Molecular Diagnosis

PL-01

Determination of Low HCV Viral Load by Abbott RealTime HCV Ultrasensitive Protocol after Direct Acting Antiviral Agents Therapy

Fabbio Marcuccilli [1], Marco Ciotti [1], Tania Guenci [1], Sara Giannella [1], Francesca Stazi [1], Valentina Serafini [1], Carlo Federico Perno [1, 2]

[1] Laboratory of Molecular Virology, Polyclinic Tor Vergata Foundation, Viale Oxford 81-00133, Rome, Italy

[2] Department of Experimental Medicine and Surgery, University Tor Vergata of Rome, Via Montpellier 1-00133, Rome, Italy

New drugs called Direct Acting Antiviral Agents (DAAs) have been developed to clear chronic HCV infection. Highly sensitive quantitative real-time PCR assays are recommended to monitor patients on antiviral therapy.

The aim of the study is to assess whether patients with detectable but not quantifiable viremia have more frequently a return of viral replication compared to patients with undetectable viral load.

For this reason we used an ultrasensitive (US) protocol by introducing a modification of the Abbott RealTime HCV assay: larger sample input volume (1 ml) was used to detect and quantify HCV RNA below the validated LOD (Limit of detection) of 12 IU/ml of the standard assay. RNA extraction was performed with the Abbott *m*2000sp and amplification/quantification with the Abbott *m*2000rt. To evaluate the analytical performances of the US protocol a clinical sample with an HCV RNA concentration of 304292 IU/ml pre-determined by the Abbott RealTime HCV assay was diluted with Basematrix to the target concentrations of 51.4, 25.7, 12.84, 6.42, 3.21 1.60 and 0.80 IU/ml, respectively. To evaluate intra-run variation and the LOD, ten replicates of each dilution were tested in 1 run and to evaluate inter-run variability, 3 replicates of each dilution were analyzed in 4 runs.

INTRA-RUN VARIATION and LOD

The intra-run CV % spanned from 13,6% to 43,3% based on the quantified results.

Mean IU/ml	53,8	25,2	12,3	6,8	3,6	2,0	1,7
SD	7,3	3,6	3,0	2,4	1,5	0,7	0,6
CV	13,6%	14,5%	24,2%	34,9%	43,3%	36,0%	36,5%

The modified protocol showed high detection rate in the range from 51,4 IU/ml to 0,80 IU/ml: 82,8% (58/70).

Target Concentration IU/ml	51,4	25,7	12,8	6,4	3,2	1,6	0,8
Replicates							
1	60,0	29,0	16,0	4,2	3,9	2,1	1,9
2	47,0	23,0	14,0	8,4	2,5	TND	TND
3	48,0	20,0	13,0	5,9	4,1	TND	TND
4	66,0	20,0	10,9	4,1	1,9	TND	TND
5	62,0	29,0	13,0	7,0	1,9	TND	TND
6	54,0	29,0	8,5	10,6	TND	3,2	TND
7	58,0	27,0	9,0	7,2	5,3	1,8	TND
8	46,0	27,0	8,8	6,4	3,0	2,1	2,3
9	51,0	26,0	17,0	10,1	3,1	1,0	TND
10	46,0	22,0	13,0	4,0	6,4	1,7	1,0

TND: target not detected.

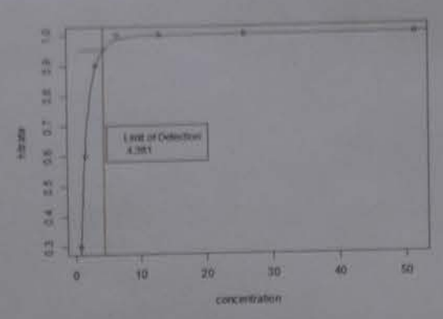

The LOD calculated by probit analysis following the CLSI Guideline EP17-A2 was 4.381 IU/ml or 0.6416 log IU/ml.

Total variation across multiple runs

The CV % across 4 runs per target concentration with 3 replicates each, respectively, spanned from 18,9 % to 82,3% based on the quantified results.

Mean IU/ml	96,1	45,1	22,8	5,1	3,5	1,9	1,0
SD	18,1	9,2	5,2	2,5	2,9	1,2	0,5
CV	18,9%	20,5%	22,8%	48,5%	82,3%	65,5%	44,8%

Conclusions: The US protocol of the Abbott RealTime HCV showed high precision, adequate LOD and it thus appropriate to evaluate the predictive value of very low on-treatment HCV RNA concentrations for DAA therapies.

Molecular Diagnosis

PL-02

PERFORMANCE EVALUATION OF ANYPLEX TMII HPV28 DETECTION KIT AND COMPARISON WITH THE HPV Sign® Genotyping Test.

FABBIO MARCUCCILLI [1], FRANCESCA FARCHI [2], MASSIMO CICCOZZI [3], PIERPAOLO PABA [4], ELENA BONANNO [5], PAOLO CASALINO [6], MARCO CIOTTI [7], CARLO FEDERICO PERNO [8]

[1-4-5-6-7-8] Fondazione "PTV" Roma, [2-3] Istituto Superiore di Sanità, [5-8] Università degli studi di Roma "Tor Vergata"

SUMMARY

Anyplex ™II HPV28 is a novel PCR assay designed for HPV genotyping. It detects up to 28 HPV types including 19 high-risk and 9 low-risk types. This study evaluted the performance of Anyplex TMII HPV28 on 123 fresh cervical samples screened in parallel with HPV Sign® Genotyping Test.

METHODS

One hundred twenty-three cervical samples obtained from women undergoing routine HPV based screening and sent to the laboratory of Molecular Virology, "Tor Vergata" University Hospital, Rome, Italy, from March to September 2013, were included in the study. The age of the women from whom the samples were collected ranged from 18 to 70 years old, mean age 34.4 years, median 34 years.

Cervical cells were collected by cytobrush, rinsed in the PreservCyt solution (Hologic, Marlborough, MA, USA) and stored according to the manufacturer's instructions until analysis.

Total DNA/RNA was extracted using the NucliSENS® easyMAG® kit on the Easy-Mag automatic extractor (bioMerieux S.A., Marcy l'Etoile, France) following the manufacturer's instructions. Two aliquots of the extracted DNA were used with the HPV sign® Genotyping Test and Anyplex™II HPV28 kit, respectively.

The study was conducted according to the indications of the Ethical Committee. All information regarding the patients was kept anonymous.

RESULTS

Of the 123 samples screened, 93 were positive, 15 negative, and 15 discordant. The total number of HPV positive samples combined was 108: 38 single infections and 70 multiple infections. The agreement between the two tests was 87.8%, κ = 0.592. Genotype specific agreement was strong for HPV 16 (k=0.761), HPV 18 (k=0.674), and HPV 35 (k=0.796). Sensitivity and specificity of Anyplex™II HPV28 assay using HPV Sign® Genotyping Test as reference was 84.8% and 94%; conversely, sensitivity and specificity of HPV Sign® Genotyping Test was 29% and 99.5%. **(see Tables 1.2.3.4)**

Table 1. Detection of HPV by Seegene and Qiagen assays

	Seegene results, No. of samples		
Qiagen results	Neg	Pos	Total
Neg	15	9	24
Pos	6	93	99
Total	21	102	123

Table 3. Distribution of HPV genotype in single and multiple infections

		No of cases				
		Single infection		Multiple infection		
Genotype		Discordant	Concordant	Discordant	Concordant	P^1
High Risk	31	0	0	10	1	-
	51	0	0	6	0	-
	52	0	1	8	0	0,111
	53	0	0	15	0	-
	56	0	2	11	2	0,057
	58	0	0	11	2	-
	59	0	0	7	1	-
	66	3	0	18	3	1,000
	73	0	2	6	10	0,529
Low risk	6	2	1	12	2	0,465
	42	3	0	20	0	-
	44	0	0	7	0	-
	54	1	0	5	0	-
	61	0	0	9	0	-

Table 4. Distribution of HPV types according to viral load

		No. of samples						
		+ (50-100 cp/reaction)		++ (10^2-10^5 cp/reaction)		+++ (>10^5 cp/reaction)		
Genotype		Disc.	Conc.	Disc.	Conc.	Disc.	Conc.	P^1
High risk	31	0	0	7	0	3	1	0.018
	51	0	0	1	0	5	0	-
	52	1	0	5	1	2	0	0.49
	53	3	0	8	0	4	0	-
	56	3	0	2	1	6	3	0.18
	58	5	0	4	1	2	1	0.08
	59	1	0	3	0	3	1	0.10
	66	4	0	9	0	7	3	0.025
	73	1	1	3	8	2	3	0.68
Low risk	6	4	0	6	1	4	2	0.08
	42	5	0	7	0	10	0	-
	44	4	0	3	0	0	0	-
	54	4	0	2	0	0	0	-
	61	2	0	4	0	3	0	-

Table 2. HPV genotype by Seegene and Qiagen assays
1: S, Seegene; Q, Qiagen; S-/Q-, negative with both tests; S-/Q+, Seegene negative and Qiagen positive;
S+/Q-, Seegene positive and Qiagen negative;
S+/Q+, positive with both tests;

Genotype		[1]S-/Q-	S-/Q+	S+/Q-	S+/Q+	% Agreement	k	Meaning	McNemar
High Risk	16	76	7	6	34	89.4	0.761	strong	1.000
	18	110	2	4	7	95.12	0.674	strong	0.688
	26	123	0	0	0	100	1.000	perfect	1.000
	31	112	0	10	1	91.87	0.154	poor	0.002
	33	117	1	4	1	95.9	0.269	weak	0.375
	35	120	0	1	2	99.19	0.796	strong	1.000
	39	120	1	2	0	97.56	-0.011	no	1.000
	45	117	1	3	2	96.75	0.484	moderate	0.625
	51	117	0	6	0	95.12	0.000	no	0.031
	52	114	0	8	1	93.5	0.188	poor	0.008
	53	108	0	15	0	87.8	0.000	no	<0.0001
	56	108	0	11	4	91.06	0.390	weak	0.001
	58	110	0	11	2	91.06	0.245	weak	0.001
	59	115	0	7	1	94.31	0.211	weak	0.016
	66	99	1	20	3	82.93	0.177	poor	<0.0001
	68	119	0	4	0	96.75	0.000	no	0.125
	69	123	0	0	0	100	1.000	perfect	1.000
	73	105	0	6	12	95.12	0.774	strong	0.031
	82	118	0	5	0	95.93	0.000	no	0.063
Low risk	6	106	0	14	3	88.62	0.270	weak	<0.0001
	11	118	0	3	2	97.56	0.561	moderate	0.250
	40	119	0	4	0	96.75	0.000	no	0.125
	42	100	1	22	0	81.3	-0.016	no	<0.0001
	43	117	0	4	2	96.75	0.488	moderate	0.125
	44	116	0	7	0	94.31	0.000	no	0.016
	54	117	0	6	0	95.12	0.000	no	0.031
	61	114	0	9	0	92.68	0.000	no	0.004
	70	121	0	1	1	99.19	0.663	strong	1.000
Total genotype sample cominations									
High and low risk		3159	14	193	78	93.80	0.406	moderate	<0.0001
High risk		2131	13	123	70	93.86	0.480	moderate	<0.0001
Low risk		1028	1	70	8	93.67	0.173	poor	<0.0001

CONCLUSIONS

Anyplex™II HPV28 assay is a sensitive and specific assay suitable for HPV genotyping but requires clinical validation.

Molecular Diagnosis

PL-03

The 32nd World Congress of Biomedical Laboratory Science (IFBLS2016)

Serum microRNAs for early diagnosis of acute radiation syndrome

Mitsuru Chiba and Satoru Monzen

Graduate School of Health Sciences, Hirosaki University, 66-1, Hon-cho, Hirosaki, Aomori, 036-8564, Japan

HIROSAKI UNIVERSITY

Abstract

[Aim] Exposure to a high dose of ionizing radiation causes acute radiation syndrome (ARS) in humans and animals. ARS patients require immediate blood transfusions and bone marrow transplant. The biological assessment of exposure dose is performed by chromosomal tests, such as the dicentric and premature chromosome condensation assays, using peripheral blood lymphocytes. However, a rapid measurement of the biological exposure dose using these assays is difficult. Therefore, we aimed to identify novel biological markers in serum microRNAs using mice exposed to lethal ionizing radiation.

[Methods] In the present study, 8-week-old male C57BL/6NJcl mice exposed to an X-ray dose of 7.0 Gy (1.0 Gy/min) were used. We explored whether serum microRNAs increased in these irradiated mice using Agilent microRNA microarray system. Extracellular vesicles (EVs) were collected from the serum using ExoQuick reagent. Gene and microRNA expressions were analyzed using quantitative polymerase chain reaction. Irradiated tissue damage was examined by hematoxylin and eosin staining and TdT-mediated dUTP nick end labeling method.

[Results and discussion] We focused on miR-375-3p increase in the serum and found that it increased two-fold at 72 h after irradiation ($p<0.05$) and was highly expressed in the small intestine. It was assumed that serum miR-375-3p was contained in EVs. In addition, cell death, such as by apoptosis and/or necrosis, was partially induced in the irradiated small intestine. On the other hand, sphingomyelin phosphodiesterase 3 encoding neutral sphingomyelinase 2 involved in exosome secretion was upregulated in the small intestine at 72 h after irradiation ($p<0.01$). These results suggest that the irradiated small intestine releases miR-375-3p-containing EVs, such as exosomes and/or apoptotic bodies, to extracellular spaces.

[Conclusions] The present study indicates that serum miR-375-3p may be a biomarker for the early diagnosis of ARS.

Introduction

The changes of survival rate and body weight in mice exposed to 7 Gy of IR

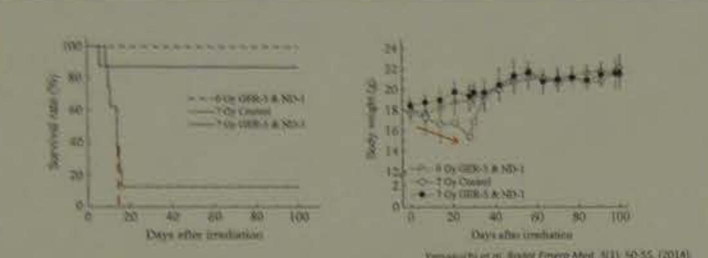

Yamaguchi et al. Radiat Emerg Med. 3(1): 50-55, (2014).

The survival rate of 7 Gy irradiated mice is less than 50% in 2-weeks. In addition, body weight in mice decrease after exposure to 7 Gy of ionizing radiation (IR).

It is necessary to provide the emergency medical care to patients in radiation accidents. Therefore, a novel biomarker for dosimetry of the internal radiation dose is required.

Intracellular microRNAs are secreted to extracellular space

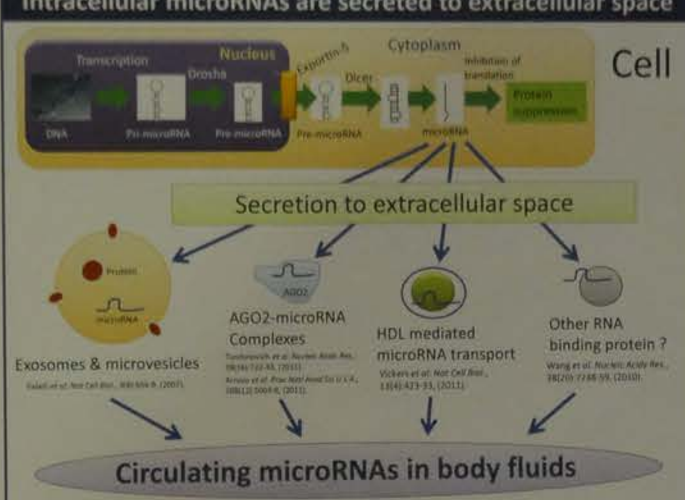
Cell
Nucleus
Transcription
Drosha
Exportin-5
Cytoplasm
Dicer
Inhibition of translation
Protein suppression
DNA
Pri-microRNA
Pre-microRNA
microRNA
Secretion to extracellular space
Exosomes & microvesicles
AGO2-microRNA Complexes
HDL mediated microRNA transport
Other RNA binding protein ?
Circulating microRNAs in body fluids

Aim

The present study aimed to identify increasing serum microRNAs within 72 hour (h) using mice exposed to 7 Gy of IR.

Results

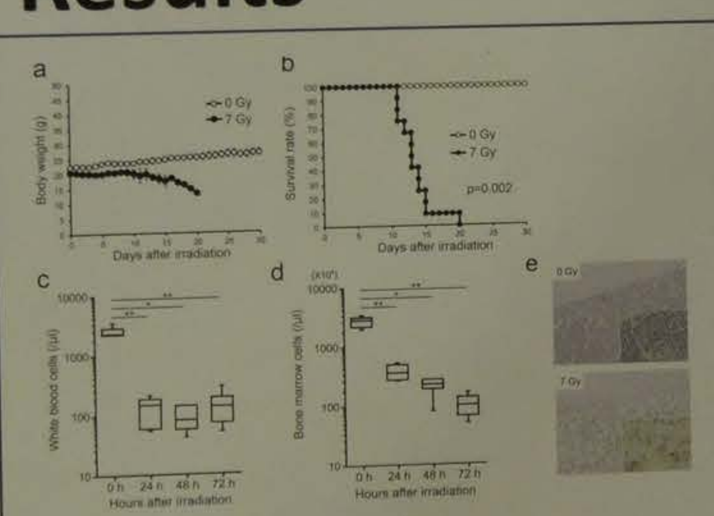

Figure 1. Effects on exposure to a 7 Gy dose of X-ray irradiation in mice. **(a)** The body weight changes of irradiated group (7 Gy) (n=12) and non-irradiated group (0 Gy) (n=6) every day until 30-day after irradiation. The data are expressed as the means ± SD. **(b)** Kaplan-Meier plot for the survival of irradiated C57BL/6N male mice. The survival rate of irradiated group (n=12) and non-irradiated group (n=6) every day until 30-day after irradiation. The statistical difference was determined by log-rank test between irradiated group and non-irradiated group. Difference with $p<0.05$ was considered significant. **(c)** The number of peripheral white blood cells (PWBC) in irradiated mice. **(d)** The number of bone marrow cells in irradiated mice. PWBC and bone marrow cells decreased significantly at 24 h, 48 h and 72 h after irradiation compared to 0 h. Statistical significance was examined by Steel's test for multiple comparison (*$p<0.05$, **$p<0.01$). **(e)** Hematoxylin and eosin (HE) staining of decalcified thighbone sections in mice. HE staining was performed to visualize the fine structures of thighbone in irradiated mice. Bone marrow cells in mice at 72 h after 7 Gy irradiation decreased clearly compared to 0 Gy.

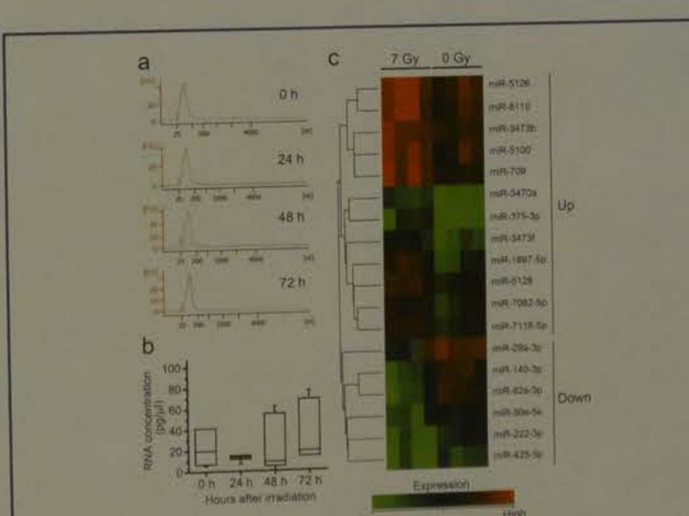

Figure 2. Identification of differentially expressed microRNAs in serum of mice exposed to X-ray 7 Gy. **(a)** Detection of extracellular RNAs in serum of irradiated mice. Sera were obtained from mice at 0 h, 24 h, 48 h and 72 h after 7 Gy irradiation. Serum RNAs were extracted using Isogen II reagent (NipponGene) as described in Methods. Extracellular small RNAs were detected in all samples using an Agilent Bioanalyzer (Agilent Technologies). **(b)** Quantitation of extracellular RNA concentrations in serum of irradiated mice. RNA concentration was measured using a Quant-iT™ RiboGreen® RNA assay and kit (Life Technologies) and showed no significant differences among groups. **(c)** Expression analysis of up-/down-regulated microRNAs in serum of irradiated mice using an Agilent mouse microRNA microarray. Heat map showing variations in a part of 18 radio-responsive microRNAs, identified by student t-test with a cut off p-value of 0.05 and 2-fold change. Up-regulated 12 microRNAs and down-regulated 6 microRNAs were identified, respectively.

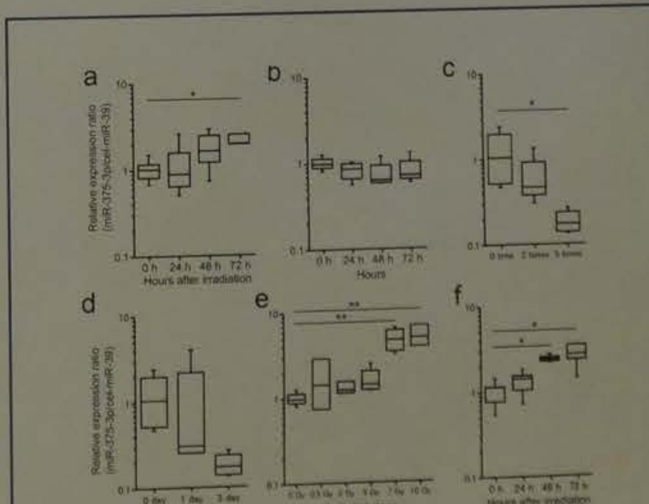

Figure 3. MiR-375-3p expressions in serum of irradiated mice of 7 Gy X-ray. The changes of miR-375-3p expressions by reverse transcription-qantitative polymerase chain reaction (RT-qPCR). **(a)** at 0 h, 24 h, 48 h and 72 h after irradiation of 7 Gy X-ray, **(b)** at each hour in non-irradiation controls, **(c)** in freeze thaw cycles (0, 2 and 5 times), **(d)** by incubation for 0 day, 1 day and 3 day at room temperature, **(e)** in each radiation dose (0, 0.5, 2, 4, 7 and 10 Gy), and **(f)** in extracellular vesicles (EVs) derive from serum of 7 Gy irradiated mice. EVs were collected using ExoQuick reagent (System Biosciences). Cel-miR-39 was used as external control. Expression levels of miR-375-3p were determined by RT-qPCR using the comparative Ct methods. Statistical significance was examined by Steel's test for multiple comparison (*$p<0.05$, **$p<0.01$).

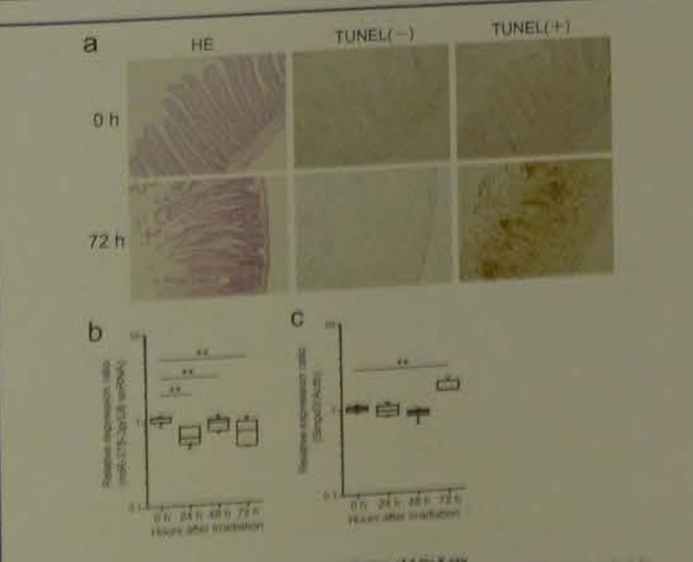

Figure 4. MiR-375-3p also releases from intestine by irradiation of 7 Gy X-ray. (a) Analysis of TdT-mediated dUNP nick end labeling (TUNEL) staining in mouse intestine. Cell death, such as by apoptosis and/or necrosis, was partially induced in the irradiated small intestine. (b) Expressions of miR-375-3p in mouse small intestine after irradiation. MiR-375-3p was downregulated in the small intestine at 24 h, 48 h and 72 h after irradiation (each $p<0.01$). (c) Expressions of Sphingomyelin phosphodiesterase 3 (Smpd3) in mouse small intestine after irradiation. Smpd3 encoding neutral sphingomyelinase 2 involved in exosome secretion was upregulated in the small intestine at 72 h after irradiation ($p<0.01$).

Conclusion

- 18 microRNAs were found to be expressed differentially in the sera of IR-exposed mice (7 Gy), with a magnitude of more than 2.0-fold change as compared to the sera of IR-unexposed mice (0 Gy).
- Serum miR-375-3p increased 2.0-fold change at 72 h after exposure to 7 Gy dose of X-ray irradiation.
- Serum miR-375-3p may be secreted from small intestine.
- Serum miR-375-3p has the potential to be used as a biomarker to identify exposure to IR.

Molecular Diagnosis

PL-04

HCV Related Cryoglobulinemia：A Case Report

Yi Shun. Chen[1], Wei Yung. Lo[2], and Ya I. Hsiao[1*]

[1]Laboratory Medicine Department, [2]Division of Rheumatology, Department of Internal Medicine, National Taiwan University Hospital Hsin-Chu Branch, Taiwan

1. INTRODUCTION

Cryoglobulins, in three main types, are a group of immunoglobulins that undergo reversible precipitation at low temperatures. Trace serum cryoglobulin levels , in the case of mixed type, could be identified in about 50% hepatitis C patients, usually together with appearance of rheumatoid factors (RF) and antinuclear antibodies (ANA). Neglecting prior hepatitis C history, clinicians might miss making pegylated interferon or anti-viral medications to work for people who have associated cryoglobulinemia due to misdiagnosed atypical rheumatoid arthritis. In clinical practice, with higher awareness, cryoglobulin test would be ordered to perform for chronic hepatitis C patients developing the following symptoms alone or in combination: purpura, arthritis, glomerulonephritis, neuritis, etc.

2. METHOD & RESULT

This report here describes a case of highly suspected hepatitis C virus (HCV) related secondary cryoglobulinemia. A 66-year-old man with HCV antibodies visited our hospital and presented with polyneuropathy on October 21, 2015. Laboratory data discovered trace-positive cryoglobulin, elevated RF (35 IU/mL), positive ANA (titer of 1:40; speckled pattern), increased erythrocyte sedimentation rate (1、2hr: 17、36mm), elevated IgG (1730 IU/mL). Four weeks later, further analyzed data revealed the appearance of HCV RNA (genotype 1b), with HCV viral load up to 3.92 x10^7 IU/mL, elevated AST/ALT (37/51 IU/mL), besides, polyclonal gammopathy could be seen in serum protein electrophoresis.

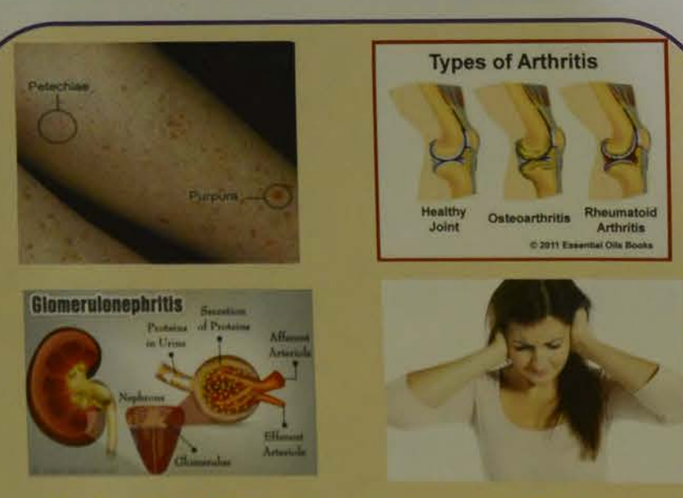

Fig1. Clinical Symptoms for Hepatitis C Patients with Cryoglobulinemia

(a) Cryoprecipitate at cold temperature
(b) Disappearance of cryoprecipitate on rewarming

Fig2. Cryoglobulin Test

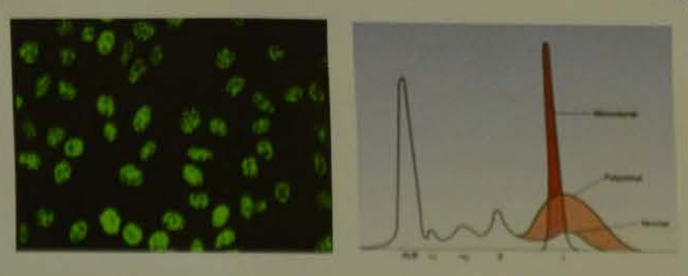

positive ANA (speckled pattern)

polyclonal gammopathy in serum protein EP

Fig3. ANA and Serum protein ElectrophoresisTest

Table1. List of Other Clinical Laboratory Testing

Item	Result	
HCV antibodies	positive	
HCV RNA	genotype 1b	
HCV viral load	3.92 x10^7 IU/mL	
RF	35 IU/mL	elevated
IgG	1730 IU/mL	elevated
AST/ALT	37 / 51 IU/mL	elevated

3. CONCLUSION

In the laboratories, cryoglobulins are hard to accurately detect because of temperature sensitive nature and generally trace amount in blood specimens. Therefore, a proper pre-analytical procedure of blood collecting is the key point. Planning how to increase the detection rate and persistent follow-up of laboratory data as well as therapeutic effects will be the goals we are striving for in the future.

Molecular Diagnosis

PL-05

Mitochondrial DNA Mutations in Thyroid disease

Hung-cheng Chou [1,2], Shu-Huei Kao[2], Chi-ChaoTu [3*]

[1] Department of Laboratory Medicine, National Taiwan University Hospital Hsin-Chu Branch, R.O.C, Taiwan;

[2]Taipei Medical University,School of Medical Laboratory Science and Biotechnology, R.O.C, Taiwan

[3*] Department of Laboratory Medicine, Keelung Hospital, Ministry of Health and Welfare, R.O.C, Taiwan

Aim

Goiter and benign thyroid disease are a common problem with prevalence about 4% in the general population. The pathogenesis of goiter and gland hyperplasia is still unclear. Human mtDNA is recognized to evolve 10–100 times faster than nuclear DNA with a number of reasons. Accumlation of human mtDNA mutations has been demonstrated to be an important factor of human aging and degenerative disease. It is well defined that thyroid hormone could contribute in the regulation of the expression of mtDNA replication and nucleus encoded mitochondrial protein.

Materials and Methods

Forty patients with thyroid hyperplasia patient from Shin-Chu Hospital were enrolled in this study. We also collected the clinical data of TSH、T3 and free T4. The large-scale mtDNA deletion were identified by long-rang PCR, primer -shift PCR and semi-quantitative PCR. There were three types of mtDNA deletion identified in this study including 4977bp, 7599bp and 5335 bp deletions.

Results

The occurrence of mtDNA deletion was 67.3%, 37.5% and 20.0% in papillary carcinoma, Nodular hyperplasia, and diffuse hyperplasia, respectively. Abnormal hormone level were correlated with the occurrence of mtDNA deletion. TSH level abnormal bearing with 7599bp deletion was about 62.5%, with 5335bp deletion was about 37.5%, with 4977bp deletion was about 25.0%. T4 level abnormal bearing with 7599bp deletion was about 80.0%, with 5335bp deletion was about80.0%, with 4977bp deletion was about 60.0%.

Conclusions

The mtDNA copy-number were detected by real-time PCR and we finned that mtDNA copy-number were decreased in tissue sample of patient (52%). The mtDNA copy-number in the blood sample of patient after operation was increase about 10% than patient before operation.

Disscuss

It reveals that patient after operation treatment may increase there mtDNA copy-number. We suggest that mutations and/or depletion of mtDNA might play some important role in the progression and pathogenesis of thyroid hyperplasia.

Table 1 Primer pair in this study

Primer pair sequenc	Nucleotide positi	Oligonucleotid
L7901	7901-7920	5'- TGACCTACGGTACACACCGA- 3'
L8150	8150-8166	5'- CCGGGGGTATACTACGGTCA- 3'
L8251	8251-8270	5'- GCCCGTATTTACCCTATAGC- 3'
L8531	8531-8550	5'- ACGAAAATCTGTTCGCTTAC- 3'
H13650	13650-13631	5'- GGGGAAGCGAGGTTGACCTG- 3'
H13845	13845-13862	5'- GTCTAGGGCTGTTAGAAGCT- 3'
H13905	13905-13886	5'- GGAGAAATAAAATGTGCATA- 3'
H14020	14020-14001	5'- ATAGCTTTTCTAGTCAGGTT- 3'
H16255	16255-16236	5'- CTTTGGAGTTGCAGTTGATG- 3'
H16450	16450-16431	5'- CGAGGAGAGTAGCACTCTTG- 3'

Table 2 Mutated mtDNA in Thyroid cancer patients

	Amplified region (nucleotide position)	Length of PCR product amplified from normal mtDNA(bp)	Length of PCR product amplified from mutated mtDNA(bp)	Length of mutated mtDNA(bp)
20	8150-14020	5871	894	4977
			536	5335
45	8150-13845	5696	719	4977
			361	5335
05	8251-13905	5655	360	5335
45	8251-13845	5595	260	5335
50	8251-13650	5400	423	4977
55	7901-16255	8335	756	7599
55	8251-16255	8005	406	7599
45	8531-13845	5315	415	7599
50	8531-16450	7920	321	7599

Table 3 Thyroid hormone level results

Type of disease	Sample No.	TSH (uIu/ml)	T4 (ng/dl)	T3 (nmol/L)
Normal control	5	1.58±0.48	1.14±0.38	1.16±0.07
Papillary carcinoma	3	45.31±22.31	0.43±0.17	ND
Nodular hyperplasia	32	1.51±0.19	1.12±0.12	1.024±0.15
Diffuse hyperplasia	5	1.54±0.56	1.16±0.06	ND

ND, no detection.

Reference values of TSH is 0.25-4.0(uIu/ml)

Reference values of fT4 is 0.8-1.9 (ng/dl)

Reference values of T3 is 0.84-1.72(nmol/L)

Figure 1 Pathologic conformed in study

Figure 2 Pathologic conformed in study

Figure 3 Result of 7599bp deleted

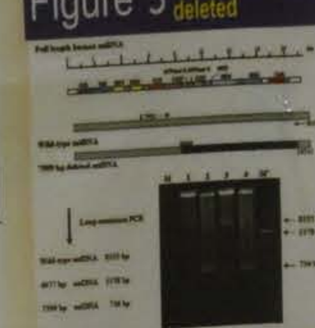

Figure 4 Result of 4977 and 5335 bp deleted

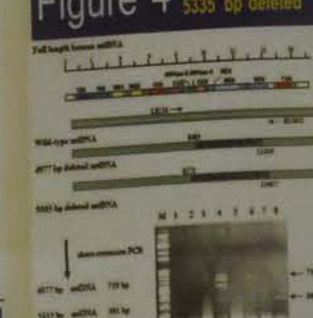

Figure 5 Result of 4977 bp deleted

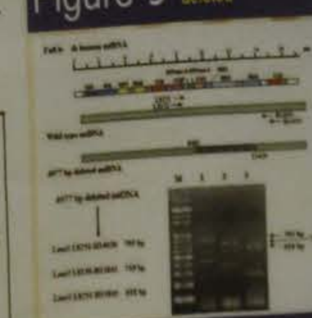

Table 8 Frequences of MtDNA deletion

[illegible]

Figure 6 Results of conformed sequence of MtDNA

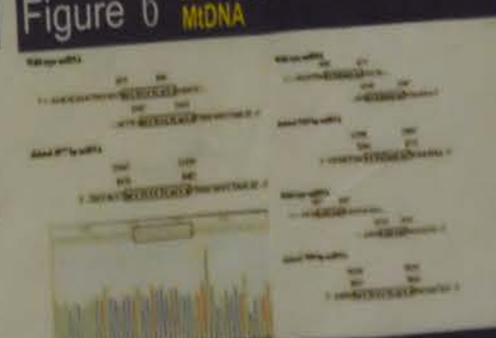

Figure 7 Result of MtDNA deleted Thyroid hormone level

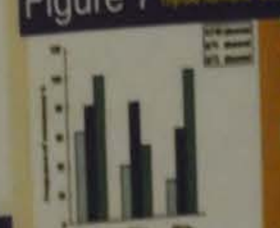

Table 4 Results of normal control

[illegible]

Table 5 MtDNA deleted in 3 cancer patients

[illegible]

Figure 10 RtPCR result of mutated MtDNA copynumber

台大醫院 國立臺灣大學醫學院附設醫院新竹分院
新竹分院 National Taiwan University Hospital Hsin-Chu Branch

Molecular Diagnosis

PL-06

PL-06 Genetic and Phylogenetic Analysis of Influenza A(H1N1)pdm09 Virus in the 2015/2016 Season: How were mutations introduced in H1N1pdm09 genomes ?

Kuo-Chien Tsao[1,2,3], Yu-Nong Gong[1], Shu-Li Yang[1,2], Yi-Chun Liu[1], Shuan Yang[1], Chung-Guei Huang[1,2,3]
[1] Department of Laboratory Medicine, Linkou Chang Gung Memorial Hospital; [2] Department of Medical Biotechnology and Laboratory Science; [3] Research Center for Emerging Viral Infections, College of Medicine, Chang Gung University, Taoyuan, Taiwan

Introduction

- As swine-origin H1N1 virus (H1N1pdm09) emerged in 2009, incidence of H1N1pdm09 has significantly risen to reach a new high in 2015. In Taiwan, the H1N1pdm09 outbreak from July 2015 to March 2016 caused over 1400 severe cases and 110 deaths [1]. This outbreak might result from novel genetic mutations or antigenic drift.
- In this study, we 1) constructed phylogenetic tree based on HA1 domain for designating Taiwanese and worldwide strains to genetic clades, and 2) identified H1N1pdm09 signature residues by a position-specific entropy manner from 11 protein alignments of PB2, PB1, PA, PA-X, HA NP, NA, NS1, NS2, M1 and M2 for discussing how genomic diversity of H1N1pdm09 were introduced in this outbreak.

Materials and Methods

Sample Collection and Sequencing

- For whole genome sequencing, 10 influenza isolates were collected in Linkou Chang Gung Memorial Hospital, Taiwan, from October 2015 to March 2016. Nucleotide sequences of these strains were obtained using in-house RT-PCR and the Sanger dideoxy sequencing method by specific primer pairs.
- Sequences were downloaded from GISAID EpiFlu database (http://platform.gisaid.org/epi3/), including HA sequences of 23 worldwide reference strains and 64 Taiwanese strains from 2009 to 2016 for phylogenetic analysis, and 757 worldwide genomes from 2015 to 2016 for Entropy analysis.

Entropy and Phylogenetic Analyses

- HA1 nucleotide sequences of Taiwanese and worldwide strains were aligned using Clustal Omega (version 1.2) [2] for Bayesian evolutionary analysis by using BEAST2 [3].
- An Entropy (En) value was defined at an aligned amino acid position according to the formula $-\Sigma Pi*\log(Pi)$, in which i is the observed probability for each of the 20 amino acids [4].

Result

Bayesian Evolutionary Analysis

Figure 1 showed a clade transition of H1N1pdm09 by using HA1 sequences of Taiwanese and reference strains from 2009 to 2016, demonstrating that strains from 2009 to 2011 belonged to Clades from 1 to 4, from 2011 to 2012 to Clades 5, 7 and 8, and after 2011 to Clade 6.

In this outbreak season from 2015 to 2016, 767 HA1 sequences were designated to sub-clades 6b.1 (n=640) and 6b.2 (n=127).

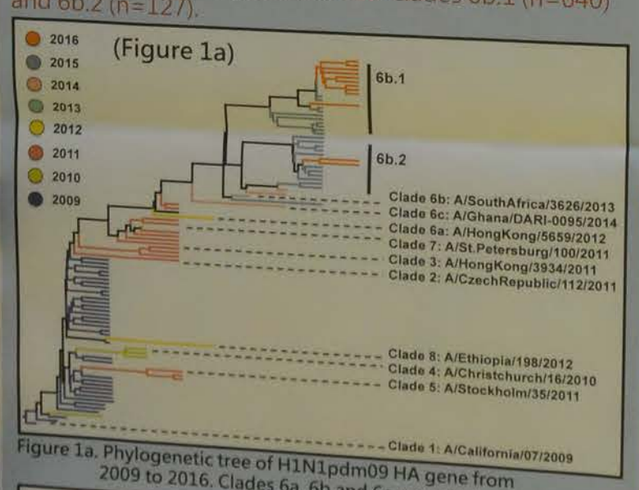

Figure 1a. Phylogenetic tree of H1N1pdm09 HA gene from 2009 to 2016. Clades 6a, 6b and 6c were derived after 2011.

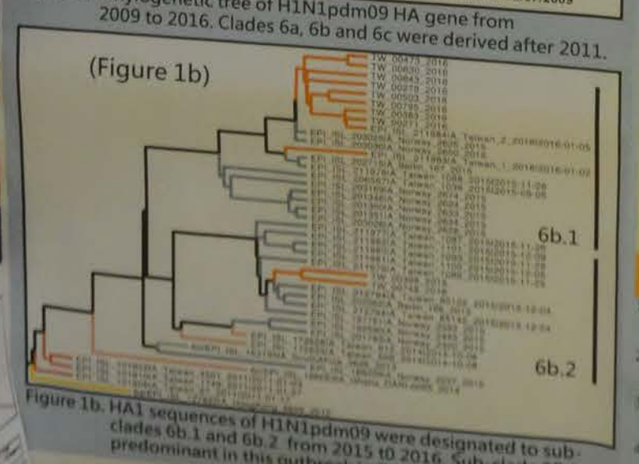

Figure 1b. HA1 sequences of H1N1pdm09 were designated to sub-clades 6b.1 and 6b.2 from 2015 t0 2016. Sub-clade 6B.1 was predominant in this outbreak in Taiwan (orange line).

Sequence and Entropy Analyses of Taiwanese and Worldwide Genomes

- 10 Taiwanese genomes shared high sequence identities. Minimum identities of nucleotide sequences in each of genes were from 98.3% to 100%, except for 97.3% of HA gene. Minimum identities of amino acid sequences in each of proteins were from 98% to 100%, except for 96.7% of NS2 protein.
- According to 6 clade-specific HA mutations [5] marked by asterisks in Table 1, an entropy threshold of 0.12 was applied on 769 genomes from this season for avoiding amino acid changes introduced by random drift. For example, Entropy values of 0.60, 0.39 and 0.12 were obtained from HA1-162, HA-13 and HA1-222, respectively. Entropy values of >0.45, 0.31–0.45 and <0.31 were highlighted with red, pink and white backgrounds, respectively.
- 16 HA signatures were identified by this threshold, together with 56 signatures from other proteins, as summarized in Table 1. Those signatures demonstrated how genomic mutations of H1N1pdm09 were introduced in this season.

Table 1. 72 Amino acid signatures of influenza A(H1N1)pdm09 virus in this 2015/2016 season

Protein	Pos	En	Composition	Protein	Pos	En	Composition
*HA1-216		0.61	T=553,I=211,P=3	PB1	374	0.22	A=727,T=35,I=4,X=1
*HA1-162		0.60	N=556,S=209,R=2		211	0.18	R=731,K=36
*HA1-84		0.45	N=635,S=132		175	0.18	N=732,D=35
HA-13		0.39	T=665,A=102		69	0.13	I=745,V=22
HA2-169		0.26	L=714,Q=49,R=4	PA	361	0.46	K=633,R=134
HA1-48		0.23	A=720,P=46,T=1		538	0.28	E=713,D=46,G=8
HA1-69		0.23	S=720,P=47		100	0.22	I=721,V=46
HA-6		0.22	V=721,A=46		61	0.18	I=736,V=28,T=2,L=1
*HA1-173		0.18	V=734,I=32,X=1		649	0.18	L=733,I=34
*HA2-152		0.18	V=735,T=30,X=2		330	0.14	V=744,I=21,A=2
HA2-324		0.17	V=721,A=46		341	0.13	V=743,M=24
HA1-222		0.17	I=738,V=30,X=1		379	0.12	V=749,M=10,L=8
HA2-305		0.16	D=737,E=30	PB2	453	0.58	T=626,S=101,P=40
HA2-295		0.16	E=738,G=29		299	0.47	K=626,R=141
*HA2-174		0.12	N=747,S=19,X=1		184	0.36	A=680,T=85,V=1,X=1
HA1-222		0.12	D=751,G=8,X=6,N=4		588	0.15	T=745,I=14,A=6,X=2
NA	264	0.40	I=664,V=102,T=1	NP	105	0.39	T=665,M=101,V=1
	270	0.38	K=667,N=100		425	0.36	V=674,I=93
	314	0.36	M=679,I=87,V=1		22	0.35	T=681,A=85,X=1
	13	0.34	I=682,V=85		444	0.34	V=682,I=85
	117	0.34	I=684,M=83		359	0.20	S=727,F=40
	450	0.23	S=721,G=44,D=2		190	0.17	A=738,T=27,V=2
	288	0.22	I=721,V=46	NS1	125	0.60	D=557,E=208,G=2
	34	0.19	V=731,I=34,L=2		2	0.59	E=555,D=211,K=1
	365	0.19	I=730,T=36,X=1		6	0.20	M=734,T=25,I=8
	67	0.17	V=735,I=32		124	0.20	M=732,T=32,I=2,X=1
	151	0.17	D=738,X=27,N=2		48	0.18	N=734,S=32,X=1
	86	0.16	A=739,T=25,V=3		131	0.15	E=740,K=27
	329	0.16	N=738,S=28,D=1		178	0.13	V=745,I=21,L=1
	381	0.16	T=737,I=30	NS2	2	0.59	E=555,D=211,K=1
	15	0.14	M=744,I=19,V=4		83	0.48	I=632,M=133,T=1,V=1
PA-X	204	0.54	S=616,N=141,G=9,X=1		6	0.20	M=734,T=25,I=8
	100	0.22	I=721,V=46		115	0.15	A=741,T=25,S=1
	61	0.18	I=736,V=28,T=2,L=1	M1	208	0.46	Q=133,K=634
	212	0.17	A=737,V=29,T=1		167	0.18	T=732,A=35
	222	0.13	T=743,I=24	M2	21	0.41	G=659,V=107,A=1

Conclusion

- A clade transition of Taiwanese and worldwide strains in phylogenetic analysis demonstrated that clades 6a, 6b and 6c were derived after 2011, and then sub-clade 6b.1 was predominant in the H1N1pdm09 population from 2015 to 2016.
- Although 10 Taiwanese genomes were sequenced from this outbreak season sharing high sequence identities, adaptive mutations contributed to the emergence of influenza H1N1pdm09 virus. A total of 72 genomic signatures were explored by a cut-off 0.12 of entropy value in 2015/2016. This manner helped us to better elucidate the rapid rise and the genomic diversity of H1N1pdm09 in this season.
- Clade transition and genomic diversity in Taiwanese and worldwide strains were provided in this study. However, links between genomic changes and clinical disease severity were still unknown and needed to be further investigated.

References

1. Taiwan Centers for Disease Control (CDC). http://www.cdc.gov.tw/list.aspx?treeid=1F07E8862BA550CF&nowtreeid=2048424A955D57 2F. Accessed date: August 10, 2016
2. Sievers F, Wilm A, Dineen D, Gibson TJ, Karplus K, Li W, et al. Fast, scalable generation of high-quality protein multiple sequence alignments using Clustal Omega. Mol Syst Biol. 2011; 7: 539
3. Bouckaert R, Heled J, Kühnert D, Vaughan T, Wu C-H, Xie D, et al., BEAST 2: A Software Platform for Bayesian Evolutionary Analysis. PLoS Computational Biology. 2014; 10(4). e1003537
4. Shannon, Claude E. (July–October 1948). "A Mathematical Theory of Communication". Bell System Technical Journal. 27 (3): 379–423
5. Influenza virus characterization, nextflu.org/reports/feb-2016/. Accessed date: August 10, 2016

Molecular Diagnosis

PL-07

Droplet Digital PCR for quantitation of human papilloma virus (HPV) 16, 18, 33 and 45.

Gabriella Lillsunde Larsson and Gisela Helenius.

Department of Laboratory Medicine, Faculty of Medicine and Health, Örebro University, SE-701 82 Örebro, Sweden. gabriella.lillsunde-larsson@regionorebrolan.se

Background

HPV infection is the cause of cervical cancer and the virus has also been strongly associated with other ano-genital malignances. For lesion development, a long-term persistent viral infection is required. Estimation of HPV viral load can be used to identify a persistent infection with slowly increasing copy numbers from a transient infection where a quick rise is followed by a copy number drop. Droplet digital PCR (ddPCR) measures absolute quantities of PCR amplified fragments, without the need for standard curves, by counting nucleic acid molecules encapsulated in volumetrically defined water-in-oil droplet partitions. Reagents and sample are positioned into 20 000 (nanoliter sized) droplets. PCR is performed and each drop is analyzed individually using a two-color detection system.

Aim

To evaluate the ddPCR method for estimation of HPV16, 18, 33 and 45 viral load in formalin fixed paraffin embedded (FFPE) samples.

Material and method

DNA from FFPE vaginal and vulvar carcinoma samples, positive for HPV16 (n= 33), 18 (n= 4), 33 (n=4) and 45 (n=1) was used for ddPCR HPV viral load quantitation together with human control gene *HBB*. Duplex PCR- reactions (HPV genotype + *HBB*) were positioned in droplets that were PCR-amplified followed by signal evaluation (VIC and FAM), using a droplet reader (Bio-Rad).

For HPV16- positive samples, data on viral load using real-time PCR was used for comparison. Standard curves were established by making serial dilutions of plasmid pBR322 containing the total HPV16 genome.

The equation of the standard curve is used to estimate copy number from sample cycle Ct. HPV16 copy number ddPCR results were compared to real-time PCR results

Results

Method validation of ddPCR showed an intra-assay precision between 0.2 % and 12.2 % (HPV18 and HPV33 respectively), while inter-assay precision was somewhat higher; 0.1-14.6 % (HPV33 and HPV45). Limit of detection was between 0.08 and 0.23 copies/µl. Viral load in 20 ng of input DNA varied between 154 and 340 200 copies for HPV16, between 12 and 1565 copies for HPV18 and between 36 and 3455 copies for HPV33, table 1.

Table 1. Viral load (copies in 20 ng DNA) in FFPE HPV-positive samples.

Genotype	n	Min	Max	Mean	Median	SD
HPV16	33	154	340 200	29 424	2820	71 284
HPV18	4	12	1565	544	300	726
HPV33	4	36	3455	1499	1253	1464
HPV45	1	67	67	67	67	N/A

Corresponding values of HPV copies/cell was between 0.27 to 573 in samples positive for HPV16, between 1.8 and 680 for HPV18, between 3 and 506 for HPV33 and 0.3 for HPV45-positive samples.

A strong correlation between methods for viral load (HPV16) was found, Pearson; r = 0.99, p=0.000 (n= 33). However, copy numbers using ddPCR were consistently lower compared to real-time PCR data.

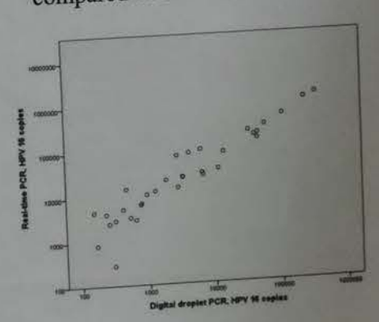

Figure 2. Correlation of realtime PCR viral load data to ddPCR viral load data for HPV 16.

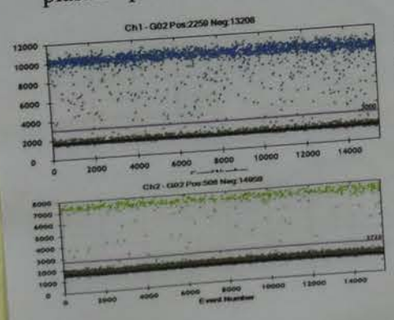

Figure 1. Detection of HPV16 and *HBB*. Upper : HPV16 detection using FAM, lower: *HBB* detection using VIC. Positive droplets in blue and green and negative droplets in grey. Degradation of FFPE DNA results in varying signal amplitud, i.e.. "droplet rain".

Conclusion

Droplet Digital PCR (ddPCR) provides a new promising tool for evaluating HPV viral load in FFPE samples.

Presenting author:
Gabriella Lillsunde Larsson
gabriella.lillsunde-larsson@regionorebrolan.se

ÖREBRO UNIVERSITY

Region Örebro County
Örebro University Hospital

Molecular Diagnosis

PL-08

馬偕紀念醫院
MacKay Memorial Hospital

Comparison of a Real-Time PCR with an in-house semi-nested PCR assay - for the Diagnosis of Herpes Simplex Virus infection

Yu-Ying Chiu[1], Yi-Jhen Chen[1], Tuan-Jen Wang[1], Chi-Kuan Chen[1,2]
Department of Laboratory Medicine[1] and Department of Pathology[2], Mackay Memorial Hospital, Taipei, Taiwan

Background: Although viral culture has been considered to be the gold standard method for diagnosis of HSV, but it's time consuming, labor-intensive and requires special equipments. PCR based methods are fast and highly sensitive tools, particularly for specimens difficult to be cultured, such as CSF.

Objective: To evaluate the performance of TIB MOLBIOL LightMix® Kit HSV-1/2 on LightCycler® 480 II system, and compare the results with a routinely used in-house semi-nested PCR combined with enzyme digestion to distinguish HSV-1 and HSV-2, using clinical samples and proficiency testing samples of College of American Pathology (CAP). 。

Results:

The sensitivity of real-time PCR and semi-nested PCR were tested triplicate using ten fold serial diluted HSV-1, the results were 10 $TCID_{50}$ and 0.1 $TCID_{50}$ respectively (Table 1).

21 clinical samples and 3 proficiency test samples were tested parallel by real-time PCR and semi-nested PCR, the total agreement between these two methods were 100%, besides, the HSV types detected by semi-nested PCR followed by enzyme digestion were all the same as the results of real-time PCR with melting curve analysis (Table 2), even with the HSV variants (Fig. 1).

The LOD of the LightMix® Kit HSV-1/2 kit was evaluated with standard of 10 copy provided in the kit, the results was 10 copies / reaction as indicated in the package insert.

The repeatability was evaluated with cumulated Coefficient of variation (CV) of the log transformed data of standards (from 10^2 to 10^6 copies / reaction), the results were all below 5.0 %.

The linearity was tested with 10 fold serial diluted 10^7 $TCID_{50}$ HSV-1 and the R-squared of linear regression analysis was 0.983 (Fig. 2).

FIG 2 Linearity results of the LightMix® Kit HSV-1/2 kit

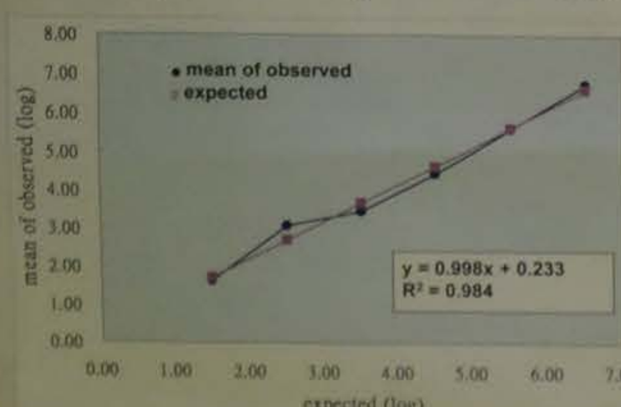

TABLE 1 comparison of the sensitivity of HSV real-time PCR and semi-nested PCR

dilution	viral titer	HSV real-time PCR			semi-nested PCR
		Cp	copies	log	PCR results
0	10^7 $TCID_{50}$	16.86	3630000	6.56	+
10^{-1}	10^6 $TCID_{50}$	20.88	175000	5.24	+
10^{-2}	10^5 $TCID_{50}$	24.19	14300	4.16	+
10^{-3}	10^4 $TCID_{50}$	27.49	1190	3.08	+
10^{-4}	10^3 $TCID_{50}$	30.73	103	2.01	+
10^{-5}	10^2 $TCID_{50}$	34.01	8.6	0.93	+
10^{-6}	10^1 $TCID_{50}$	37.13	0.82	-0.09	+
10^{-7}	1 $TCID_{50}$	-	-	-	+
10^{-8}	10^{-1} $TCID_{50}$	-	-	-	+
10^{-9}	10^{-2} $TCID_{50}$	-	-	-	-
10^{-10}	10^{-3} $TCID_{50}$	-	-	-	-

TABLE 2 agreement of HSV real-time PCR and semi-nested PCR methods

sample No.	Nucleic Acid titer	HSV real-time PCR					Semi-nested PCR		agreement
		Cp	copies	log	Tm	Types	PCR results	Types	
1	1X	20.71	455000	5.66	56.73	HSV-1	+	HSV-1	Yes
	dilute 10X	24.27	34800	4.54	66.83		+		
2	1X	[illegible]	[illegible]	0.94	NA	HSV-1	+	HSV-1	Yes
	dilute 10X	[illegible]	[illegible]	1.01	[illegible]		+		
3	1X	20.15	712000	5.85	60.06	HSV-2	+	HSV-2	Yes
	dilute 10X	23.78	49900	4.70	60.02		+		
4	1X	27.68	2940	3.47	67	HSV-1	+	HSV-1	Yes
	dilute 10X	30.68	331	2.52	67.19		+		
5	1X	27.52	3330	3.52	55.8	[illegible]	+	HSV-2	Yes
	dilute 10X	29.81	637	2.80	55.59		+		
6	1X	-	-	-	-	NA	-	NA	Yes
	dilute 10X	-	-	-	-		-		
7	1X	-	-	-	-	NA	-	NA	Yes
	dilute 10X	-	-	-	-		-		
8	1X	22.76	68100	4.83	67.59	HSV-1	+	HSV-1	Yes
	dilute 10X	28.3	5570	3.75	67.2		+		
9	1X	32.52	33.6	1.53	[illegible]	[illegible]	+	HSV-2	Yes
	dilute 10X	35.02	3.36	0.53	[illegible]		+		
10	1X	29.93	312	2.49	[illegible]	[illegible]	+	HSV-2	Yes
	dilute 10X	32.86	29.6	1.47	[illegible]		+		
11	1X	34.43	5.85	0.77	60.84	HSV-2	+	HSV-2	Yes
	dilute 10X		-	-			-		
12	1X	24.2	25700	4.41	67.21	HSV-1	+	HSV-1	Yes
	dilute 10X	27.61	2040	3.31	67.06		+		
13	1X	28.3	855	2.93	67.03	HSV-1	+	HSV-1	Yes
	dilute 10X	31.63	73.5	1.87	67.3		+		
14	1X	-	-			NA	-	NA	Yes
	dilute 10X	-	-				-		
15	1X	-	-			NA	-	NA	Yes
	dilute 10X	-	-				-		
16	1X	-	-			NA	-	NA	Yes
	dilute 10X	-	-				-		
17	1X	-	-			NA	-	NA	Yes
	dilute 10X	-	-				-		
18	1X		-			NA	-	NA	Yes
	dilute 10X	-	-				-		
19	1X					NA	+	[illegible]	Yes
	dilute 10X						-		
20	1X					NA	-	NA	Yes
	dilute 10X	-	-	-			-		
21	1X	[illegible]	1430	[illegible]	[illegible]	[illegible]	-	HSV-2	Yes
	dilute 10X	[illegible]	[illegible]	[illegible]	[illegible]		-		

FIG 1 Amplification curves and melting peaks of the HSV standards and samples, including a HSV-2 variant

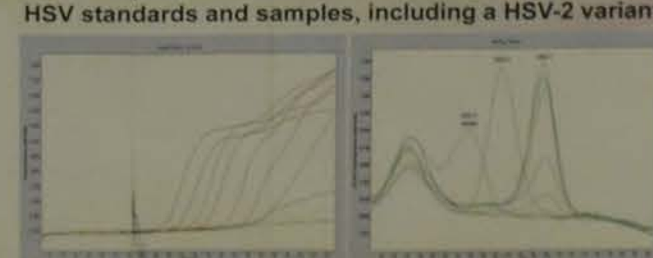

Conclusion: Although semi-nested PCR seems to be more sensitive than real-time PCR assay, however, real-time PCR assay is more rapid, labor-saving and can provide quantitative results with good repeatability and linearity. 。

Molecular Diagnosis

PL-09

The mutational spectrum of cancer-related genes from polyps to colorectal carcinoma by next generation sequencing

PL-09

Pi-Yueh Chang [1,2], Nai-Chung Chang[1], Shih-Cheng Chang[1,2], Jinn-Shiun Chen[3], Jang-Jih Lu[1]

[1]Department of Laboratory Medicine, Chang Gung Memorial Hospital at Linkou, Taoyuan, Taiwan,
[2]Department of Medical Biotechnology and Laboratory Science, Chang Gung University, Taoyuan, Taiwan, Taiwan,
[3]Department of Colorectal Surgery, Chang Gung Memorial Hospital at Linkou, Taoyuan, Taiwan

Introduction

Colorectal cancer (CRC) arises from the transition of normal epithelium to adenoma and then to carcinoma. The tumor progression model is associated with accumulated acquired DNA mutation from *APC, KRAS, TP53* and to other genes. Next generation sequencing (NGS) grant the opportunities to resequence these genes simultaneously in a cost effective manner and unveil their roles in carcinogenesis. We aim to investigate the mutational spectrum and elucidate the role of each gene on malignancy transformation.

Material and Methods

- **FFPE samples**
  - Group 1 non-neoplastic polyps: n=18 (including hyperplasia, adenomatous and tubular adenoma with diameter < 1 cm)
  - Group 2 neoplastic polyps: n=15 (tubular polyps with diameter ≧1cm, tubulovillous, and villous adenomatous polyps)
  - Group 3 adenocarcinoma: n=6 (High-grade hyperplasia or Tis)
- **DNA extraction**
  - DNA were extracted from 5 sections (10 μm/section) FFPE tissue by GeneRead™ DNA FFPE kit
- **Next generation sequencing**
  - Sequencing by AmpliSeq Cancer Hotspot Panel v2 and Ion Torrent PGM platform
  - Variant calling and annotation were conducted by Torrent Suits 4.2 and Vanno pipeline

Study design flowchart

Polyps FFPE tissue (n=39)
(1055 variants)
↓
Panel: Ampliseq cancer hotspot panel V2 (50 genes, 2855 hotspots)
Massively parallel sequencing: Ion Torrent PGM
↓
Data filtering
Variant effect: nonsynonymous or frameshift or stopgain
Region type: exonic
dbSNP-Asian Variant frequency <3%
Mutation Variant frequency > 10% and Variant coverage >30
Q-value>20, Filter sequencing artifact
↓
53 variants (37 type)
↓ Confirmed by Sanger or pyrosequencing
Reported variants

PL-09

Results

1 Germline and somatic variants detected in 39 polyps and carcinoma FFPE samples

53 variants (37 types) distributed on 12 genes were found in 27 samples (69%, 27/39). Two variants with 50% frequency were designated as germline mutations, the rest were somatic ones. Among somatic mutations, 5 were novel variants. Average number of variants in three groups were 0.6, 1.7 and 2.3 respectively. High intra- and inter-specimen heterogeneity were found.

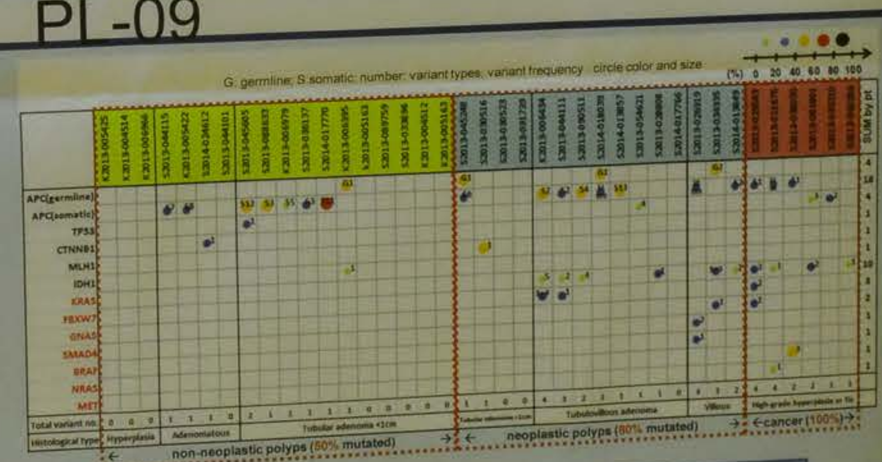

2 Somatic mutational progression from benign polyps to cancer

Among the 5 most frequently mutated genes, *APC* and *TP53* mutation occurred in whole carcinogenesis of colorectal cancer. Interestingly, mutation in *FBXW7, GNAS* and *KRAS* genes were only observed in neoplastic polyps and cancer tissues but none in non-neoplastic samples.

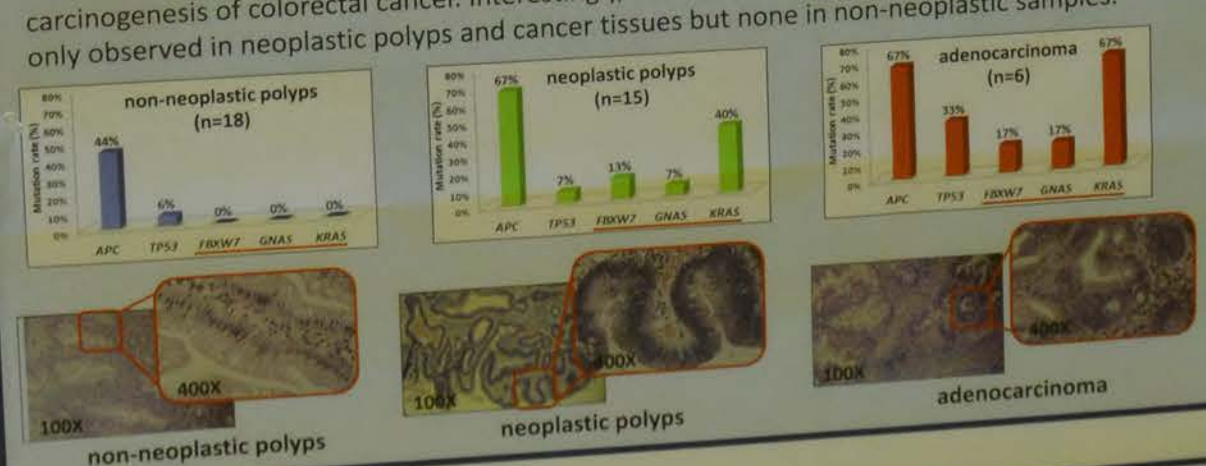

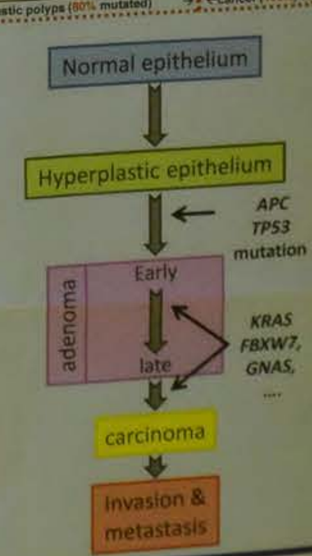

Conclusion

1 Panel based sequencing data provide direct evidence that the earliest event in the colorectal cancer progression involves the mutation of tumor suppressor genes, especially on *APC* gene. Acquiring and accumulating more somatic mutations on specific genes such as *KRAS* is essential for malignant transformation.

2 Characterization of the presence of mutational alleles across the carcinogenesis pathway helps us to stratify patients at risk to develop cancer and to design possible intervention strategies .

...or quantitation of human ...PV) 16, 18, 33 and 45.

...arsson and Gisela Helenius.
...y of Medicine and Health, Örebro University, SE-
...larsson@regionorebrolan.se

The equation of the standard curve is used to estimate cop... number from sample cycle Ct. HPV16 copy number ddPC... results were compared to real-time PCR results

Results

Method validation of ddPCR showed an intra-assa... precision between 0.2 % and 12.2 % (HPV18 and HPV3... respectively), while inter-assay precision was somewh... higher; 0.1-14.6 % (HPV33 and HPV45). Limit of detectio... was between 0.08 and 0.23 copies/µl. Viral load in 20 ng ... input DNA varied between 154 and 340 200 copies f... HPV16, between 12 and 1565 copies for HPV18 ar... between 36 and 3455 copies for HPV33, table 1.

Table 1. Viral load (copies in 20 ng DNA) in FFPE HPV-positive samples.

Genotype	n	Min	Max	Mean	Median	SD
HPV16	33	154	340 200	29 424	2820	71 28...
HPV18	4	12	1565	544	300	726
HPV33	4	36	3455	1499	1253	1464
HPV45	1	67	67	67	67	N/A

Corresponding values of HPV copies/cell was between 0.2 to 573 in samples positive for HPV16, between 1.8 and 68 for HPV18, between 3 and 506 for HPV33 and 0.3 for HPV45-positive samples.
A strong correlation between methods for viral load (HPV was found, Pearson; r = 0.99, p=0.000 (n= 33). However, copy numbers using ddPCR were consistently lower compared to real-time PCR data.

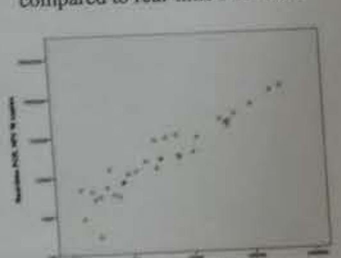

Figure 2. Correlation of realtime PCR viral load data to ddPCR viral load data for HPV 16.

Conclusion

Droplet Digital PCR (ddPCR) provides a new promising tool for evaluating HPV viral load in FFPE samples.

Örebro University
Region Örebro County
Örebro University Hospital

Molecular Diagnosis

PL-10

Evaluating diagnos... A(H1N1)pdm09 virus in the...

Why does virus culture have an unusually low sensitivity?

- Among aforementioned 11 real-time RT-PCR positive but virus-culture negative cases, 6 of 11 (or 54.5%) were treated with Oseltamivir or Zanamivir before clinical specimens collected, and 8 of 11 (or 72.7%) with lower viral load which threshold cycle values is greater than 32, as shown in Table 3.
- Routine assays needed a minimum number of viable virus particles in clinical samples. Low sensitivity of virus culture might result from a lack of viral viability before laboratory testing due to improper storage [3].
- Strategies of clinical medication in the 2015/2016 outbreak were different from in 2009's pandemic. Patients with severe symptoms were administrated with antiviral drug before their samples collected. In this circumstance, assays that are able to detect viral nucleic acid, without requiring viable viruses, offers a great advantage. [4]

Table 3 : 11 real-time RT-PCR positive, but virus-culture negative cases

Conclusions

- Viable influenza virus, residual RNA fragment and neuraminidase inhibitor (NAI) treatment are all factors that affected diagnostic test result of influenza virus infections, although virus culture was a gold standard for detecting viable virus and RIAT was useful for rapidly screening purpose.
- In the current study, we suggested that real-time RT-PCR offered a better sensitivity than RIDT and virus culture for confirming virus infections and for following-up patients with severe syndromes ; in particular, those with suspected influenza infections after NAI treatment in the outbreak season.

REFERENCES

Molecular Diagnosis

PL-10

Evaluating diagnostic methods of influenza A(H1N1)pdm09 virus in the 2015/2016 season

Shuan Yang[1], Kuo-Chien Tsao[1,2,3], Yu-Nong Gong[1], Hsin-Yao Wang[1], Shu-Li Yang[1,2], Ya-jhu Lin[1], Pi-Yueh Chang[1,2]

[1] Department of Laboratory Medicine, Linkou Chang Gung Memorial Hospital, Taoyuan, Taiwan
[2] Department of Medical Biotechnology and Laboratory Science, College of Medicine, Chang Gung University, Taoyuan, Taiwan
[3] Research Center for Emerging Viral Infections, College of Medicine, Chang Gung University, Taoyuan, Taiwan

Background

- In 2009, a novel influenza A(H1N1)pdm09 virus (designated as H1N1pdm09) emerged, with at least 18,449 deaths reported as of August 2010 [1]. While H1N1pdm09 was no longer a pandemic virus, this virus has become seasonal virus to circulate around the world [2].
- In Taiwan, an H1N1pdm09 outbreak caused severe clinical disease in the 2015/2016 season, resulting in a high mortality rate.
- Diagnostic methods currently were used for detection of influenza viruses in clinical laboratories, which included the rapid influenza diagnostic test (RIDT), viral culture, enzyme immunoassay and molecular tests such as real-time reverse-transcription polymerase chain reaction (real-time RT-PCR). It was needed for a sensitive, rapid and cost-effective assay to detect, type and sub-type influenza viruses, contrasting to cell culture method with a long turnaround time.

Objectives

In an outbreak season, a rapid and accurate diagnosis test for H1N1pdm09 became an important role for epidemiological and therapeutic purposes. Our aim was to evaluate an appropriate method for influenza virus detection by comparing RIDT, virus culture and real time RT-PCR.

Methods

Specimens

- We analyzed diagnostic results from influenza-like illness patients in Linkou Chang Gung Memorial Hospital from December 2015 to February 2016. 4727 respiratory specimens were examined by RIDT, 854 by real-time RT-PCR and 1041 by virus culture.

Influenza Diagnostic Rapid Test

- RIDT was performed by using Formosa One Sure Flu A/B Rapid Test kit(card) of Formosa Biomedical Technology Corporation.

Virus isolation

- Madin-Darby Canine Kidney (MDCK) cell or R-Mix cell shell vial (R-Mix SV, DHI, USA) was used for influenza viral isolation.

Real-time Reverse transcription polymerase chain reaction

- RNA extraction was performed by using 300 µl of sample and the Labturbo Virus mini kit (Taigen Bioscience, Taiwan). Specific primers was used to detect and type of influenza viruses targeting amplification of matrix protein, and to sub-type H1N1 and H3N2 targeting hemagglutinin (HA) and neuraminidase (NA) proteins.

Result

The sensitivity and specificity of real-time RT-PCR comparing to virus culture and RIDT

- When referenced to real-time RT-PCR of 102 cases, RIDT exhibited a sensitivity and specificity of 45.1% and 94.5%, respectively, and of 50.0% and 98.8% for virus culture, respectively, as shown in Tables 1 and 2.
- Among 102 samples examined by both RT-PCR and virus culture, 11 of 22 (or 50.0%) RT-PCR positive cases were virus-culture negative; on the contrary, only one of 12 (or 8.3%) virus-culture positive cases was RT-PCR negative, as shown in Table 2. Virus culture had an unusually low sensitivity of 50.0% compared with 2009's pandemic.

Table 1 ： 463 cases examined by real-time RT-PCR and RIDT

	Real-time RT-PCR	
RIDT	TP = 46	FP=20
	FN = 56	TN=341
	SS = 45.1%	SP=94.5%

True positive=TP; True negative=TN; False positive=FP; False negative=FN; Sensitivity=SS; Specificity=SP

Table 2 ： 02 cases examined by real-time RT-PCR and virus culture

	Real-time RT-PCR	
Virus culture	TP = 11	FP=1
	FN = 11	TN=79
	SS = 50.0%	SP=98.8%

Why does virus culture have an unusually low sensitivity?

- Among aforementioned 11 real-time RT-PCR positive but virus-culture negative cases, 6 of 11 (or 54.5%) were treated with Oseltamivir or Zanamivir before clinical specimens collected, and 8 of 11 (or 72.7%) with lower viral load which threshold cycle values is greater than 32, as shown in Table 3.
- Routine assays needed a minimum number of viable virus particles in clinical samples. Low sensitivity of virus culture might result from a lack of viral viability before laboratory testing due to improper storage [3].
- Strategies of clinical medication in the 2015/2016 outbreak were different from in 2009's pandemic. Patients with severe symptoms were administrated with antiviral drug before their samples collected. In this circumstance, assays that are able to detect viral nucleic acid, without requiring viable viruses, offers a great advantage. [4]

Table 3 ： 11 real-time RT-PCR positive, but virus-culture negative cases

CASE NO	PCR-SPECIMEN TYPE	Ct	VIRUS CULTURE-SPECIMEN TYPE	SEVERE/NON-SEVERE	SPECIMEN COLLECTED	ANTIVIRUS	ANTIVIRUS INITIAL DATE	Adm before Collect
1	TH	33.2	TH	NON-SEVERE	20160120	Oselt	20160120	N
2	TH	33.7	TH	NON-SEVERE	n/a	n/a	n/a	N
3	TH	35.5	TH	SEVERE	20160220	Oselt	20160220	N
4	BAL	33.5	BAL	SEVERE	20160126	Oselt	20160129	N
5	SP	32.4	TH	SEVERE	20160218	Oselt	20160217	Y
6	TH	28.8	TH	SEVERE	20160122	Oselt	20160121	Y
7	TH	32.9	TH	SEVERE	20160220	Oselt	20160218	Y
8	TH	33.8	TH	SEVERE	20160223	Zana	20160222	Y
9	NP	36.2	NP	NON-SEVERE	20160225	Zana	20160223	Y
10	SP	25.1	TH	SEVERE	20160202	Oselt	20160202	N
11	TH	27.2	TH	SEVERE	20160203	Oselt	20160202	Y

TH= throat swab; BAL= Bronchoalveolar lavage; NP= Nasopharyngeal swab; SP= sputum; Oseltamivir=Oselt; Zanamivir=Zana; CT=Threshold cycle

Conclusions

- Viable influenza virus, residual RNA fragment and neuraminidase inhibitor (NAI) treatment are all factors that affected diagnostic test result of influenza virus infections, although virus culture was a gold standard for detecting viable virus and RIAT was useful for rapidly screening purpose.
- In the current study, we suggested that real-time RT-PCR offered a better sensitivity than RIDT and virus culture for confirming virus infections and for following-up patients with severe syndromes ; in particular, those with suspected influenza infections after NAI treatment in the outbreak season.

REFERENCES

1. World Health Organization. Pandemic (H1N1) 2009-Update 112, 6 August 2010. Available from: http://www.who.int.csr/don/2010_08_06/en/index.hmt [Last accessed on 2011 Oct 12].
2. World Health Organization. Global alert and response (GAR) (2011). Summary review of the 2010-2011 northern hemisphere winter influenza season. Available from: http://www.who.int/influenza/surveillance_monitoring/2010_2011_GIP_surveillance_seasonal_review/en/. [Last accessed on 2012 Aug 28].
3. Cherian T, Bobo L, Steinhoff MC, Karron RA, Yolken RH. Use of PCR-enzyme immunoassay for identification of influenza A virus matrix RNA in clinical samples negative for cultivable virus. J Clin Microbiol 1994;32:623-8.
4. Claas EC, van Milaan AJ, Sprenger MJ, Ruiten-Stuiver M, Arron GI, Rothbarth PH, *et al*. Prospective application of reverse transcriptase polymerase chain reaction for diagnosing influenza infection in respiratory samples from a children's hospital. J Clin Microbiol 1993;31:2218-21.

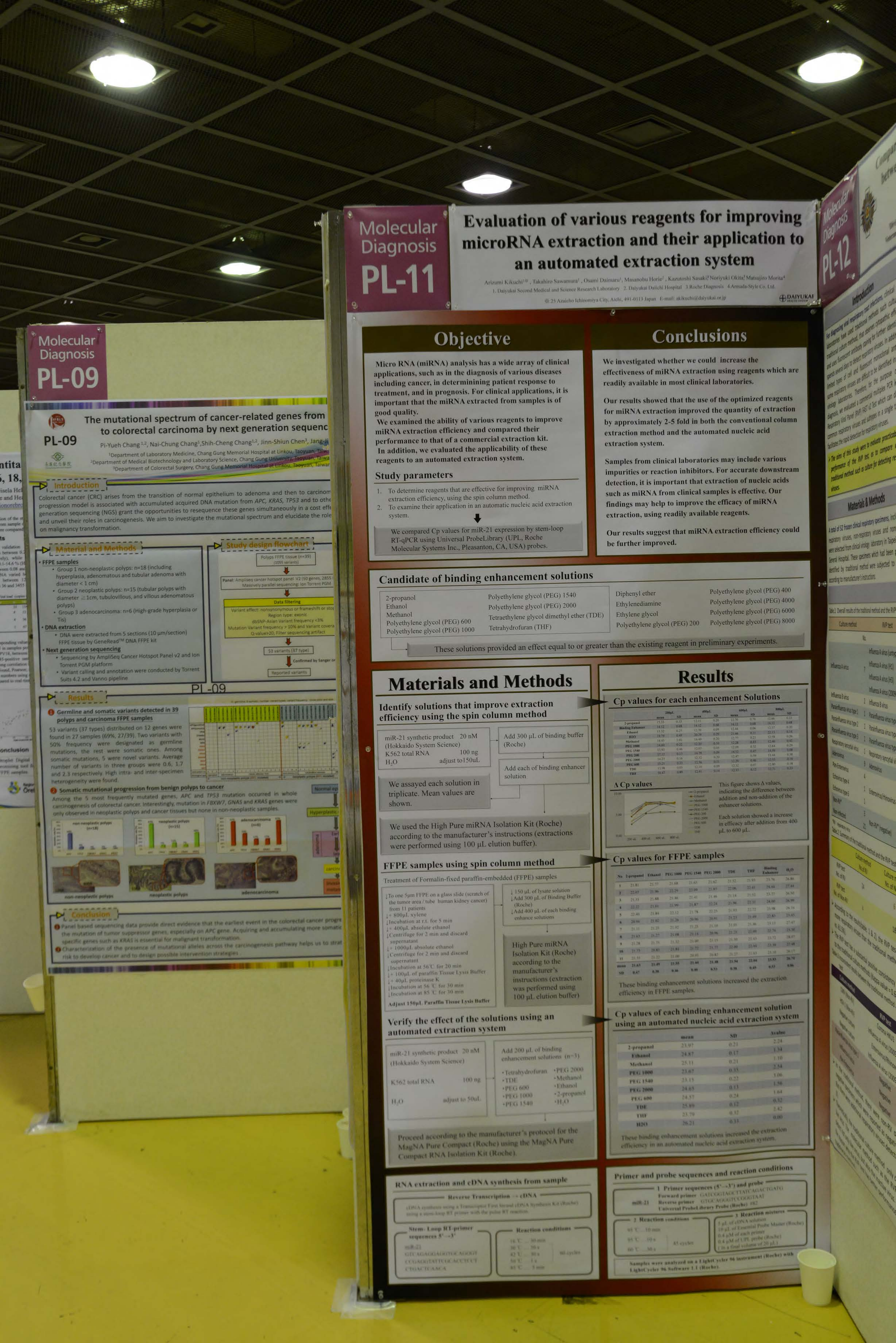

Molecular Diagnosis
PL-11
Evaluation of various reagents for improving microRNA extraction and their application to an automated extraction system
Arizumi Kikuchi, Takahiro Sawamura, Osami Daimaru, Masanobu Horie, Kazutoshi Sasaki, Noriyuki Okita, Matsujiro Morita
1. Daiyukai Second Medical and Science Research Laboratory 2. Daiyukai Daiichi Hospital 3. Roche Diagnosis 4. Armada-Style Co. Ltd.
25 Azaicho Ichinomiya City, Aichi, 491-0113 Japan E-mail: akikuchi@daiyukai.or.jp
DAIYUKAI
Objective
Micro RNA (miRNA) analysis has a wide array of clinical applications, such as in the diagnosis of various diseases including cancer, in determinining patient response to treatment, and in prognosis. For clinical applications, it is important that the miRNA extracted from samples is of good quality.
We examined the ability of various reagents to improve miRNA extraction efficiency and compared their performance to that of a commercial extraction kit.
In addition, we evaluated the applicability of these reagents to an automated extraction system.
Study parameters
1. To determine reagents that are effective for improving miRNA extraction efficiency, using the spin column method.
2. To examine their application in an automatic nucleic acid extraction system.
We compared Cp values for miR-21 expression by stem-loop RT-qPCR using Universal ProbeLibrary (UPL, Roche Molecular Systems Inc., Pleasanton, CA, USA) probes.
Conclusions
We investigated whether we could increase the effectiveness of miRNA extraction using reagents which are readily available in most clinical laboratories.
Our results showed that the use of the optimized reagents for miRNA extraction improved the quantity of extraction by approximately 2-5 fold in both the conventional column extraction method and the automated nucleic acid extraction system.
Samples from clinical laboratories may include various impurities or reaction inhibitors. For accurate downstream detection, it is important that extraction of nucleic acids such as miRNA from clinical samples is effective. Our findings may help to improve the efficacy of miRNA extraction, using readily available reagents.
Our results suggest that miRNA extraction efficiency could be further improved.
Candidate of binding enhancement solutions
2-propanol
Ethanol
Methanol
Polyethylene glycol (PEG) 600
Polyethylene glycol (PEG) 1000
Polyethylene glycol (PEG) 1540
Polyethylene glycol (PEG) 2000
Tetraethylene glycol dimethyl ether (TDE)
Tetrahydrofuran (THF)
Diphenyl ether
Ethylenediamine
Ethylene glycol
Polyethylene glycol (PEG) 200
Polyethylene glycol (PEG) 400
Polyethylene glycol (PEG) 4000
Polyethylene glycol (PEG) 6000
Polyethylene glycol (PEG) 8000
These solutions provided an effect equal to or greater than the existing reagent in preliminary experiments.
Materials and Methods
Identify solutions that improve extraction efficiency using the spin column method
miR-21 synthetic product 20 nM (Hokkaido System Science)
K562 total RNA 100 ng
H2O adjust to150uL
Add 300 μL of binding buffer (Roche)
Add each of binding enhancer solution
We assayed each solution in triplicate. Mean values are shown.
We used the High Pure miRNA Isolation Kit (Roche) according to the manufacturer's instructions (extractions were performed using 100 μL elution buffer).
FFPE samples using spin column method
Treatment of Formalin-fixed paraffin-embedded (FFPE) samples
To one 5μm FFPE on a glass slide (scratch of the tumor area / tube human kidney cancer) from 11 patients
+ 800μL xylene
Incubation at r.t. for 5 min
+ 400μL absolute ethanol
Centrifuge for 2 min and discard supernatant
+ 1000μL absolute ethanol
Centrifuge for 2 min and discard supernatant
Incubation at 56℃ for 20 min
+ 100μL of paraffin Tissue Lysis Buffer
+ 40μL proteinase K
Incubation at 56 ℃ for 30 min
Incubation at 85 ℃ for 30 min
Adjust 150μL Paraffin Tissue Lysis Buffer
150 μL of lysate solution
Add 300 μL of Binding Buffer (Roche)
Add 400 μL of each binding enhance solutions
High Pure miRNA Isolation Kit (Roche) according to the manufacturer's instructions (extraction was performed using 100 μL elution buffer)
Verify the effect of the solutions using an automated extraction system
miR-21 synthetic product 20 nM (Hokkaido System Science)
K562 total RNA 100 ng
H2O adjust to 50uL
Add 200 μL of binding enhancement solutions (n=3)
•Tetrahydrofuran •TDE •PEG 600 •PEG 1000 •PEG 1540 •PEG 2000 •Methanol •Ethanol •2-propanol •H2O
Proceed according to the manufacturer's protocol for the MagNA Pure Compact (Roche) using the MagNA Pure Compact RNA Isolation Kit (Roche).
RNA extraction and cDNA synthesis from sample
Reverse Transcription → cDNA
Stem-Loop RT-primer sequences 5'→3'
Reaction conditions
Results
Cp values for each enhancement Solutions
Δ Cp values
This figure shows Δ values, indicating the difference between addition and non-addition of the enhancer solutions.
Each solution showed a increase in efficacy after addition from 400 μL to 600 μL.
Cp values for FFPE samples
These binding enhancement solutions increased the extraction efficiency in FFPE samples.
Cp values of each binding enhancement solution using an automated nucleic acid extraction system
These binding enhancement solutions increased the extraction efficiency in an automated nucleic acid extraction system.
Primer and probe sequences and reaction conditions
1 Primer sequences (5'→3') and probe
miR-21
2 Reaction conditions
3 Reaction mixtures
Samples were analyzed on a LightCycler 96 instrument (Roche) with LightCycler 96 Software 1.1 (Roche).
Molecular Diagnosis
PL-09
The mutational spectrum of cancer-related genes from to colorectal carcinoma by next generation sequenc
Pi-Yueh Chang, Nai-Chung Chang, Shih-Cheng Chang, Jinn-Shiun Chen, Jang-Ji
Introduction
Material and Methods
Study design flowchart
Results
Conclusion
Molecular Diagnosis
PL-12
Introduction
Materials & Methods

Molecular Diagnosis

PL-12

Comparing respiratory viral identification efficacy between traditional culture methods and RVP

Chia-Lin Lee[1], Wen-Sung Weng[1], Yu-Han Huang[1], Huei-Yuan Lee[1], Pao-Chu Chiu[1], Yu-Jiun Chan[1,2]

[1]Division of Microbiology, Department of Pathology & Laboratory Medicine, Veterans General Hospital; and [2]National Yang-Ming University, Taipei, TAIWAN

Introduction

For diagnosing viral respiratory tract infections, clinical virology laboratories have used traditional methods such culture. The traditional culture method, that observes cytopathic effect(CPE) and uses fluorescent antibody staining for further identification, spends several days to detect respiratory viruses. In addition, the limited types of cell and fluorescent monoclonal antibodies, some respiratory viruses are difficult to be identified in general virology laboratories. Therefore, for the purpose of rapid diagnosis, we evaluated a commercial multiplex PCR kit, xTAG Respiratory Viral Panel (RVP) FAST v2 Test which can detect 16 common respiratory viruses and subtypes in a single test. This facilitates the rapid detection for respiratory viruses.

➢ ***The aims of this study were to evaluate practicability and performance of the RVP test, as to compare with the traditional method such as culture for detecting respiratory viruses.***

Materials & Methods

A total of 52 frozen clinical respiratory specimens, including the respiratory viruses, non-respiratory viruses and non-infected, were selected from clinical virology laboratory in Taipei Veterans General Hospital. These specimens which had been previously identified by traditional method were subjected to RVP test according to manufacturer's instructions.

The xTAG Respiratory Viral Panel (RVP) FAST v2 Test (Luminex®) is a qualitative nucleic acid multiplex test intended for the simultaneous detection and identification of multiple respiratory viruses. The virus types and subtypes detected by RVP FAST v2 are influenza A (H1/H3/2009H1N1), influenza B, respiratory syncytial virus, parainfluenza virus (subtype 1/2/3/4), adenovirus, human metapneumovirus, enterovirus/rhinovirus, human bocavirus, coronavirus (299E/OC43/NL63/HKU1).

☐ **The xTAG RVP FAST v2 Technology：**

A. Nucleic acid extraction (QIAGEN QIAamp®)

B. Multiple target specific RT-PCR amplification

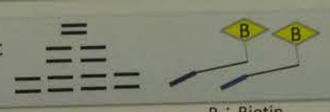

B：Biotin

C. Beads hybridization

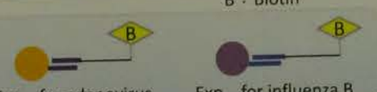

D. Detection

SAPE：Streptavidin-phycoerythrin

E. Analysis (Luminex®)

Results

Table.1 Overall results of the traditional method and the RVP test

Culture method		RVP test	
	No.		No.
Influenza A virus	7	Influenza A virus (untype)	0
		Influenza A virus (H1)	0
		Influenza A virus (H3)	0
		Influenza A virus (2009H1N1)	8
Influenza B virus	2	Influenza B virus	4
Parainfluenza virus type 1	1	Parainfluenza virus type 1	0
Parainfluenza virus type 2	1	Parainfluenza virus type 2	1
Parainfluenza virus type 3	1	Parainfluenza virus type 3	1
Respiratory syncytial virus	1	Respiratory syncytial virus	1
Adenovirus	9	Adenovirus	9
Pan-Enterovirus	4		
Echovirus type 4	1	Enterovirus/rhinovirus	8
Echovirus type 6	1		
Non-RV*	3	Non-RV* (negative)	18
Non-infected	21		

*RV：respiratory virus

Table.2 Summary of the traditional method and the RVP test

	Culture method No.of RV	Culture method No. of Non-RV
RVP test No. of RV	24	6
RVP test No. of Non-RV	4	18

➢ According to the results(table. 1 & 2), the RVP test detected more respiratory viruses than the traditional method. (53.8% vs. 61.5%).

➢ The RVP test has a substantial positive consistency compared to the traditional culture methods (Kappa value = 0.688).

Table.3 Inconsistent results between the traditional method and the RVP test

Culture method	RVP test
CMV (Non-RV)	Corona HKU1
HSV-1 (Non-RV)	Influenza A virus (2009H1N1)
Negative culture	Enterovirus/Rhinovirus
Negative culture	Influenza A virus (2009H1N1)
Parainfluenza virus type 1	Negative
Influenza A virus	Negative
Pan-Enterovirus	Negative

➢ In the traditional method, there were non-RV or culture-negative specimens which were reported as negative results. But there were additional respiratory viruses detected. (table. 3)

➢ Theoretically, the traditional culture method only can detect live virus. The molecular method such as the RVP test can detect not only live virus, but also the inactive virus. It may be the reason why the RVP test has better performance than the traditional method.

➢ There were 4 samples have been cultured respiratory viruses, but were reported as negative results in RVP test. (table. 3). We thought that RNA viruses were difficult to preserve for a long time, and RNA was easy to degrade, therefore using fresh specimen maybe better.

Table.4 Co-infecting viruses detected by the RVP test

Culture method	Co-infecting virus detected by the RVP test
Herpes simplex virus type 1	Influenza A virus (2009H1N1) (HSV is not included)
Herpes simplex virus type 1	Enterovirus/rhinovirus (HSV is not included)
Adenovirus	Adenovirus Enterovirus/rhinovirus
Pan-Enterovirus	Enterovirus/rhinovirus Influenza B virus
Echovirus type 6	Enterovirus/rhinovirus Influenza B virus
Cytomegalovirus	Coronavirus HKU1 (CMV is not included)

➢ There were 6 samples(11.5%) showed to be co-infections. Especially, in the traditional method, 2 samples were detected as HSV-1 and CMV, but were co-infected with respiratory virus in the RVP method.

➢ The cells, infected by HSV, were showed destructive cytopathic effect. Therefore, it is difficult to detect virus which produce cytopathic effect slowly. This may cause us to miss some important pathogenic infection.

➢ In addition, limited to cell types such as Vero cells and fluorescent monoclonal antibody which do not use in our laboratory, thus coronavirus can not be cultured.

Fig.1 The time spent on the traditional method and the RVP test

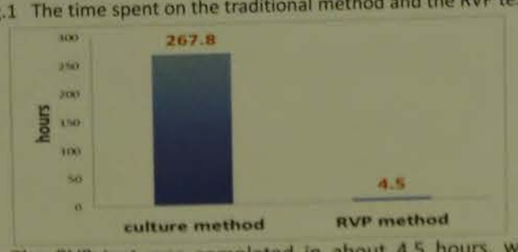

➢ The RVP test was completed in about 4.5 hours, while the traditional method required 11.1 days on average for identifying the respiratory virus.

➢ For rapid diagnosis of respiratory virus, the RVP test can be shorten 98.3% of the time.

Conclusion

➢ **The RVP test is convenient for rapid detection of respiratory virus and it can provide more detection for respiratory viruses, including co-infection, compared to the traditional method.**

➢ **The RVP molecular method may shorten the respiratory virus identification process and facilitate immediate diagnosis and provide timely information for appropriate treatment decisions.**

Molecular Diagnosis
PL-13

Molecular Diagnosis
PL-15

馬偕紀念醫院
MacKay Memorial Hospital

Evaluation of a RUO qPCR Assay for Detecting PML-RARα to Assist Diagnosis APL

- A case of developing a reliable process for extending RUO assay to assist diagnosis

Chun-Lan Lu[1], Yu-Ying Chiu[1], Tuan-Jen Wang[1], Chi-Kuan Chen[1,2]
Department of Laboratory Medicine[1] and Department of Pathology[2], Mackay Memorial Hospital, Taipei, Taiwan

ABSTRACT

To help the clinical physician in diagnosis of acute promyelocytic leukemia (APL), we develop the methods to assess the detection of PML-RARα of chromosome translocation t(15:17) (q22:q21) with Roche LightCycler 480 II LED and the LightMix PML-RAR t(15:17). For realizing the accuracy, specification, lowest detection limit, linearity and the reproducibility, the extraction control and the NB4 cell line with chromosome translocation were also set as control in the experiment. Results of DNA sequencing showed that the sequence of PML-RARα in NB4 cells was identical to reference sequence. Excellent linearity was valid with cloned PML-RARα plasmid, the detection limitation is 10 copies of target sequence, the linear range was from 10^2-10^6 copies (R^2=0.9921, CV is less than 3%). Another experiment, $10^{1.58}$-$10^{5.58}$copies of PML-RARα sequence with 10^3-10^5 copies of extraction control (Zebrafish qStandard) had been performed to check the interference of each other, and the results were not detected. At last stage, the method had been performed with clinical APL samples which had been verified by physician, showing the consistent results in 3 positive clinical samples. The data showed that have introduced a method for helping diagnosis of acute promyelocytic leukemia.

METHODS

The cDNA of PML-RAR t(15;17) was generated by LightMix PML-RAR t(15:17) kit and detected by LightCycler®480 II Instruments (Roche). To achieve our purpose, procedures were showed by following steps:

1. Accuracy: NB4 cell lines (including PML-RARα fusion gene) were used to perform conventional RT-PCR and sequencing analysis. (Table 1) Sequence identity was calculated by comparing the data from sequencing results with reference sequence (gbM73779).
2. Lowest detection limit (LOD): 10 copies of standard provided by LightMix PML-RAR t(15:17) kit was used to test the lowest detection limit.
3. Linearity: To generate high concentration of plasmid containing PML-RAR fusion gene, segment of PML-RAR in NB4 cells was amplified and cloned into plasmid. Plasmids were transformed into *E. coli* (DH5α) and then bacteria was cultured at 37℃ for 14 hours. 2 mL of bacteria was used to extract plasmid DNA by extraction kit to generated high concentration plasmid containing PML-RAR. High concentration plasmid was diluted by serial dilution ($10^{1.58}$ to $10^{6.58}$ copies) to evaluate linearity.
4. Reproducibility: 10^2-10^6 copies of standards in each run was used to calculate CV in log scale.
5. Examination of interference from extraction control (Zebrafish qStandard): Concentration of stock solution containing plasmid with PML-RAR fragment was $10^{6.58}$ copies/uL. Stock solution was diluted to $10^{5.58}$ copies/uL, $10^{4.58}$ copies/uL, $10^{3.58}$ copies/uL, $10^{2.58}$ copies/uL, $10^{1.58}$ copies/uL by 10-fold serial dilution. Each concentration of plasmid was mixed with 1ul of different concentration of Zebrafish qStandard (10^3 to 10^5 copies) in triplicate.
6. Clinical specimen tests: Blood specimens from 6 APL patients were used to evaluate the accuracy of this RUO qPCR assay for detecting PML-RARα.

Table 1. NB4 cell lines (including PML-RARα fusion gene) were used to perform conventional RT-PCR

Database references

Chromosome aberration	Gene	Name	Accession number	Date
t(15;17)	PML	HUMPML	M73779	8-Jan-95
	RARA	HSRAR	X06538	12-Sep-93

Primers for RT-PCR analysis of t(15;17)(q22;q21) with the PML-RARA fusion gene

Primer code	5' Position(size)	Sequence (5'–3')
PML-C1(Fwd)	1546 (21)	CAAGATGGAGTCTGAGGAGG
RARA-D(Rev)	426 (20)	CTGCTGCTCTGGGTCTCAAT

Figure 1. Linearity of real-time PCR assay for detection of PML-RARα

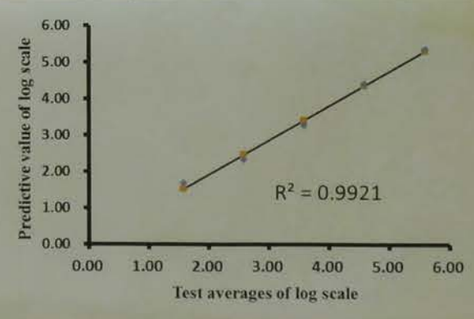

RESULTS

Accuracy: Sequence of PML-RARα fusion gene in NB4 cell line was compared to reference sequence form NCBI (Sequence ID: gbM73779.1). The identity between these two sequences is 100%.

2.Lowest detection limitation: The total of 26 test results showed that calibrator containing 10 copies of target sequence can be detected. The lowest detection limit can be in accordance with the instruction which claim the LOD is 10 copies/reaction.

3.Linearity: The R^2 value is 0.9921 which is higher than 0.950. The results indicate that linearity is excellent. (Figure 1)

4.Reproducibility: 10^2 to 10^6 copies of standards in different batches and were detected by real-time PCR. CVs of each of copy number in log scale are less than 3%. (Table 2)

5.Examination of interference from extraction control (Zebrafish qStandard): Average values of CVs for different copies of PML-RARα DNA fragment in log scale are less than 0.5. Results from real-time PCR showed that there was no interfere when samples mixed with 10^4 to 10^5 copies of extraction control. We also mixed clinical samples with 10^4 or 10^5 copies of extraction control and detect target sequence in clinical samples.

6.Clinical specimen tests: 6 clinical specimen from patients were used. 3 of 6 samples from patients who would be confirmed as APL and were detected as positive results for PML-RAR, indicating that results from this assay were consistent with clinical diagnosis.

Table 2. Reproducibility of real-time PCR for detection of PML-RARα of each copy number

log copies of standards	2	3	4	5	6
1st	1.92	2.98	3.93	5.06	5.96
2nd	2.10	2.94	4.00	5.08	5.96
3rd	1.96	3.00	4.05	5.01	6.00
4th	1.98	3.03	3.98	5.02	5.99
5th	2.04	3.05	3.99	5.01	5.99
6th	2.00	2.91	4.00	5.00	6.00
7th	1.95	3.00	3.97	5.02	5.99
8th	2.03	3.01	4.02	5.01	5.99
9th	2.04	3.01	3.98	5.03	6.00
Mean	2.00	2.99	3.99	5.03	5.99
SD	0.05	0.04	0.03	0.03	0.02
CV	2.7%	1.4%	0.9%	0.5%	0.3%

DISCUSSION

We confirm the accuracy, specificity, lowest detection limitation, linearity and the reproducibility of RUO real-time PCR qualitative assay detecting PML-RARα by LightCycler® 480 II instrument. Furthermore, results from this assay are consist with clinical diagnosis of APL. Thus, We have evaluated reliability of this RUO assay which could help the clinical physician diagnose acute promyelocytic leukemia (APL). Because there were 3 clinical specimens used to evaluate the reliability of this assay, positive results should contain report notes: "Analytical use only."

D-2

Molecular Diagnosis

PL-16

Evaluation of mRNA Expression in different stages of Colon Cancer Cell Lines

(Colorectal Cancer Cell Lines regulated through mRNA expression of different signal transduction pathway)

Junn-Liang Chang[1], Hung-Sheng Shang[2], Cherng-Lih Perng[2], Ya-Ling Li[3], Jun-Yi Kao[3], Lei-Fa Chang[3]

[1]Department of Pathology and Laboratory Medicine, Taoyuan Armed Forces General Hospital, Taoyuan, Taiwan

[2]Division of Clinical Pathology, Tri-Service General Hospital, Department of Pathology, National Defense Medical Center, Taipei, Taiwan

[3]Asia Med Medical Reference Laboratory, Taipei, Taiwan

BACKGROUND

Colorectal cancer (CRC) is one of the most common cancers worldwide. In Taiwan, CRC is the third among the top ten leading causes of death and the top cancer by incidence. CRC originates from abnormal proliferation of epithelial cells and accumulation of many genetic aberrations, including activation of oncogenes and inactivation of tumor suppressor genes.

OBJECTIVE

To investigate the relation between stages of CRC cell lines and expression of different genes in signal transduction pathway.

MATERIAL AND METHOD

RNA was extracted from four cell lines Caco2, SW48, SW480, COLO205 that represent different stages of CRC using TRI-Reagent and stored at −80°C. Single-stranded cDNA was prepared using High-Capacity cDNA Archive Kit (Applied Biosystems). mRNA expression was quantified by real-time PCR on an Applied Biosystems StepOne™ Real-Time PCR System. To control between-sample variability, mRNA levels were normalized to GAPDH for each sample, and fold change was calculated using the relative quantification $2^{-(\Delta Ct)}$ method.

RESULT

In Caco2 and SW480, higher expression of *EGFR* and *SMAD4* that closely related with tumor cell proliferation and angiogenesis was found. SW48 revealed increased *CXCL3* mRNA expression relative comparison with other three CRC cell lines. mRNA expression of *PTEN* and *TGF*B in SW480 and COLO205 CRC cell lines are higher than CRC cell lines of the other two stages. The results indicate that the up-regulation of *PTEN* and *TGFB* may relate to colorectal cancer cell invasion and metastasis. However, *WNT1* and *WNT2* showed no significant difference of expression among these CRC cell lines, indicating that WNT signaling may regulate with other molecular mechanisms involved in whole colon tumorigenesis. Paired tissue RNA samples were analyzed the expression level of by real time reverse transcription-PCR. We observed increased *EGFR*, *CXCL3*, *TGFBR2* and *AKT1* relative gene expression in tumor tissue compared to adjacent normal tissue.

FIGURE 1

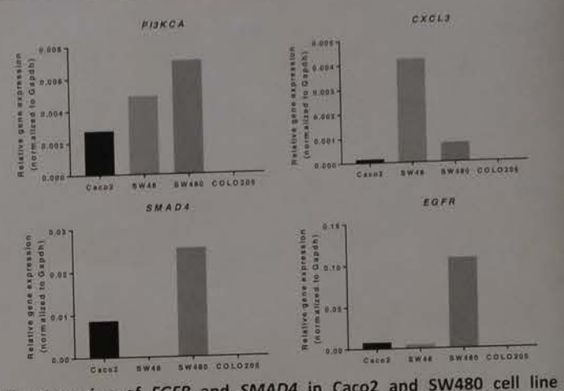

Up-expression of *EGFR* and *SMAD4* in Caco2 and SW480 cell line indicated these molecule upregulate initiated formation of colorectal cancer cell proliferation and angiogenesis. *GAPDH* was used as the endogenous control to allow for normalization between individual samples

FIGURE 2

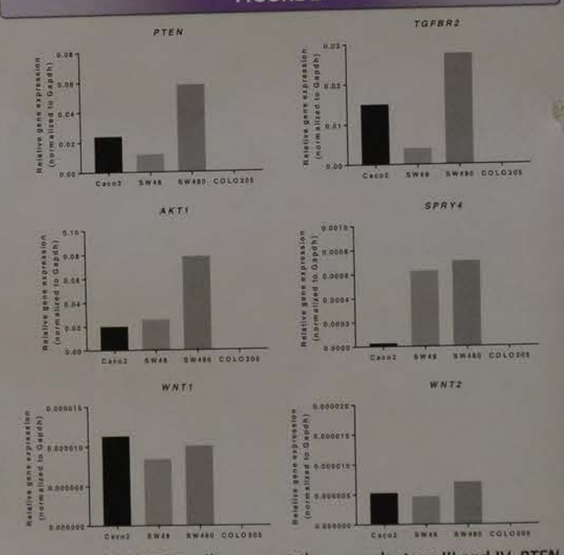

SW480 and COLO205 cell represent the cancer's stage III and IV. *PTEN* and *TGF*B show higher mRNA expression at these two stages CRC cell lines and perform closely related with invasion and metastasis. *GAPDH* was used as the endogenous control to allow for normalization between individual samples

FIGURE 3

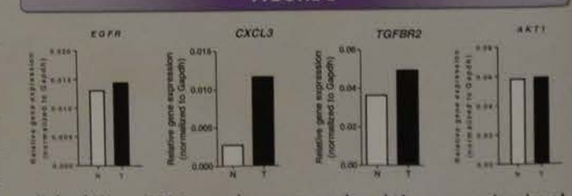

Paired tissue RNA samples were analyzed the expression level of *EGFR, CXCL3, TGFBR2* and *AKT1* by real time reverse transcription-PCR. These four gene expression are higher in tumor part compared with normal part tissue. *GAPDH* was used as the endogenous control to allow for normalization between individual samples. N mean the average of expression of 5 normal parts of tissue. T means the average of expression of 5 tumor parts of tissue.

CONCLUSION

These four stages of CRC cell lines are regulated through different signal pathway as EGFR, PTEN, TGFb and WNT signaling.

PI-15

Public Health

PI-16

Aiming at provision of quality healt
checkup services in a developing co
- Lessons learnt from Cambodia -

Molecular Diagnosis
PL-17

Molecular Diagnosis
PL-18

Evaluation of two real-time RT-PCR assays for detection of influenza virus

Shu-Yuan Ho[1], Kuo-Chen Weng[1], Chuan-Liang Kao[2]
Department of Laboratory Medicine, National Taiwan University Hospital, Taipei, Taiwan[1],
Department of Clinical Laboratory Sciences and Medical Biotechnology, National Taiwan University, Taipei , Taiwan[2]

Background & Aim

- Influenza viruses (Flu) and respiratory syncytial virus (RSV) are frequently causes upper and lower respiratory tract infections in adults and children.
- These infections often clinically misjudged as similar signs and symptoms.
- Monospecific real-time RT-PCR of viral identification is time-consuming and expensive, and so multiplex real-time RT-PCR has been developed.
- We aim to describe the performance of a multiplex real-time RT-PCR for detection of influenza virus and co-infection of RSV.

Materials and Methods

- Performance of RIDAGENE Flu&RSV was evaluated by comparing it to our in-house RT-qPCR, virus isolation (VI), and fluorescent immunoassay (FIA) for influenza virus assay on throat swab (TS) and sputum samples collected during an influenza season (Tab.1, January to March 2016).
- In-house RT-qPCR targeting the genes of influenza A (Flu A, M-gene) and influenza B (Flu B, NP1-gene), but commercial kit provides the ability of further genetic characterization of RSV (F-gene).
- We evaluated the performance of RIDAGENE Flu&RSV on the CFX96™ real-time system.

Results

- 30 respiratory samples tested with VI had 12 Flu positive (Flu A, n=3; Flu B, n=9) and 18 negatives (Tab.2, 6 VI negative were RIDAGENE Flu&RSV positive).
- 46 respiratory samples tested with FIA had 15 Flu positive (Flu A, n= 6; Flu B, n=5; Flu A&B, n=4) and 31 negatives (Tab.3, 6 FIA negative were RIDAGENE Flu&RSV positive).
- Compared to in-house RT-qPCR, RIDAGENE Flu&RSV tested on 50 respiratory samples submitted in the influenza season showed sensitivities of 100% (9/9) for FluA, 100% (9/9) for FluB (Tab.4).
- All specimens (32/32) that were negative by in-house RT-qPCR were Flu A/B negative by RIDAGENE Flu&RSV.
- Two RSV positive were detected in Flu A/B negative samples (6.25%, 2/32) by RIDA GENE Flu&RSV(Tab.5).

Conclusions

- The results indicate the performance of multiplex real-time RT-PCR kit is a precise tool to differentiate 2 viral infections.
- It is particularly suited to simultaneous screening of Flu and RSV during epidemic months.

Table 1. Total Flu testing for all subjects

Method	No. / Positive	No.	%
Virus isolation	12	30	40.0
Fluorescent immunoassay	15	45	33.3
In-house RT-qPCR	18	50	36.0
RIDAGENE Flu&RSV	18	50	36.0

Table.2: Correlation of Flu results with RIDAGENE Flu&RSV and VI

		Virus isolation (VI)		
		Positive	Negative	total
RIDAGENE Flu&RSV	Positive	11	6	17
	Negative	1	12	13
	total	12	18	30

Table.3: Correlation of Flu results with RIDAGENE Flu&RSV and FIA.

		Fluorescent immunoassay (FIA)		
		Positive	Negative	total
RIDAGENE Flu&RSV	Positive	9	6	15
	Negative	6	25	31
	total	15	31	46

Table.4: Correlation of Flu results with two RT-qPCR.

		In-house RT-qPCR		
		Positive	Negative	total
RIDAGENE Flu&RSV	Positive	18	0	18
	Negative	0	32	32
	total	18	32	50

Table.5: Differences between two RT-qPCR in 32 Flu negatives

In-house RT-qPCR						RIDAGENE Flu&RSV					
Flu A	Flu B	RSV	Results	No.	%	Flu A	Flu B	RSV	Results	No.	%
+	-	-	A[1]	9	18	+	-	-	A	9	18
-	+	-	B[2]	9	18	-	+	-	B	9	18
+	+	-	A/B[3]	0	0	+	+	-	A/B	0	0
-	-	+	RSV	n/a[4]	n/a	-	-	+	RSV	2	4
-	-	-	Neg.[5]	32	64	-	-	-	Neg.	30	60
			Total	50	100				Total	50	100

1, Flu A; 2, Flu B ; 3, combined Flu A and B; 4, Not applicable; 5, Negative

NTUH Care Outreach Research Education

Molecular Diagnosis

PL-19

Mutation Patterns to Rifampicin and Isoniazid of *M. tuberculosis* by GenoType MTBDRplus Test in Taiwan

Cherng-Lih Perng[1, 2], Yi-Hui Wang[1], Xin-Yi Zhong[1], Ming-Zhi Jian[1], Xiao-Wei Li[1], Tzong-Shi Chiueh[1]

[1]Division of Clinical Pathology, Department of Pathology, Tri-Service General Hospital;
[2]Graduate Institute of Pathology, National Defence Medical Center, Taipei, Taiwan

Introduction

The GenoType MTBDRplus line probe assay (LPA) is used for the rapid detection of Mycobacterium tuberculosis (MTB) complex and its associated susceptibilities to Rifampicin (RIF) and Isoniazid (INH) by detection of the most significant mutations of the rpoB, katG, and inhA genes. The resistance is interpreted by the loss of wild type probe's signal or the presence of mutant probe's signal.

The comparison between the interpretation of RIF and INH resistance by GenoType MTBDR*plus* molecular method and traditional drug susceptibility testing by cultural based method showed some inconsistences. We analyzed these different banding patterns to show that some special ones should be interpreted very carefully.

Materials and methods

A total of 6,810 sputum sediments collected from 4,175 cases from year 2012 to 2015 were tested by GenoType MTBDRplus assay compared with MTB traditional culture and drug susceptibility testing (DST) from patients who were belong to treatment loss, treatment failure, relapsed cases, and other high MTB Resistant Groups from hospitals all over in Taiwan.

Principle of GenoType MTBDRplus

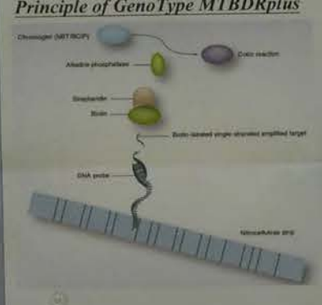

Nucleic acid extraction

Multiplex PCR amplification

Interpretation of hybridization banding patterns for GenoType MTBDRplus

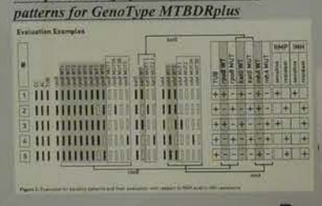

Susceptible pattern for RIF (rpoB) and INH (katG & inhA)

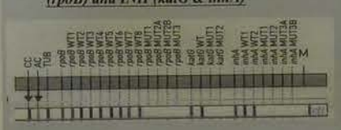

Results

Table 1: The results of GenoType MTBDRplus test from different special TB groups

AFB Stain	Special TB Groups	Samples	GenoType MTBDRplus Test: MTB detection Neg.	MTB detection Pos.	MTB detection Pos. rate	Resistance RIF	Resistance INH	Resistance RIF & INH (MDRTB)	Resistant rate
Smear (−)	Treatment failure	313	239	74	24%	3	13	1	23%
	Treatment loss	48	42	6	13%	0	0	0	0%
	Relapsed	791	734	57	7%	1	1	1	5%
	MDRTB Contacts	30	30	0	0%	0	0	0	-
	High risk group at mountain village	451	442	9	2%	0	1	0	11%
	Live more than 1 month at high-burden countries	0	0	0	-	0	0	0	-
Subtotal		1633	1487	146	9%	4	15	2	14%
Smear (+)	Treatment failure	2080	695	1385	67%	29	85	30	10%
	Treatment loss	80	22	58	73%	2	2	5	16%
	Relapsed	2310	1045	1265	55%	52	64	65	14%
	MDRTB Contacts	99	20	79	80%	7	5	37	62%
	High risk group at mountain village	370	95	275	74%	8	10	14	12%
	Live more than 1 month at high-burden countries	238	45	193	81%	6	14	12	17%
Subtotal		5177	1922	3255	63%	104	180	163	14%
Total		6810	3409	3401	50%	108	195	165	13%

Results

Table 2: RIF resistance with different rpoB patterns compared with traditional culture DST

Traditional culture	Mol. Method: GenoType MTBDR*plus* TB Positive & RIF resistant (*rpoB* mutation)	WT1(-)	WT2(-)	WT2,3(-)	WT2,3,4(-)	WT3,4(-)	WT3,4,7(-) /MUT2B(+)	WT5(-)
TB culture	RIF resistant	0	2	2	7	21	5	0
	RIF susceptible	0	9	0	0	0	0	5
	TB Negative	5	4	0	0	2	0	0
	NTM	0	2	0	0	0	0	0
Frequency		1.8%	6.2%	0.7%	2.6%	8.4%	1.8%	1.8%

Traditional culture	Mol. Method: GenoType MTBDR*plus* TB Positive & RIF resistant (*rpoB* mutation)	WT6(-)	WT7(-)	WT7(-) /MUT2A(+)	WT7(-) /MUT2B(+)	WT8(-)	WT8(-) /MUT3(+)	WT8(weak)	TB Neg. NA
TB culture	RIF resistant	5	0	14	5	18	127	0	21
	RIF susceptible	0	5	0	0	5	2	5	0
	TB Negative	0	0	5	0	0	12	4	0
	NTM	0	0	0	0	2	0	0	0
Frequency		1.8%	1.8%	7.0%	1.8%	9.2%	51.6%	3.3%	-

Table 3: INH resistance with different katG/inhA patterns compared with traditional culture DST

Traditional culture	Mol. Method: GenoType MTBDR*plus* TB Positive & INH resistant (*katG* or *inhA* mutation)	INH High conc.	INH Low conc.	katG wt(-) /MUT1(+)	katG wt(+) MUT1(+)	inhA WT1(-)	inhA WT1(-) /MUT1(+)	inhA WT2(-) /MUT3A(+)	inhA WT2(-) /MUT3B(+)	katG wt(-) /MUT1(+);inhA WT1(-) /MUT1(+)	Suscep-tible	TB Neg.
TB culture	R	R	127	7	0	36	7	0	6	32	5	
	S	R	0	0	5	25	0	0	0	37	10	
	-	R	2	0	0	7	0	0	0	0	0	
	S	S	0	0	0	2	0	0	0	0	0	
TB Negative			76	2	7	42	0	7	2	0	0	
Frequency			56.9%	2.5%	3.3%	31.1%	1.9%	1.9%	2.2%	-	-	

Figure 1: The hybridization strip pictures of different rpoB/katG/inhA patterns

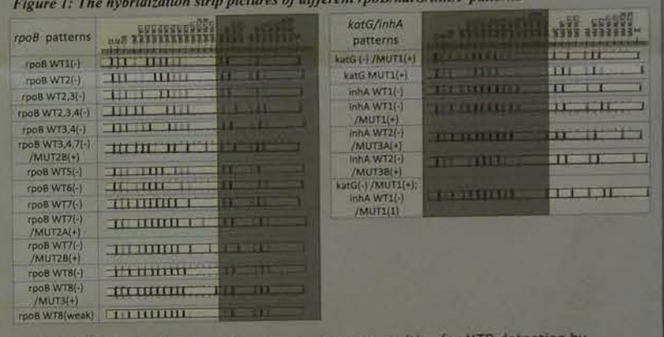

- About 50% (3,401/6,810) sputum specimens were positive for MTB detection by GenoType MTBDR*plus* assay (Table 1). But only 273 samples with *rpoB* gene variations (Table 2) and 360 samples with *katG*/*inhA* gene variations were interpreted as RIF or INH resistant (Table 3).
- The most frequent mutations in the rpoB gene were S531[WT8(-)/MUT3(+)] (51.6%), L533 [WT8(-)] (12.5%), D516 [WT3(-)/WT4(-)] (8.4%), H526 [WT7(-)/MUT2A(+)] (7%), and L511 [WT2(-)] (6.2%). The most frequent mutations in the katG/inhA genes were katG S315 [katG WT(-)/MUT1(+)] (56.9%) and inhA -15 [inhA WT1(-)/MUT1(+)] (31.1%).
- In 60.5% of rifampin resistant strains, there was also resistance to isoniazid. And 42.4% of isoniazid resistant strains, there was also resistance to rifampin. Therefore, in Taiwan the rifampin or isoniazid single resistance is not reliable marker for MDR strains of M. tuberculosis.
- In *rpoB* gene banding patterns (Figure 1), the loss of *rpoB* WT2, WT5, or WT7 probe only without mutant probe presentation showed all susceptible to RIF and the loss of *rpoB* WT2+3, WT2+3+4, WT3+4, WT6, or WT8 probe only without mutant probe presentation showed all resistant to RIF.
- In *katG*/*inhA* gene banding patterns, the loss of WT probe with or without mutant probe presentation showed all resistant to INH.

Conclusion

The GenoType MTBDR*plus* assay only screens the nucleic acid sequence and not the amino acid sequence. It is suggested that the DNA sequencing should be performed when only the wild type probe's signal is absent. The interpretation as resistant is more confident when mutant probe's signal is present. It should be very carefully interpreted the resistance of RIF or INH when only the wild type probe is absent.

There is no significant difference of the mutation patterns of rpoB, katG, and InhA genes found in Taiwan compared to other countries. The GenoType MTBDRplus assay could successfully detection of not only rifampin or isoniazid single resistance but also MDRTB strains.

References

1. Kambli P, et al. Defining multidrug-resistant tuberculosis: correlating GenoType MTBDRplus assay results with minimum inhibitory concentrations. Diagn Microbiol Infect Dis. 2015 Jan 29.
2. Singhai R, et al. Early detection of multi-drug resistance and common mutations in Mycobacterium tuberculosis isolates from Delhi using GenoType MTBDRplus assay. Indian J Med Microbiol. 2015 Feb;33 Suppl:46-52.

Molecular Diagnosis

PL-17

Evaluation of two real-time RT-PCR assay for detection of influenza virus

Shu-Yuan Ho[1], Kuo-Chen Weng[1], Chuan-Liang Kao[2]

Department of Laboratory Medicine, National Taiwan University Hospital, Taipei.
Department of Clinical Laboratory Sciences and Medical Biotechnology, National Taiwan Univ

Background & Aim

- Influenza viruses (Flu) and respiratory syncytial virus (RSV) are frequently causes upper and lower respiratory tract infections in adults and children.
- These infections often clinically misjudged as similar signs and symptoms.
- Monospecific real-time RT-PCR of viral identification is time-consuming and expensive, and so multiplex real-time RT-PCR has been developed.
- We aim to describe the performance of a multiplex real-time RT-PCR for detection of influenza virus and co-infection of RSV.

Materials and Methods

- Performance of RIDAGENE Flu&RSV was evaluated by comparing it to our in-house RT-qPCR, virus isolation (VI), and fluorescent immunoassay (FIA) for influenza virus assay on throat swab (TS) and sputum samples collected during an influenza season (Tab.1, January to March 2016).
- In-house RT-qPCR targeting the genes of influenza A (Flu A, M-gene) and influenza B (Flu B, NP1-gene), but commercial kit provides the ability of further genetic characterization of RSV (F-gene).
- We evaluated the performance of RIDAGENE Flu&RSV on the CFX96™ real-time system.

Results

- 30 respiratory samples tested with VI had 12 Flu positive (Flu A, n=3; Flu B, n=9) and 18 negatives (Tab.2, 6 VI negative were RIDAGENE Flu&RSV positive).
- 46 respiratory samples tested with FIA had 15 Flu positive (Flu A, n= 6; Flu B, n=5; Flu A&B, n=4) and 31 negatives (Tab.3, 6 FIA negative were RIDAGENE Flu&RSV positive).
- Compared to in-house RT-qPCR, RIDAGENE Flu&RSV tested on 50 respiratory samples submitted in the influenza season showed sensitivities of 100% (9/9) for FluA, 100% (9/9) for FluB (Tab.4).
- All specimens (32/32) that were negative by in-house RT-qPCR were Flu A/B negative by RIDAGENE Flu&RSV.
- Two RSV positive were detected in Flu A/B negative samples (6.25%, 2/32) by RIDA GENE Flu&RSV(Tab.5).

Conclusions

- The results indicate the performance of multiplex real-time RT-PCR kit is a precise tool to differentiate 2 viral infections.
- It is particularly suited to simultaneous screening of Flu and RSV during epidemic months.

Table 1. Total Flu testing for all subje

Method	No. / Positive
Virus isolation	12
Fluorescent immunoassay	15
In-house RT-qPCR	18
RIDAGENE Flu&RSV	18

Table.2: Correlation of Flu results wi and VI

		Virus isol
		Positive
RIDAGENE Flu&RSV	Positive	11
	Negative	1
	total	12

Table.3: Correlation of Flu results wi and FIA.

		Fluorescent (F
		Positive
RIDAGENE Flu&RSV	Positive	9
	Negative	6
	total	15

Table.4: Correlation of Flu results wi

		In-house
		Positive
RIDAGENE Flu&RSV	Positive	18
	Negative	0
	total	18

Table.5: Differences betv negatives

In-house RT-qPCR						
Flu A	Flu B	RSV	Results	No.	%	
+	-	-	A[1]	9	18	+
-	+	-	B[2]	9	18	-
+	+	-	A/B[3]	0	0	+
-	-	+	RSV	[illegible]	[illegible]	-
-	-	-	Neg.[5]	32	64	-
			total	50	100	

1, Flu A. 2, Flu B ; 3, combined Flu A a
5, Negative

Molecular Diagnosis PL-19

Molecular Diagnosis PL-20

Rapid screening of extended RAS mutations using BNA Real-Time PCR in colorectal cancer

Takao Iida[1)], Yukie Mizuno[1)], Yasuharu Kaizaki[2)]
1) Department of Clinical Laboratory, Fukui Prefectural Hospital
2) Department of Pathology, Fukui Prefectural Hospital

Background

RAS (KRAS and NRAS) testing is required to predict anti-EGFR treatment efficacy in advanced colorectal cancer (CRC). A diagnostic kit providing rapid and cost-effective method for identification of KRAS exons 2-4 and NRAS exons 2-4 mutations status would be clinically beneficial. We evaluated the BNA Real-Time PCR Mutation Detection Kit Extended RAS (Riken Genesis), a novel modification of the conventional real-time PCR method that selectivity amplifies minority RAS mutations by Bridged Nucleic Acid (BNA) clamping technology (Figure 1).

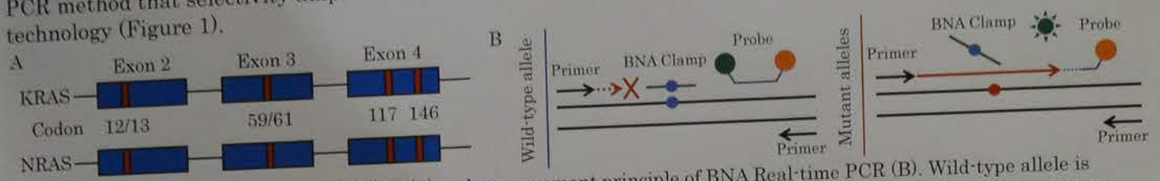

Figure 1. Measuring codons of extended RAS (A) and measurement principle of BNA Real-time PCR (B). Wild-type allele is suppressed PCR amplification by wild-type allele specific BNA clamp. Mutant alleles are amplified by PCR and fluorescence increases by cleaving the common probe of wild-type allele and mutant alleles.

Methods

- FFPE samples from 23 patients with histologically diagnosed CRC were used.
- Figure 2 shows RAS testing procedures using BNA Real-time PCR.
- The concordance rate between RAS mutations identified with the assay and reference assay of the KRAS Mutation Detection Kit (TrimGen) or the MEBGEN™ RASKET KIT (MBL).

Deparaffinized FFPE sample of tumor cells processed by manual micro-dissection

↓ QIAamp DNA FFPE tissue kit (Qiagen)

Rapid screening of RAS mutations

Genomic DNA

↓ BNA Real-time PCR Mutation Detection Kit Extended RAS (Riken Genesis)
↓ BNA Real-time PCR UNG (Uracil N-Glycosylase) (Riken Genesis)

BNA Real-time PCR
Running time: ~2 hours

StepOnePlus (Thermo Fisher Scientific)

Data analysis
Detection sensitivity: 1~5% mutant DNA in background of wild-type DNA

↓ Positive / Negative

Subsequent Sanger sequencing

Post-BNA Real-time PCR product

↓ QIAquick PCR Purification Kit (Qiagen)
↓ RAS Sequencing Primer Set Extended RAS (Riken Genesis)
↓ Big Dye® Terminator Cycle Sequencing kit v.3.1 (Thermo Fisher Scientific)

Cycle Sequencing reaction

↓ Big Dye® XTerminator™ Purification kit (Thermo Fisher Scientific)

Capillary electrophoresis

3500Dx Genetic Analyzer (Thermo Fisher Scientific)

Data analysis ····· Sequencing Analysis Software v.5.4 (Thermo Fisher Scientific)

Figure 2. RAS testing procedures. Rapid screening of RAS mutations and subsequent Sanger sequencing are indicated in the red and the blue square respectively.

Results

- Among 23 CRC samples, both the assay and the reference assay detected 10 RAS mutations (Table 1).
- Representative results of the detected RAS mutations in FFPE samples of CRC are shown in Figure 3.
- The between-method concordance rate of RAS mutation detection was 100% (Table 2). The results of RAS genotype were concordant between the assays.

Table 1. Frequency of RAS mutations in CRC.

RAS status		CDS mutation*	AA mutation*	No. of cases
KRAS	Exon 2			8 (34.8%)
	Codon 12	c.35G>A	p.G12D	1
		c.35G>T	p.G12V	3
		c.35G>C	p.G12A	1
	Codon 13	c.38G>A	p.G13D	3
	Exon 4			1 (4.3%)
	Codon 146	c.437C>T	p.A146V	1
NRAS	Exon 2			1 (4.3%)
	Codon 12	c.35G>A	p.G12D	1
Wild-type RAS				13
Overall				23

* CDS, coding DNA sequence; AA, amino acid

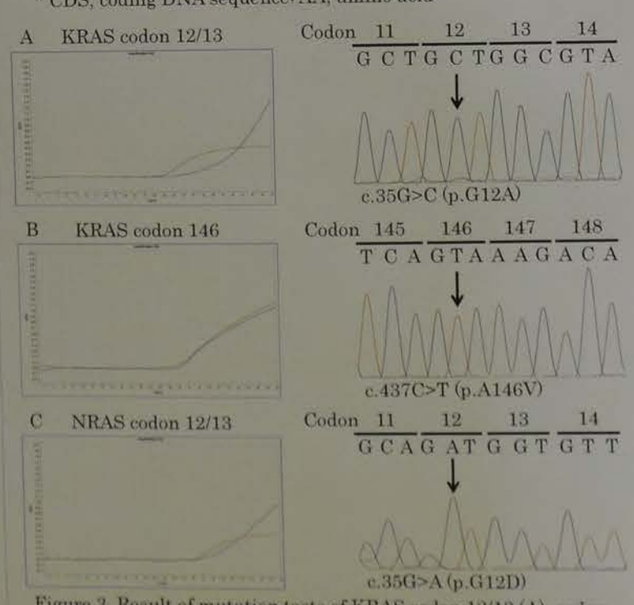

Figure 3. Result of mutation tests of KRAS codon 12/13 (A), codon 146 (B) and NRAS codon 12/13 (C). Each of the mutations were amplified by BNA Real-time PCR (blue line). The red line indicates the internal positive control. Subsequent Sanger sequencing identified the following specific nucleotide change (allows).

Table 2. Concordance of mutations detected with the assay versus the reference assay (n = 23).

Concordance		The reference assay		
		Positive	Negative	Total
The assay	Positive	10	0	10
	Negative	0	13	13
	Total	10	13	23

Overall percent agreement: 100%
Positive percent agreement: 100%
Negative percent agreement: 100%

Conclusions

The BNA Real-Time PCR Mutation Detection Kit Extended RAS will enable rapid screening of RAS mutations prior to anti-EGFR treatment in clinical setting.

Molecular Diagnosis PL-22

Impact of RNA amount on the efficacy of re… transcription
—Aiming at full-automatic quantification of leukemia genes tra…

Tsukimi SHOJI, Tamao WATANABE, Yuto KIDA, Nana KURODA, Yuko HISAM…
Atsumi ISHIDA, Miki NAGAO, Shuichi SHIGA, Satoshi ICHIYAMA
Department of Clinical Laboratory, KYOTO University Hospital

- The quantitative Reverse Transcription PCR (qRT-PCR) methods are generally used for … of leukemia gene transcripts like *WT1* mRNA.
- We evaluated the impact of amount of RNA on the quantification of *WT1* mRNA by qRT-…
- Our results indicate here that the RNA amount in RT does not make major impact on the … *WT1* mRNA for internal control gene *ABL1*.

Disclosure of Conflict of Interest : I have no COI with …

Introduction

Universal Quantitation Protocol for mRNA

Specimen
↓
…A Extraction
↓
…easurement of …A concentration
↓ qRT-PCR
…erse Transcription; RT (cDNA Synthesis)
↓
…al-time PCR

- The number of leukocytes is various.
- The quantity and concentration of RNA of each sample is different.
- Absorbance measurement isn't automated.
- 1 µg RNA is used for a RT reaction.

Is it possible that the broad range of RNA amount is available for RT reaction?

- Leukemia genes and internal control gene are amplified simultaneously.

…e broad range of RNA amount can be available for RT …ion, the measurement and preparation of RNA …entration are not necessary, and full-automatic …tificational approach will be facilitated.

Method

35 RNA Extracts

Reverse Tra…

1 µL RNA
3 µL RNA
5 µL RNA

SuperScript® VILO™ …
RNA
Nuclease-free Wate…

2 µL
↓
WT1-PCR

WT1 copy / AB…

Thirty five RNA samples were obtained f… and 8 peripheral blood of patients with A… transcription was performed with three … (1µl, 3µl, 5µl) for each RNA extract. *WT1* … control) were amplified from 2µL cDNA a… TaqMan real-time PCR system. The PCR re… 20µL.

Results

…RNA amount of each sample

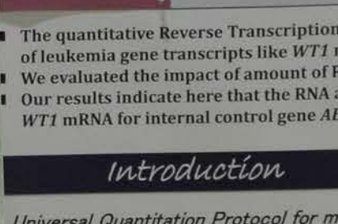

…mples used in this study consisted of various …tration of RNA (0.07 ~ 1.00µg/µl). The graph shows …ount of RNA corresponding to the volume (1µl, 3µl, …dded to RT reaction.

…Comparison of ΔCt

i. 1µl - 3µl

ii. 1µl - 5µl

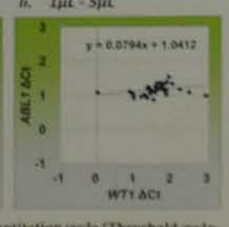

…ΔCt was the decline in quantitation cycle (Threshold cycle) …in real-time PCR when the volume of RNA added to RT …tion was increased from 1µl to 3µl or 5µl. The ΔCt of *ABL1* … small compared with *WT1*. It suggested that *ABL1* was not …ified sufficiently by qRT-PCR corresponding to increase of …

III. Correlation and Difference of WT…

i. 1µl vs 3µl

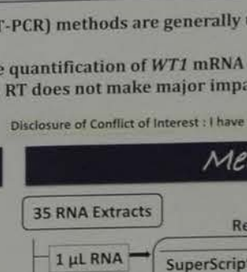

ii. 1µl vs 5µl

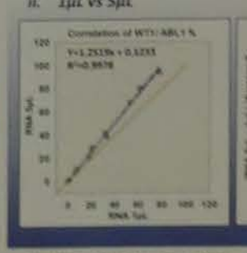

The *WT1*/ *ABL1* % values obtained from the … of RNA correlated well. There was the tende… *ABL1* % values obtained from 3 or 5µl RNA … that from 1µl RNA, and its tendency was also … of 19.5 and 25.7 units respectively in Bland … (right). Using Mann-Whitey U test, no signifi… resulted from the RNA amount were detecte… 0.573, 1µl vs 5µl: P = 0.474).

…nclusion

The relative values of *WT1* mRNA for *ABL1* were robust, irrespective of the RNA amount … transcription reaction.
Our data raised the possibility that the large amount of RNA in reverse transcription rea… plateau or decline of qRT-PCR efficacy, especially in case of high expression genes like A… biased relative value.
We will have further investigate that the bias presented in this study has no effect on foll… patients and the differences within mean ± 1.96 SD are not clinically important.

Molecular Diagnosis

PL-21

Examination of minimal residual disease (MRD) in the Neuroblastoma using the Real-time PCR.

Makoto Ikejiri[1], Maki Nakamura[1], Makoto Morimoto[1], Keiko Sakata[2], Shoutarou Iwamoto[2], Kazushi Sugimoto[1], Masahiro Hirayama[2], Kaname Nakatani[1]

1 Division of Clinical Laboratory, Mie University Hospital
2 Departments of Pediatrics, Mie University Graduate School of Medicine

MIE UNIVERSITY HOSPITAL

Object

Neuroblastoma is the most common extra-cranial solid neoplasm in children. It has a poor prognosis in the high-risk group, and long-term survival rate is approximately 30%. In recent years, it is useful to monitor an evaluation of the treatment response by minimal residual disease (MRD), and there is a report suggested that it can become the prognostic factor in a neuroblastoma. Therapeutic effect of the remission induction therapy was monitored by MRD in the neuroblastoma using Real-time PCR, and we assessed its usefulness in this study.

Method

We examined a diagnosis, the neuroblastoma that we treated in Mie university hospital from April, 2010. A bone marrow and the peripheral blood were obtained after treatment of the remission induction therapy and performed Real-time PCR (*TH, PHOX2B*) as an evaluation of MRD. Then, those in remission survival group and non-remission / recurrence group were compared. We simultaneously evaluated urinary vanilylmandelic acid (VMA) and the homovanillic acid (HVA).

Sampling point

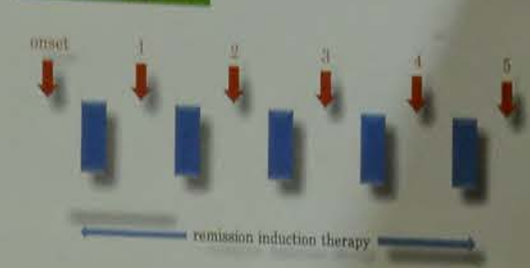

Real-time PCR

- Target gene
  - *PHOX2B* (paired-like homeobox 2b)
  - *TH* (Tyrosin hydroxylase)
- Primer & Probe

Case

Untreated onset neuroblastoma (Stage IV)

Case		①	②	③	④	⑤
Outcome		Remission survival	Remission survival	Recurrence death	Non-remission death	Non-remission death
Age of the month at diagnosis		24	22	93	42	33
Observation period (month)		67	16	15	12	7
Sex		M	F	F	F	F
Primary lesion		adrenal gland	adrenal gland	adrenal gland	adrenal gland	adrenal gland
Infiltration	Lymph node	○	○	○	○	
	bone marrow	○	○	○	○	○
	Bone	○	○	○	○	○
	liver		○			
Pathology*		UF	UF	UF	UF	UF
MYCN		×	○	nd	○	○
Ploidy		Diploid	Diploid	nd	Diploid	Diploid

*UF : unfavorable

Flow chart of the risk classification

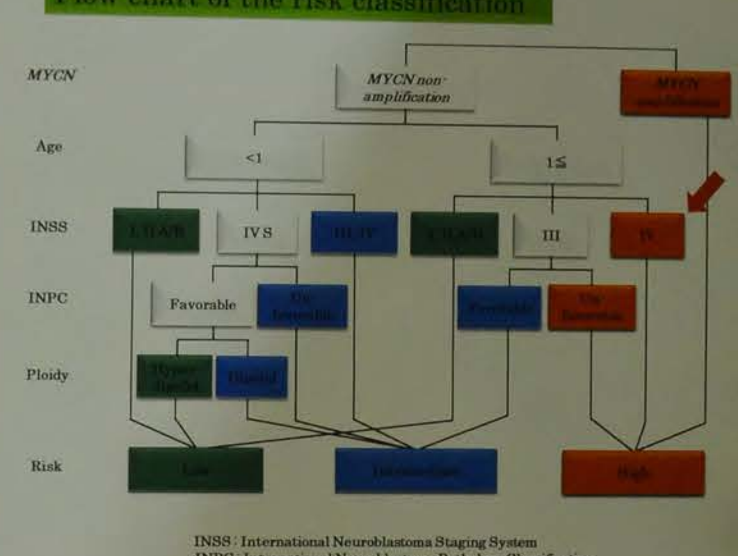

INSS : International Neuroblastoma Staging System
INPC : International Neuroblastoma Pathology Classification

Change of the MRD monitoring

remission induction therapy

① Remission survival	Onset	1	2	3	4	5
PHOX2B	1.6*10^6	nd	Negative	Negative	Negative	1.2*10^2
TH	3.0*10^5	nd	Negative	Negative	Negative	Negative
VMA	nd	nd	2.5	nd	nd	3.2
HVA	nd	nd	2.4	nd	nd	4.5
② Remission survival	Onset	1	2	3	4	5
PHOX2B	3.1*10^6	Negative	Negative	Negative	Negative	Negative
TH	1.5*10^3	Negative	Negative	Negative	Negative	Negative
VMA	1.2	0.7	0.8	0.8	0.9	nd
HVA	13.8	1.2	1.4	1.4	1.7	nd
③ Recurrence death	Onset	1	2	3	4	5
PHOX2B	1.4*10^7	3.8*10^3	Negative	Negative	Negative	Negative
TH	1.2*10^6	3.6*10^2	Negative	Negative	Negative	Negative
VMA	nd	nd	nd	nd	nd	nd
HVA	nd	nd	nd	nd	nd	nd
④ Non-remission death	Onset	1	2	3	4	5
PHOX2B	1.6*10^6	4.8*10^7	2.1*10^3	1.6*10^3	Negative	4.9*10^2
TH	4.1*10^5	Negative	1.9*10^2	2.2*10^3	Negative	Negative
VMA	nd	nd	2.7	22.7	nd	nd
HVA	nd	nd	4.6	14.3	nd	nd
⑤ Non-remission death	Onset	1	2	3		
PHOX2B	1.7*10^6	1.5*10^3	Negative	6.5*10^3		
TH	5.1*10^5	Negative	Negative	3.4*10^3		
VMA	11.7	2.2	14.9	3.9		
HVA	169.7	8.5	29	15.2		

PHOX2B, TH : copy/μgRNA

Standard Value
VMA 1.3-4.3 mg/day
HVA 1.5-6.6 mg/day

Positive ratio of MRD

		Nagative	Positive	Positive ratio
Remission Survival group	*PHOX2B*	8	1	11.1%
	TH	9	0	0.0%
	VMA	6	0	0.0%
	HVA	6	0	0.0%
Non-remission / Recurrence group	*PHOX2B*	6	7	53.9%
	TH	9	4	30.8%
	VMA	3	2	40.0%
	HVA	1	4	80.0%
Total	*PHOX2B*	14	8	36.4%
	TH	18	4	18.2%
	VMA	9	2	18.2%
	HVA	7	4	36.4%

Result

- We were able to identify tumor cells in the bone marrow and peripheral blood of all the cases at diagnosis.
- The MRD-positive rate was higher in the non-remission / recurrence group than those in the survival group after the remission induction therapy.
- Negative conversion was early confirmed in the remission survival group.
- The increase of urinary VMA and HVA were almost in accord with positive conversion of MRD, but some recurrent cases did not show such an increase.

Discussion

- *PHOX2B* had high positive rate in this examination. Also, BM, PB and PBSC do not have detectable expression, and there is the report to be a high sensitive maker. Thus, it is thought to be useful as a marker of MRD monitoring.
- *PHOX2B* is thought to be more useful than VMA and HVA where there was the case that did not show increase at a recurrence.

Conclusion

It was suggested that the MRD monitoring by the Real-time PCR (*PHOX2B*) was useful to evaluate therapeutic effect in the remission induction therapy. Further studies are required to evaluate it.

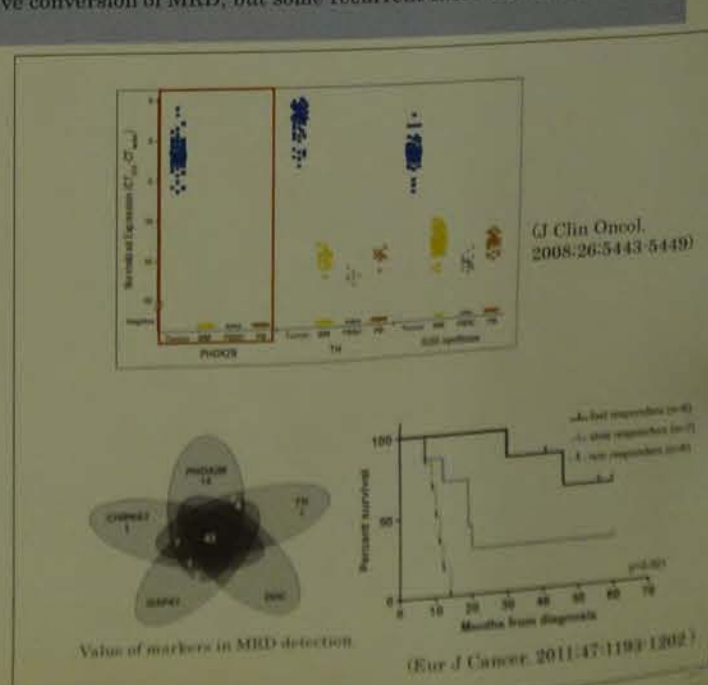

(J Clin Oncol. 2008;26:5443-5449)

Value of markers in MRD detection

(Eur J Cancer. 2011;47:1193-1202)

Molecular Diagnosis

PL-22

Impact of RNA amount on the efficacy of reverse transcription

—Aiming at full-automatic quantification of leukemia genes transcripts—

Tsukimi SHOJI, Tamao WATANABE, Yuto KIDA, Nana KURODA, Yuko HISAMOTO, Aya NISHIMURA, Atsumi ISHIDA, Miki NAGAO, Shuichi SHIGA, Satoshi ICHIYAMA

Department of Clinical Laboratory, KYOTO University Hospital

- **The quantitative Reverse Transcription PCR (qRT-PCR) methods are generally used for the quantification of leukemia gene transcripts like *WT1* mRNA.**
- **We evaluated the impact of amount of RNA on the quantification of *WT1* mRNA by qRT-PCR.**
- **Our results indicate here that the RNA amount in RT does not make major impact on the relative values of *WT1* mRNA for internal control gene *ABL1*.**

Disclosure of Conflict of Interest : I have no COI with regard to our presentation.

Introduction

Universal Quantitation Protocol for mRNA

Specimen → *RNA Extraction* → *Measurement of RNA concentration* → qRT-PCR: *Reverse Transcription; RT (cDNA Synthesis)* → *Real-time PCR*

- The number of leukocytes is various.
- The quantity and concentration of RNA of each sample is different.
- Absorbance measurement isn't automated.
- 1 μg RNA is used for a RT reaction.

Is it possible that the broad range of RNA amount is available for RT reaction?

- Leukemia genes and internal control gene are amplified simultaneously.

If the broad range of RNA amount can be available for RT reaction, the measurement and preparation of RNA concentration are not necessary, and full-automatic quantificational approach will be facilitated.

Method

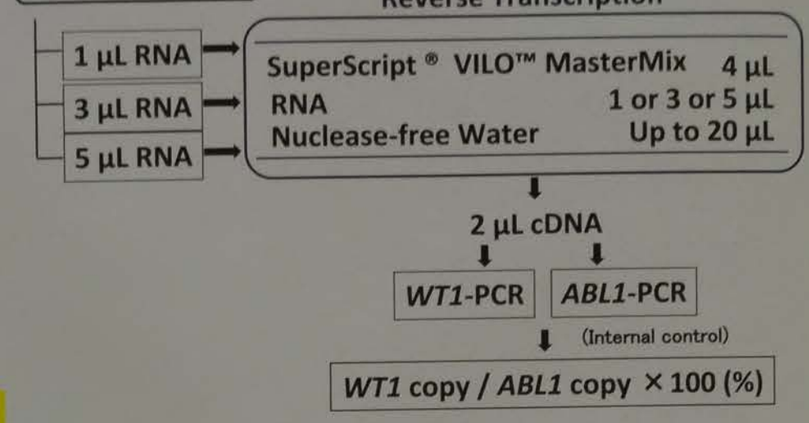

Thirty five RNA samples were obtained from 27 bone-marrow and 8 peripheral blood of patients with AML. The reverse transcription was performed with three different RNA volume (1μl, 3μl, 5μl) for each RNA extract. *WT1* and *ABL1* (as internal control) were amplified from 2μL cDNA and quantitated by TaqMan real-time PCR system. The PCR reaction volume was 20μL.

Results

I. RNA amount of each sample

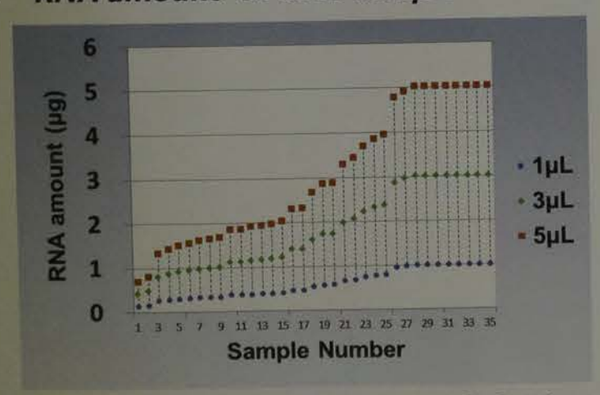

The samples used in this study consisted of various concentration of RNA (0.07 – 1.00μg/μl). The graph shows the amount of RNA corresponding to the volume (1μl, 3μl, 5μl) added to RT reaction.

II. Comparison of ΔCt

i. 1μL - 3μL

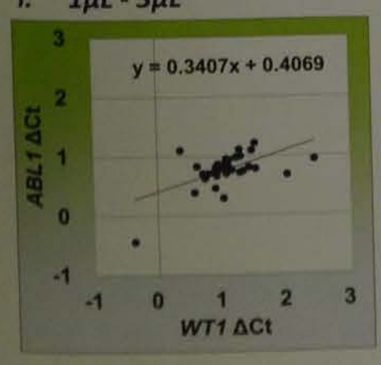

ii. 1μL - 5μL

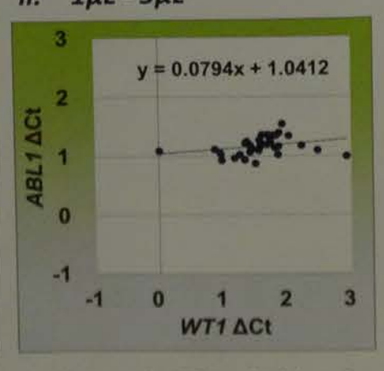

The ΔCt was the decline in quantitation cycle (Threshold cycle: Ct) in real-time PCR when the volume of RNA added to RT reaction was increased from 1μl to 3μl or 5μl. The ΔCt of *ABL1* was small compared with *WT1*. It suggested that *ABL1* was not amplified sufficiently by qRT-PCR corresponding to increase of RNA.

III. Correlation and Difference of WT1 /ABL1 % value

i. 1μL vs 3μL

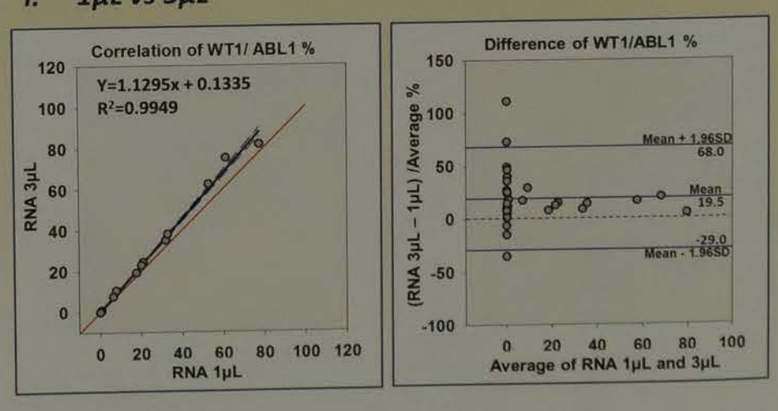

ii. 1μL vs 5μL

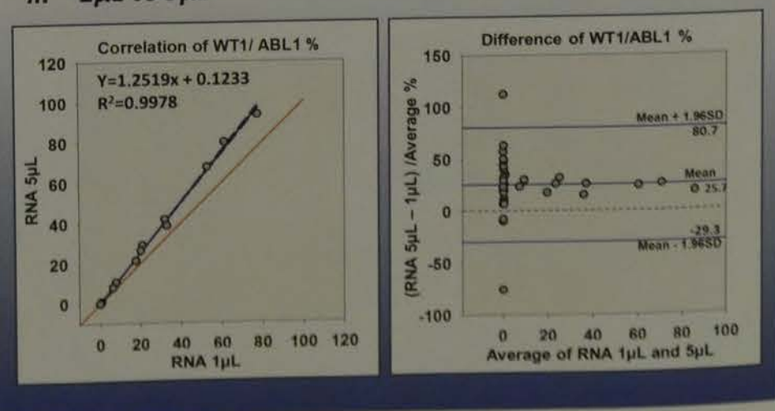

The *WT1/ ABL1* % values obtained from the different amount of RNA correlated well. There was the tendency that the *WT1/ ABL1* % values obtained from 3 or 5μl RNA were higher than that from 1μl RNA, and its tendency was also showed as the bias of 19.5 and 25.7 units respectively in Bland-Altman graph (right). Using Mann-Whitey U test, no significant differences resulted from the RNA amount were detected (1μl vs 3μl: P = 0.573, 1μl vs 5μl: P = 0.474).

Conclusion

- **The relative values of *WT1* mRNA for *ABL1* were robust, irrespective of the RNA amount added to reverse transcription reaction.**
- **Our data raised the possibility that the large amount of RNA in reverse transcription reaction can cause plateau or decline of qRT-PCR efficacy, especially in case of high expression genes like *ABL1*, resulting in biased relative value.**
- **We will have further investigate that the bias presented in this study has no effect on follow-up of patients and the differences within mean±1.96 SD are not clinically important.**

Molecular Diagnosis

PL-23

Reverse transcription loop-mediated isothermal amplification for simple and rapid detection of *PML-RARα* mRNA

Yuki Hashimoto[1)], Yuki Hatayama[1)], Nao Kojima[1)], Shota Morishita[1)], Satoko Matsumoto[1)], Yuzuru Hosoda[2)], Ayako Hara[1)], Toru Motokura[1,2)]

[1)]Division of Clinical Laboratory, Tottori University Hospital, Yonago, Tottori, Japan

[2)]Division of Clinical Laboratory Medicine, Department of Pathophysiological and Therapeutic Science, Tottori University Faculty of Medicine, Yonago, Tottori, Japan

TOTTORI UNIVERSITY GRADUATE SCHOOL OF MEDICAL SCIENCES

Introduction

Loop-mediated isothermal amplification (LAMP) method is very rapid and directly amplifies the target region from an RNA sample (1). Acute promyelocytic leukemia (APL) is a disease characterized by expression of *promyelocytic leukemia–retinoic acid receptor α* (*PML-RARα*) chimeric mRNA (2). Although APL is curable, early death due to hemorrhage is a major problem (3). Here, we report the development of a simple and rapid diagnostic method for APL based on reverse transcription (RT)-LAMP.

Materials and Methods

Targets

Three different types of *PML-RARα* mRNA

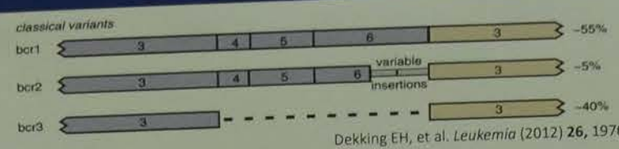

Dekking EH, et al. *Leukemia* (2012) **26**, 1976–1985

Samples

Positive controls : Three different plasmid DNAs—containing bcr1, bcr2, and bcr3 *PML-RARα* mRNA sequences.

Negative controls : IVS-0035 RNA (Invivoscribe Technologies, San Diego, CA, USA), Distilled water (DW)

Clinical samples : bcr1 RNA n = 4, bcr3 RNA n = 3

※ RNA extracted from bone marrow aspirates of six patients with APL. The samples were frozen at −80° C until the study.

Methods

- An RT-LAMP primer set was designed to detect three types of *PML-RARα* mRNA in a single reaction.
- The specificity of RT-LAMP assay was confirmed by restriction enzyme digestion of amplified RT-LAMP products using *Dde*I.
- Serial dilutions of plasmid DNA containing bcr1, bcr2, or bcr3 *PML-RARα* sequences were used to compare the sensitivities of RT-LAMP and nested PCR assays.
- Seven clinical RNA samples were tested to compare the qualitative results of RT-LAMP and nested PCR assays.

Results

Table 1. Primers for detection of *PML-RARα* mRNA by RT-LAMP

Primers	Sequence (5' → 3')
bcr1,2 FIP	TCCCCTCCTCAGACTCCATCTTGAAGAGGAAGTGCAGCCAGA
bcr1,2 F3	CTCCAATACAACGACAGCC
bcr3 FIP	TTGAACTCGTCGAAGCCATCGGCTGGACATGCACGGTT
bcr3 F3	AAGTGCTACGCCTCGGA
BIP	TGAGACCCAGAGCAGCAGTTGTAGATGCGGGGTAGA
B3	TGACAGACAAAGCAAGGC
bcr1,2 LF	GATGACCTTCCTGGGGCA
bcr3 LF	ACGGCAGCTTGCAGGCT
LB	TGAAGAGATAGTGCCCAGCCCT

Primer sets were designed using PrimerExplorer v.4 software. The primer sets were modified to detect the three types of *PML-RARα* mRNA in a single tube.

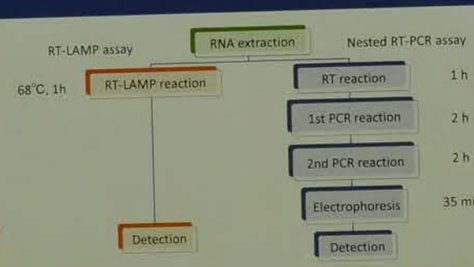

Figure 1. Flow chart of *PML-RARα* mRNA detection from RNA extraction. The reaction time of RT-LAMP assay was > 4 h shorter than the nested RT-PCR assay.

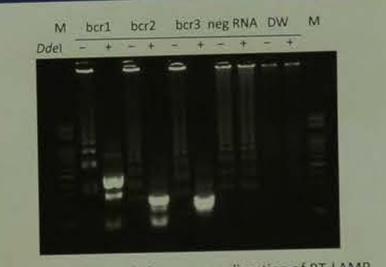

Figure 2. *Dde*I restriction enzyme digestion of RT-LAMP products. M, 100-bp ladder size marker; neg RNA, IVS-0035 RNA (negative control); DW, distilled water (negative control).

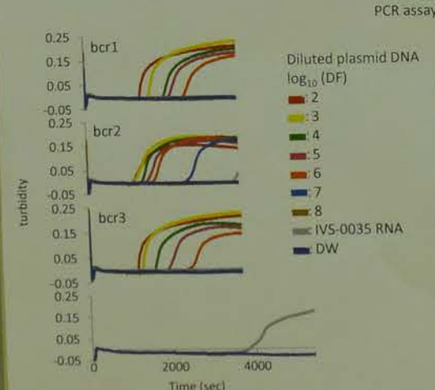

Figure 3. Detection of *PML-RARα* in plasmid DNA by RT-LAMP. RT-LAMP was able to detect 880, 78, and 800 copies/tube of bcr1, bcr2, and bcr3 plasmid, respectively. Plasmid DNAs containing bcr1, bcr2, and bcr3 sequences (starting amounts: 8.8×10^8, 7.8×10^8, and 8.0×10^8 copies/tube, respectively) were diluted by the indicated dilution factor (DF). DF of the indicated plasmid DNA is shown as a logarithmic value.

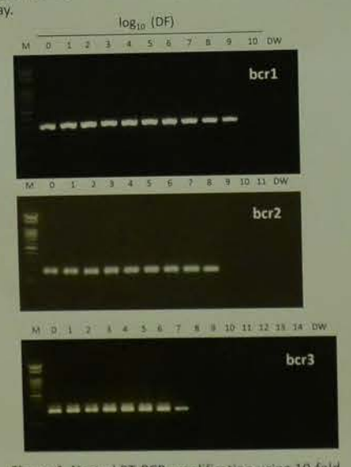

Figure 4. Nested RT-PCR amplification using 10-fold serial dilutions of plasmid DNA. Nested RT-PCR assay was able to detect 0.88, 7.8, and 80 copies/tube of bcr1, bcr2, and bcr3 plasmid , respectively.

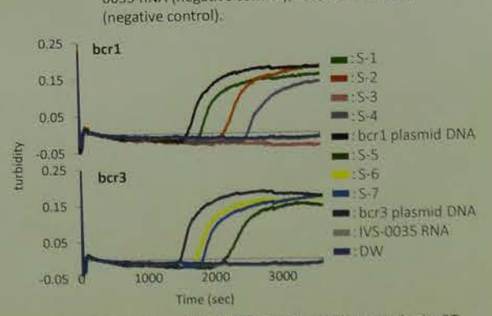

Figure 5. Detection of *PML-RARα* in clinical RNA samples by RT-LAMP. Clinical samples (S-1 through -7) from APL patients were analyzed by RT-LAMP. IVS-0035 RNA and distilled water were used as negative controls. RT-LAMP and nested RT-PCR yielded similar results in the analysis of clinical samples (see Table 2).

Table 2. Comparison between RT-LAMP and nested RT-PCR using clinical samples

Sample number	Breakpoint type	RNA concentration (ng/μL)	Absorbance ratio (260 nm/280nm)	RIN value	RT-LAMP	Nested RT-PCR
S-1	bcr1	250.8	2.04	9.60	(+)	(+)
S-2	bcr1	535.0	2.04	10	(+)	(+)
S-3	bcr1	361.9	1.98	NM	(-)	(-)
S-4	bcr1	1141.0	2.06	NA	(+)	(+)
S-5	bcr3	389.8	2.06	9.50	(+)	(+)
S-6	bcr3	309.2	2.05	9.90	(+)	(+)
S-7	bcr3	59.9	2.04	8.50	(+)	(+)

NM, not measured due to pattern deformation; NA, not available; Samples 5 and 6 were from the same patient—S-5, at the initial visit and S-6, at the time of relapse.

Discussion

Specificity of the RT-LAMP assay

- Each type of *PML-RARα* sequence was specifically amplified by RT-LAMP. Each *PML-RARα* breakpoint as well as non-specific amplification could be distinguished by digesting the products with *Dde*I.

Clinical samples analysis

- This study suggests that RT-LAMP has clinical utility as a diagnostic test, especially at initial presentation when a sufficient amount of *PML-RARα* mRNA is available

Sensitivity of the RT-LAMP assay

- The sensitivity of the current RT-LAMP assay was lower than that of the nested RT-PCR assay. Some RT-LAMP assays have greater sensitivity than nested RT-PCR (4), while others have lower sensitivity (5). This depends on the primers used, which determine the amplification efficiency and has a significant effect on the sensitivity of gene amplification. It is virtually impossible to test all candidates, although a primer set with better amplification efficiency may exist.

Time and efficiency of the test

- The RT-LAMP assay is therefore more useful for early diagnosis and determination of an appropriate intervention. In addition, the amount of sample that is lost with RT-LAMP is minimal because the extracted RNA is used directly in the amplification reaction. This simplifies the procedure, thereby reducing the labor and cost of laboratory testing.

Conclusion

We developed an RT-LAMP assay for detection of *PML-RARα* mRNA in clinical samples from APL patients. This assay is more simple and rapid than nested RT-PCR, and can lead to the development of an automated system that can be used for point-of-care testing and diagnosis of APL.

References

1. Notomi T, et al. Loop-mediated isothermal amplification of DNA. *Nucleic Acids Res* 2000; **28**: E63.
2. Kakizuka A, et al. Chromosomal translocation t(15;17) in human acute promyelocytic leukemia fuses RAR alpha with a novel putative transcription factor, PML. *Cell* 1991; **66**: 663–74.
3. Breccia M, Cicco FL. Thrombo-hemorrhagic deaths in acute promyelocytic leukemia. *Thromb Res* 2014; **133**: 5112–56.
4. Lee S, et al. Loop-mediated isothermal amplification assay to rapidly detect wheat streak mosaic virus in quarantined plants. *Plant Pathol J* 2015; **31**: 438–40.
5. Hanaki K, et al. Reverse transcription-loop-mediated isothermal amplification for the detection of rodent coronaviruses. *J Virol Methods* 2013; **187**: 222–7.

Acknowledgments

We would like to thank Mr. Yasuharu Sasaki for technical advice and Editage (www.editage.jp) for English editing. This study was supported by a grant from Seeds Research Project at Tottori University Hospital.

Molecular Diagnosis

PL-24

PL-24

The mutation profile of *JAK2*, *CALR*, and *MPL* in Japanese patients with Philadelphia chromosome-negative myeloproliferative neoplasms

Yuta Miyahara[1)], Naoko Okayama[1)], Sayuri Hayashi[1)], Mitsuaki Nishioka[1)], Hidekazu Mizuno[1)], Yutaka Suehiro[2)], Takahiro Yamasaki[1) 2)]

1) Department of Clinical Laboratory, Yamaguchi University Hospital
2) Department of Oncology and Laboratory Medicine, Yamaguchi University Graduate School of Medicine

Background

According to the 2008 WHO classification, the Philadelphia chromosome-negative myeloproliferative neoplasms (MPNs) was classified as polycythemia vera (PV), essential thrombocythemia (ET) and primary myelofibrosis (PMF). The *JAK2 V617F* mutation has been observed frequently in MPNs patients. Recently, other specific mutational events, notably *JAK2* exon 12, *MPL* exon 10 and *CALR* exon 9 have been identified in patients with *JAK2 V617F*-negative MPNs. We elucidated the association of somatic mutations with clinical characteristics in Japanese MPNs patients.

Materials and methods

Peripheral blood samples
178 patients with MPNs
PV : 42 patients
ET : 121 patients
PMF : 15 patients

Evaluate gene of mutation
JAK2 V617F
JAK2 exon 12
CALR exon9
MPL exon 10

Deteciton method
Direct sequencing
High resolution melting

Results

Figure 1 *JAK2, MPL and CALR* mutations in Japanese MPNs patients.

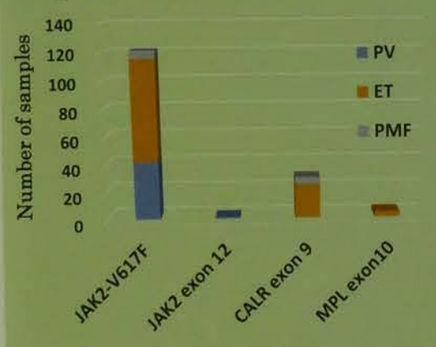

Figure 2 The frequency of somatic mutations in Japanese MPNs patients.

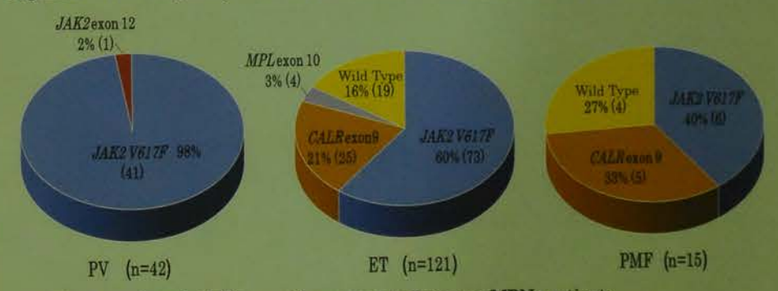

- The mutation of *JAK2* exon 12 was rare in Japanese MPNs patients. (2 % in PV , 0.6 % in all MPNs)
- The *CALR* exon 9 mutations were present in various types.
- The mutation of *MPL* exon 10 showed two types.

Table 1 *JAK2* exon12, *CALR* and *MPL* mutations in MPNs.

JAK2 exon 12 mutated	1
CALR mutated	30
-52 bp *	12
+5 bp **	11
-46 bp *	4
-34 bp *	2
-19 bp *	1
MPL mutated	4
W 515 K	3
W 515 L	1

* This mutation showed two types.
** 5 patients with PMF identified only this type.

Figure 3 Distribution of *CALR* exon 9 mutations.

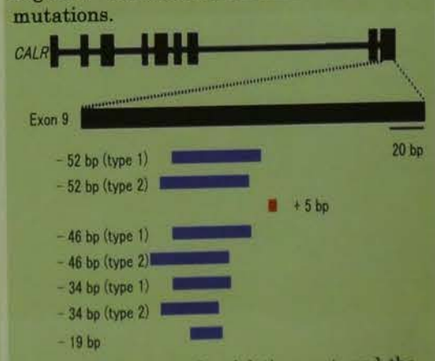

The blue bar showed a deletion part, and the red bar showed an insertion part.

Table 2 Alignment *CALR* C-terminal domain in *CALR* exon 9 mutant protein.

Wild Type	-KQDEE	QRLKEEEEDKKRKEEE·····VPGQAKDEL*	
-52bp type-1	-KQDEE	QRT	RRMMRTKMRMRR·····CREACLQGWTEA*
-52bp type-2	-KQDEE	QRL	RRMMRTKMRMRR·····CREACLQGWTEA*
+5bp	-KQDEE	QRLKEEEEDKK RKEEEEAEDNC	RRMMRTKMRMRR·····CREACLQGWTEA*
-46bp type-1	-KQDEE	QRQRT	RRMMRTKMRMRR·····CREACLQGWTEA*
-46bp type-2	-KQDEE	RRQRT	RRMMRTKMRMRR·····CREACLQGWTEA*
-34bp type-1	-KQDEE	QRRRRRQRT	RRMMRTKMRMRR·····CREACLQGWTEA*
-34bp type-2	-KQDEE	QRLRRRQRT	RRMMRTKMRMRR·····CREACLQGWTEA*
-19bp	-KQDEE	QRLKEELRRR QRT	RRMMRTKMMRR·····CREACLQGWTEA*

Same amino acid sequence identified in all samples(brown). However, mutated samples showed specific sequence(blue).

Figure 4 Data of direct sequence about mutations of *JAK2* exon12.

Table 3 Clinical characteristics of *CALR* mutated ET.

	JAK2 mutated n=73	*CALR* mutated n=25	*P*
WBC (/μl)	12567	7832	< 0.01
Hb (g/dl)	13.9	12.6	< 0.05
Ht (%)	42.6	38.1	< 0.01
PLT (x10⁴/μl)	90.1	99.6	0.48
Sex	Male : 35 (48%)	Male : 16 (64%)	0.25
Age	68.5	58.7	< 0.01
Thrombosis	16(22%)	1(4%)	0.03

Table 4 ET patients with *CALR* mutation have particular clinical characteristics as compared with those with *JAK2* mutation.

References	Sex	Age	WBC	Hb	PLT	Survival	Thrombosis
Klampfl et al[11]			Lower	Lower	Higher	Better	Less
Namgalia et al[9]				Lower	Higher	ND	
Chen et al[6]	ND	Younger	Lower	ND	Higher		Less
Rumi et al[5]	M>	Younger	Lower	Lower	Higher	ND	Less
Rotunno et al[8]	M>	Younger	Lower	Lower	Higher		Less
This study	ND	Younger	Lower	Lower	ND	NA	Less

Conclusions

We showed the somatic mutation profile of *JAK2, CALR* and *MPL* in Japanese MPNs patients. Clinical characteristics of ET patients with *CALR* mutation may be similar to previous reports in North American and European patients.

Molecular Diagnosis

PL-25

Rapid diagnosis of APL with the *PML-RARA* fusion gene using droplet-RT-PCR and instant-quality FISH

Shohei Shigeto [a], Kazuyuki Matsuda [a], Akemi Yamaguchi [b], Akane Sueki [a], Masayuki Uehara [b], Mitsutoshi Sugano [a], Takeshi Uehara [a], Takayuki Honda [a]

[a] Department of Laboratory Medicine, Shinshu University Hospital, Matsumoto, Japan
[b] Core Technology Development Center, Seiko Epson Corporation, Suwa, Japan

[Background] Acute promyelocytic leukemia (APL) is a highly aggressive disease presenting hemorrhagic complications from a characteristic coagulopathy. The presence of the *PML-RARA* fusion gene, which results from a balanced reciprocal translocation, t(15;17)(q24;q21), is the molecular hallmark of APL. All-trans retinoic acid (ATRA) with chemotherapy or ATRA with arsenic trioxide (AsO3) is effective and yields higher cure rates with complete remission. ATRA and AsO3 have specific reactivity for different parts of the PML-RARA fusion protein, which serves as the molecular basis for highly effective molecular targeted therapies. Therefore, rapid detection and quantitative assessment of the *PML-RARA* fusion gene, carried out using reverse-transcription polymerase chain reaction (RT-PCR) and fluorescence in situ hybridization (FISH), influence the prognoses of the patients with APL. Unfortunately, conventional analysis by RT-PCR and FISH requires one to two days. Here, we developed a rapid assay for identifying and measuring the *PML-RARA* fusion gene in patients with APL using droplet-reverse transcription-polymerase chain reaction (droplet-RT-PCR) and instant-quality fluorescence in situ hybridization (IQ-FISH).

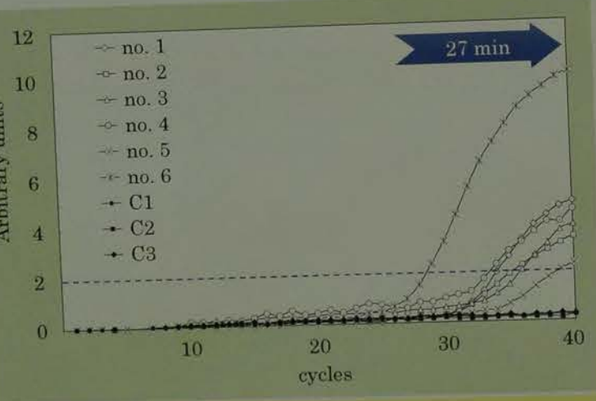

[Methods]

- Materials

RNA for droplet-RT-PCR and Carnoy's fixed interphase cells for IQ-FISH were prepared from six patients with APL and three unafected controls.

- One-step droplet-RT-PCR

The primers and TaqMan probes for the *PML-RARA* fusion gene were designed as previously reported (1). The Droplet-RT-PCR assay was performed using a droplet-PCR machine (Seiko Epson). The one-step RT-PCR reaction mixture contained RNA, SuperScript III/Platinum Taq Mix (Life Technologies, Grand Island, NY), reaction buffer composed of Tris–HCl pH 9.0, KCl and MgCl2, 0.8 µmol/L of each primer, and 0.2 µmol/L of the TaqMan probe in a final volume of 10 µL. One microliter of each reaction mixtures was used for the droplet-PCR assay.

- IQ-FISH

IQ-FISH analysis was performed using an IQ-FISH Fast Hybridization Buffer, Sure FISH PML-RARA Dual fusion probe (Agilent Technologies, West Cedar Creek, TX) and a Dako Cytology FISH Accessory Kit (Dako, Glostrup, Denmark) for slide pretreatment and wash. IQ-FISH Hybridization Buffer uses the less toxic solvent ethylene carbonate as substitute for formamide and thus, the hybridization time is dramatically reduced (2, 3). we evaluated the signal clarity and hybridization time compared with conventional FISH using Vysis LSI Hybridization buffer. We scored 500 nuclei form PB or BM samples to determine the number of yellow fusion signals using a microscope (Axio Imager Z2).

[Results]

- **Droplet-RT-PCR for detection of the *PML-RARA* fusion gene**

we set an arbitrary standard for evaluating the amplification; samples were considered positive when the fluorescent level of amplification was more than 2.0. The *PML-RARA* fusion gene was detected by droplet-RT-PCR in all samples from the six patients with APL (long-type PML-RARA, patients nos 1-5; short-type PML-RARA, patient no 6) within 27 min. No amplification was observed from control samples (C1- C3).

- IQ-FISH

IQ-FISH showed the same strong, clear signals by 60 min hybridization as obtained by conventional FISH by 16 h hybridization. There were no significant differences in positive signal percentage obtained by IQ-FISH and conventional FISH.

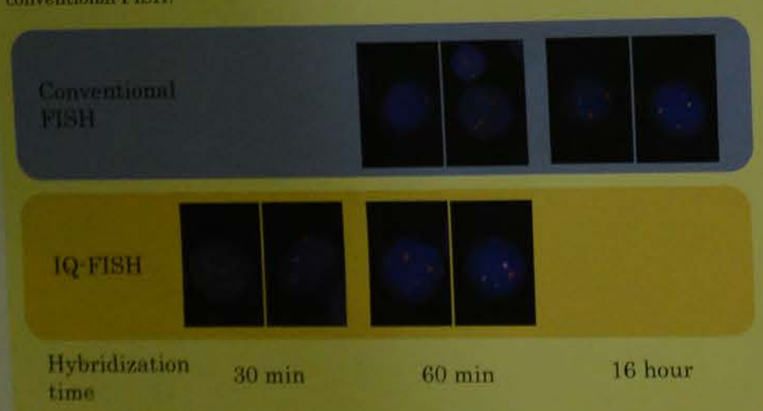

FISH signal for PML/RARA(%)

scored 500 nuclei from samples

Patient No.	Conventional FISH	IQ FISH
1	86.8	85.0
2	85.8	86.8
3	81.0	79.0
4	91.4	90.0
5	95.0	96.4
6	88.4	92.0

[Conclusions]

Simultaneous droplet-RT-PCR and IQ-FISH, in addition to morphological examination of blood smears, can diagnose patients as having APL within 4 h based on molecular/cytogenetic results. Rapid diagnosis can allow effective therapies to be started promptly.

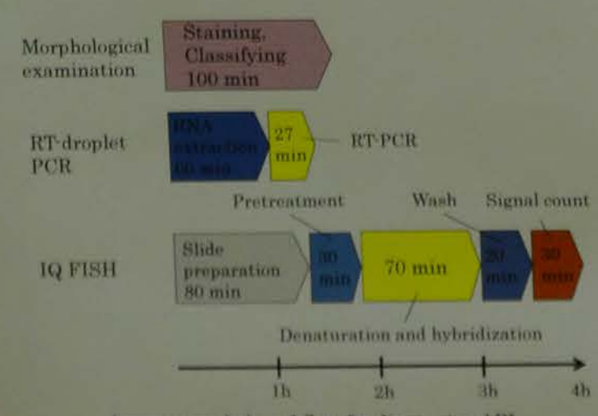

A recommended workflow for diagnosing APL with the *PML-RARA* fusion gene.

[References]

1. Gabert J, et al. Standardization and quality control studies of 'real-time' quantitative reverse transcriptase polymerase chain reaction of fusion gene transcripts for residual disease detection in leukemia - A Europe Against Cancer Program. Leukemia 2003;17 2318-57

2. Matthoesen SH, Hansen CM. Fast and Non-Toxic In Situ Hybridization without Blocking of Repetitive Sequences. PLOS One 2012;7:7

3. Tefe LJ, et al. Rapid fluorescence in situ hybridisation (FISH) for HER2 (ERBB2) assessment in breast and gastro-oesophageal cancer. J Clin Pathol 2015;68:4 306-8

Shinshu University Hospital

Molecular Diagnosis

PL-27

Loop-Mediated Isothermal Amplification for detection of atypical mycobacteria

Using universal primers for *Mycobacterium sp.* and specific primers for *M. avium* and *M. intracellulare*

Ken-ichi Sato[1)], Kazuhiro Shinto[2)], Kyohei Kato[2)], Hiroki Hanaiwa[2)], Taeko Narita[2)], Yumiko Funashima[1)], Zenzo Nagasawa[1)], Tetsuhiro Harada[2)] and Tsukuru Umemura[2)]

1) Department of Medical Technology and Sciences, International University of Health and Welfare, Fukuoka, Japan.
2) Department of Clinical Laboratory, Medical Kouhoukai Takagi Hospital, Fukuoka, Japan.

Background

Loop-Mediated Isothermal Amplification (LAMP) is an isothermal nucleic acid amplification method which does not employ a series of thermal cycling. The rapidity, high specificity, and high amplification efficiency of this method lend it importance in the clinical testing, primarily in detection of pathogens responsible for infectious disease. As LAMP can detect *Mycobacterium tuberculosis* (MTB), this method has been widely implemented by clinical laboratories in Japan. However, when acid-fast microscopy detects acid-fast bacilli in specimens for which the LAMP test is negative for MTB, it cannot be determined whether there was a failure in nucleic acid amplification or the acid-fast bacilli are atypical mycobacteria. Therefore, our objective is to develop a specific LAMP-based assay for clinical application using universal primers for detection of Mycobacterium sp. and specific primers for *M. avium* (MAV) and *M. intracellulare* (MIN) to diagnose the *M. avium complex* pulmonary disease.

Materials and Methods

Samples

35 Mycobacteria isolated by Ogawa medium from clinical specimens

DNA extraction

① Suspended colonies in sterile purified water of 1.5 mL tubes
② Boiled for 10 min at 95°C
③ Centrifuged for 1 min at 15,000 X g
④ Used supernatant diluted to 1/1000 as LAMP template

LAMP assay

- Reagents and Instrument
  - *Bst* DNA Polymerase kit (Nippon gene) and LoopampEXIA® (Eiken Chemical) were used for assay
- Primers
  - Universal primers targeted conserved region of *16S rRNA* gene
  - Specific primers for MAV and MIN targeted *gyrB* gene
- Condition
  - A reaction mixture (25 µL)

10× Reaction Mix	2.5 µL
dNTP mix (2.5 mM)	14.0 µL
Primers Mix*	1.3 µL
H2O	3.2 µL
Bst DNA polymerase	2.0 µL
template DNA	2.0 µL
total	25.0 µL

  - Primers mix contained 1.6 µM each inner primer, 0.2 µM each outer primer, 0.8 µM each loop primer
  - Incubated at 65°C for 60 min to extension and 80°C for 2 min to terminate reaction

Direct sequencing and homology search

- Reagents and Instrument sequencing
  - BigDye Terminator v3.1 cycle Sequencing Kit and Genetic analyzer 3500 (Thermo Fisher Scientific) were used for *16SrRNA* and *rpoB* gene sequencing
- Homology search
  - Used NCBI BLAST (https://blast.ncbi.nlm.nih.gov/), EzTaxon-e (http://eztaxon-e.ezbiocloud.net/ezt_identify), and Le BIBI

Results

Sample #	Species*	Amplification by LAMP primer: universal	MAV	MIN
1	*M.abscessus*	+	–	–
2	*M.marinum*	+	–	–
3	*M.peregrinum*	+	–	–
4	*M.avium*	+	+	–
5	*M.abscessus*	+	–	–
6	*M.xenopi*	+	–	–
7	*M.kansasii* or *M.gastri*	+	–	–
8	*Mscrofulaceum*	+	–	+
9	*M.intracellulare*	+	–	+
10	*M.intracellulare*	+	–	–
11	*M.Abscessus* or *M.chelonae*	+	–	–
12	*M.kansasii*	+	–	–
13	*M.kansasii* or *M.gastri*	+	–	–
14	*M.avium*	+	+	–
15	*M.fortuitum*	+	–	–
16	*M.bovis*	+	–	–
17	*M.intracellulare*	+	–	+
18	*M.marinum*	+	–	–
19	*M.intracellulare*	+	–	+
20	*M.kansasii*	+	–	–
21	*M.terrae*	+	–	–
22	*M.fortuitum*	+	–	–
23	*M.abscessus*	+	–	–
24	*M.intracellulare*	+	–	–
25	*M.intracellulare*	+	–	+
26	*M.scrofulaceum*	+	–	+
27	*M.abscessus*	+	–	–
28	*M.xenopi*	+	–	–
29	*M.peregrinum*	+	–	–
30	*M.Abscessus* or *M.chelonae*	+	–	–
31	*M.abscessus*	+	–	–
32	*M.terrae*	+	–	–
33	*M.abscessus*	+	–	–
34	*M.tuberuclosis*	+	–	–
35	*M.tuberuclosis*	+	–	–

* Identified by homology search of *16SrRNA* and *rpoB* gene sequences

- All of 35 mycobacteria specimens were identified by the universal primers.
- There were no false-positive and false-negative, using MAV and MIN specific primers.

conclusion

- We developed LAMP assays that can be used to *Mycobacteria* identification.
- The results obtained were rapid and accurate identifications of *Mycobacteria* using the universal primers and MAV and MIN using the specific primers.
- These LAMP assays may be applicable for routine identification of *Mycobacteria* in clinical laboratories.

Molecular Diagnosis

PL-26

Preanalytical evaluation of COBAS TaqMan MTB testing of MGIT samples at Chiba University Hospital

Kouichi Kitamura[1, 2], Takayuki Ishige[1, 2], Kenichi Sato[3], Sakae Itoga[1, 2], Shota Murata[1], Yuji Sawabe[1], Kazuyuki Matsushita[1, 2]

[1] Division of Laboratory Medicine, Chiba University Hospital, Chiba, Japan.
[2] Department of Molecular Diagnosis, Graduate School of Medicine, Chiba University, Chiba, Japan.
[3] Department of Medical Technology and Sciences, International University of Health and Welfare, Fukuoka, Japan.

CHIBA UNIVERSITY

Background

Mycobacterium tuberculosis (MTB) can be detected more rapidly by the mycobacteria growth indicator tube (MGIT, Becton Dickinson) than Ogawa medium.

At our clinical laboratory, 100-fold diluted MGIT samples of COBAS TaqMan MTB tests (Roche Diagnostics) are used prepared by the SOL-M kit (SHIMADZU). In this study, we evaluated the precision of our method especially on the dilution of MGIT samples.

Methods

Samples
✓ MGIT samples spiked with MTB colony and MTB-positive clinical specimen.

Reagents
✓ COBAS TaqMan MTB kit
✓ Specimen Preparation kit (SOL-M kit)

Instruments
✓ COBAS TaqMan 48 analyzer (Roche Diagnostics)
✓ BACTEC MGIT 960 (Becton Dickinson)

Workflow of this experimental protocol.

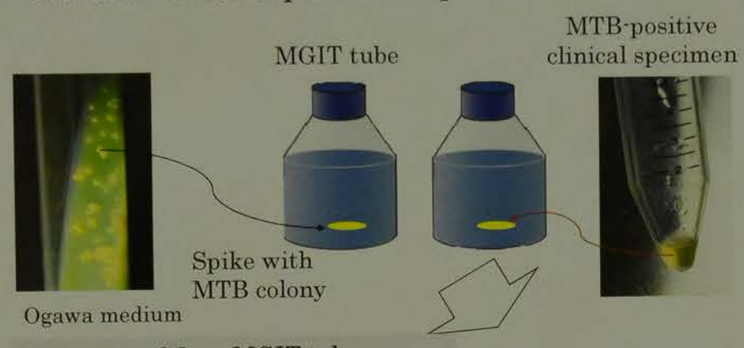

Our protocol for a MGIT tube
① Voltex a MGIT tube for 10 sec
② Spin down a MGIT tube at 2000 rpm for 1 min at 4℃.
③ Add 100 µl of MGIT sample from the bottom to 1.5ml tube.
④ Centrifuge the tube at 15,000 g for 5 min.
⑤ Remove the supernatant and add 100µl of SOL-L solution.
The usual procedures follow here after.

MGIT positive after several days

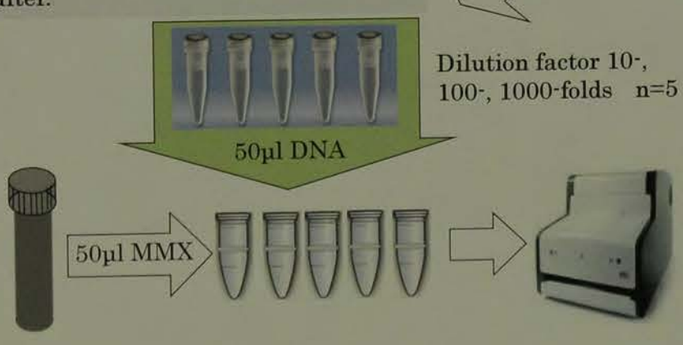

Results

1. The within-run reproducibility of Ct values and CV of MGIT samples (n=5) spiked with MTB colony.

Dilution factor	Average of Ct values		CV(%)	
	MTB	IC*	MTB	IC
x10	34.8	38.1	4.5	1.0
x100	39.7	38.7	0.9	0.9
x1000	44.8	38.7	3.4	1.4

* IC; internal control

2. The within-run reproducibility of Ct values and CV of MGIT samples (n=5) spiked with MTB-positive clinical specimen.

Dilution factor	Average of Ct values		CV(%)	
	MTB	IC	MTB	IC
x10	34.4	38.3	1.0	2.2
x100	38.5	38.8	0.6	0.8
x1000	42.1	39.2	3.5	2.3

3. The measurements of Ct-MTB values in each dilution factor (additional number of samples were prepared using the same batch).

(A). MGIT samples with MTB colony. CV of Ct-MTB values.

10-folds (yellow) — 3.0% (n=10)
100-folds (red) — 1.2% (n=10)
1000-folds (green) — 4.0% (n=9)

(B). MGIT samples with MTB-positive clinical specimen. CV of Ct-MTB values.

10-folds (yellow) — 1.4% (n=20)
100-folds (red) — 1.1% (n=20)
1000-folds (green) — 3.9% (n=19)

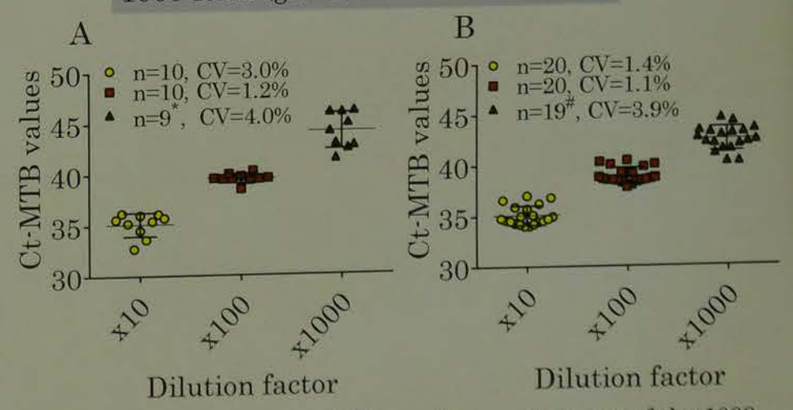

*,# One sample gave a MTB-negstive result in one of the 1000-fold diluted specimen.

Conclusion

The 100-fold dilution is the best for COBAS TaqMan MTB tests of MGIT samples because such samples exhibit the finest reproducibility.

Molecular Diagnosis

PL-27

Loop-Mediated Isothermal Amplification for detection of atypical mycobacteria

Using universal primers for *Mycobacterium sp.* and specific primers for *M. avium* and *M. intracellulare*

Ken-ichi Sato[1)], Kazuhiro Shinto[2)], Kyohei Kato[2)], Hiroki Hanaiwa[2)], Taeko Narita[2)], Yumiko Funashima[1)], Zenzo Nagasawa[1)], Tetsuhiro Harada[2)] and Tsukuru Umemura[2)]

1) Department of Medical Technology and Sciences, International University of Health and Welfare, Fukuoka, Japan.
2) Department of Clinical Laboratory, Medical Kouhoukai Takagi Hospital, Fukuoka, Japan.

Background

Loop-Mediated Isothermal Amplification (LAMP) is an isothermal nucleic acid amplification method which does not employ a series of thermal cycling. The rapidity, high specificity, and high amplification efficiency of this method lend it importance in the clinical testing, primarily in detection of pathogens responsible for infectious disease. As LAMP can detect *Mycobacterium tuberculosis* (MTB), this method has been widely implemented by clinical laboratories in Japan. However, when acid-fast microscopy detects acid-fast bacilli in specimens for which the LAMP test is negative for MTB, it cannot be determined whether there was a failure in nucleic acid amplification or the acid-fast bacilli are atypical mycobacteria. Therefore, our objective is to develop a specific LAMP-based assay for clinical application using universal primers for detection of Mycobacterium sp. and specific primers for *M. avium* (MAV) and *M. intracellulare* (MIN) to diagnose the *M. avium complex* pulmonary disease.

Materials and Methods

Samples

35 Mycobacteria isolated by Ogawa medium from clinical specimens

DNA extraction

① Suspended colonies in sterile purified water of 1.5 mL tubes
② Boiled for 10 min at 95°C
③ Centrifuged for 1 min at 15,000 X g
④ Used supernatant diluted to 1/1000 as LAMP template

LAMP assay

- Reagents and Instrument
  - *Bst* DNA Polymerase kit (Nippon gene) and LoopampEXIA® (Eiken Chemical) were used for assay
- Primers
  - Universal primers targeted conserved region of *16S rRNA* gene
  - Specific primers for MAV and MIN targeted *gyrB* gene
- Condition
  - A reaction mixture (25 µL)

10× Reaction Mix	2.5 µL
dNTP mix (2.5 mM)	14.0 µL
Primers Mix*	1.3 µL
H2O	3.2 µL
Bst DNA polymerase	2.0 µL
template DNA	2.0 µL
total	25.0 µL

  - Primers mix contained 1.6 µM each inner primer, 0.2 µM each outer primer, 0.8 µM each loop primer
  - Incubated at 65℃ for 60 min to extension and 80℃ for 2 min to terminate reaction

Direct sequencing and homology search

- Reagents and Instrument sequencing
  - BigDye Terminator v3.1 cycle Sequencing Kit and Genetic analyzer 3500 (Thermo Fisher Scientific) were used for *16SrRNA* and *rpoB* gene sequencing
- Homology search
  - Used NCBI BLAST (https://blast.ncbi.nlm.nih.gov/), EzTaxon-e (http://eztaxon-e.ezbiocloud.net/ezt_identify), and Le BIBI

Results

Sample #	Species*	Amplification by LAMP primer: universal	MAV	MIN
1	*M.abscessus*	+	–	–
2	*M.marinum*	+	–	–
3	*M.peregrinum*	+	–	–
4	*M.avium*	+	+	–
5	*M.abscessus*	+	–	–
6	*M.xenopi*	+	–	–
7	*M.kansasii* or *M.gastri*	+	–	–
8	*Mscrofulaceum*	+	–	–
9	*M.intracellulare*	+	–	+
10	*M.intracellulare*	+	–	+
11	*M.Abscessus* or *M.chelonae*	+	–	–
12	*M.kansasii*	+	–	–
13	*M.kansasii* or *M.gastri*	+	–	–
14	*M.avium*	+	+	–
15	*M.fortuitum*	+	–	–
16	*M.bovis*	+	–	–
17	*M.intracellulare*	+	–	+
18	*M.marinum*	+	–	–
19	*M.intracellulare*	+	–	+
20	*M.kansasii*	+	–	–
21	*M.terrae*	+	–	–
22	*M.fortuitum*	+	–	–
23	*M.abscessus*	+	–	–
24	*M.intracellulare*	+	–	–
25	*M.intracellulare*	+	–	+
26	*M.scrofulaceum*	+	–	+
27	*M.abscessus*	+	–	–
28	*M.xenopi*	+	–	–
29	*M.peregrinum*	+	–	–
30	*M.Abscessus* or *M.chelonae*	+	–	–
31	*M.abscessus*	+	–	–
32	*M.terrae*	+	–	–
33	*M.abscessus*	+	–	–
34	*M.tuberuclosis*	+	–	–
35	*M.tuberuclosis*	+	–	–

* Identified by homology search of *16SrRNA* and *rpoB* gene sequences

- All of 35 mycobacteria specimens were identified by the universal primers.
- There were no false-positive and false-negative, using MAV and MIN specific primers.

conclusion

- We developed LAMP assays that can be used to *Mycobacteria* identification.
- The results obtained were rapid and accurate identifications of *Mycobacteria* using the universal primers and MAV and MIN using the specific primers.
- These LAMP assays may be applicable for routine identification of *Mycobacteria* in clinical laboratories.

Molecular Diagnosis
PL-28

The analysis of functional polymorphisms in *VDR*, *GC* and *CYP2R1* in autoimmune thyroid diseases

Naoya Inoue[1,2], Mikio Watanabe[2], Yuka Katsumata[2], Yoh Hidaka[1], Yoshinori Iwatani[2]

[1]*Laboratory for Clinical Investigation, Osaka University Hospital*
[2]*Department of Biomedical Informatics Division of Health Sciences Osaka University Graduate School of Medicine*

Introduction

Hashimoto's Disease (HD)
(Positive for thyroid specific autoantibodies)

Destruction rate of thyroid follicles

HIGH → **Severe**　　*LOW* → **Mild**

Difficult to predict

Graves' Disease (GD)
(Positive for thyrotrophin receptor antibody(TRAb))

medical treatment (anti-thyroid drug)

Still positive for TRAb for at least five years → **Intractable**
Negative for TRAb → **remission**

The associations of Vitamin D in immune reactions

Liver $25(OH)D_3$ converted by **CYP2R1**

↓ Transport by **Group-specific component (GC)**

Kidney $1,25(OH)_2D_3$ converted from $25(OH)D_3$

↓ Transport by **Group-specific component (GC)**

Cells Bind **Vitamin D receptor (VDR)**
These complex bind **vitamin D response element (VDRE)**

→ **Suppress immune reaction**

The polymorphisms genotyped in this study

Gene	Polymorphism	The function of polymorphism	
VDR	rs7975232 C/A	AA genotype > CC genotype	(serum $25(OH)_2D_3$ concentration)
	rs1544410 A/G	A allele > G allele	(IFN-γ production in PBMC)
	rs2228570 C/T	TT genotype > CC genotype	(serum $25(OH)_2D_3$ concentration)
	rs731236 T/C	T allele > C allele	(VDR expression)
GC	rs7041 and rs4588	Gc1 allele > Gc2 allele	(serum $25(OH)_2D_3$ concentration)
CYP2R1	rs10741657 A/G	AA genotype > AG or GG genotype	(serum $25(OH)_2D_3$ concentration)

Objective

To clarify the associations between *VDR, GC, CYP2R1* polymorphisms and autoimmune thyroid diseases (AITD), we genotyped these polymorphisms.

Results

***1. VDR* rs731236, rs7975232, rs2228570 polymorphisms were associated with GD development**

***2. GC* Gc1Gc1 genotype, *CYP2R1* rs10741657AG genotype were associated with GD intractability**

Table 1. The frequencies of Vitamin D SNPs in AITD patients

		Control	All patients with AITD		All patients with GD		All patients with HD	
VDR rs731236	TT	58 (77·3%)	196 (81·3%)	n.s.*	109 (87·2%)	0·0147*§	87 (75·0%)	n.s.*
	TC	17 (22·7%)	43 (17·9%)		15 (12·0%)	n.s.*	28 (24·1%)	
	CC	0 (0%)	2 (0·8%)		1 (0·8%)		1 (0·9%)	
	T allele	133 (88·7%)	435 (90·2%)	n.s.*	233 (93·2%)	n.s.*	202 (87·1%)	n.s.*
	C allele	17 (11·3%)	47 (9·8%)		17 (6·8%)		30 (12·9%)	
VDR rs7975232	CC	31 (41·3%)	114 (49·1%)	0·0256*	65 (50·4%)	0·0280*	51 (47·7%)	n.s.*
	CA	32 (42·7%)	105 (45·3%)		56 (44·8%)		49 (45·8%)	
	AA	12 (16·0%)	13 (5·6%)		6 (4·8%)		7 (6·5%)	
	C allele	94 (62·7%)	333 (71·8%)	0·037*	182 (72·8%)	0·0349*	151 (70·6%)	n.s.*
	A allele	56 (37·3%)	131 (28·2%)		68 (27·2%)		63 (29·4%)	
VDR rs2228570	CC	25 (32·9%)	100 (41·8%)	n.s.*	46 (34·9%)	n.s.*	54 (50·5%)	0·0174*†, 0·0149*‡
	CT	42 (55·3%)	113 (47·3%)		70 (53·0%)		43 (40·2%)	n.s.*
	TT	9 (11·8%)	26 (10·9%)		16 (12·1%)		10 (9·3%)	
	C allele	92 (59·2%)	313 (65·5%)	n.s.*	162 (61·4%)	n.s.*	151 (70·6%)	0·0458*, 0·0348†
	T allele	60 (40·8%)	165 (34·5%)		102 (38·6%)		63 (29·4%)	
VDR rs1544410	AA	3 (4·7%)	7 (3·4%)	n.s.*	3 (2·7%)	n.s.*	4 (4·1%)	n.s.*
	AG	11 (17·2%)	56 (17·3%)		15 (13·7%)		21 (21·4%)	
	GG	50 (78·1%)	165 (79·3%)		92 (83·6%)		73 (74·5%)	
	A allele	17 (13·3%)	50 (12·0%)	n.s.*	21 (9·5%)	n.s.*	29 (14·8%)	n.s.*
	G allele	111 (86·7%)	366 (88·0%)		199 (90·5%)		167 (85·2%)	
GC	Gc1Gc1	57 (61·7%)	131 (54·6%)	n.s.*	64 (50·8%)	n.s.*	67 (56·8%)	n.s.*
	Gc1Gc2	19 (31·7%)	97 (40·4%)		54 (42·9%)		43 (37·7%)	
	Gc2Gc2	4 (6·6%)	12 (5·0%)		8 (6·3%)		4 (3·5%)	
	Gc1 allele	93 (77·5%)	359 (74·8%)	n.s.*	182 (72·2%)	n.s.*	177 (77·6%)	n.s.*
	Gc2 allele	27 (22·5%)	121 (25·2%)		70 (27·8%)		51 (22·4%)	
CYP2R1 rs10741657	GG	25 (40·3%)	97 (38·2%)	n.s.*	54 (38·9%)	n.s.*	43 (37·4%)	n.s.*
	GA	26 (41·9%)	111 (43·7%)		60 (43·2%)		51 (44·4%)	
	AA	11 (17·8%)	46 (18·1%)		25 (17·9%)		21 (18·2%)	
	G allele	76 (61·3%)	305 (60·3%)	n.s.*	168 (60·4%)	n.s.*	137 (59·6%)	n.s.*
	A allele	48 (38·7%)	203 (39·7%)		110 (39·6%)		93 (40·4%)	

Analysed by χ^2 tests *versus controls †versus HDs ‡versus GDs §TT versus TC + CC ¶CC versus CT + TT; n.s. = not significant. AITD = autoimmune thyroid disease.

Table 2. The frequencies of Vitamin D SNPs in GD and HD

		Control	GD			HD	
			Intractable	In remission		Severe	Mild
VDR rs731236	TT	58 (77·3%)	45 (84·9%)	32 (86·5%)	n.s.*	42 (79·3%)	30 (75·0%)
	TC	17 (22·7%)	7 (13·2%)	5 (13·5%)		10 (18·9%)	10 (25·0%)
	CC	0 (0%)	1 (1·9%)	0 (0%)		1 (1·8%)	0 (0%)
	T allele	133 (88·7%)	97 (91·5%)	69 (93·2%)	n.s.*	94 (88·7%)	70 (87·5%)
	C allele	17 (11·3%)	9 (8·5%)	5 (6·8%)		12 (11·3%)	10 (12·5%)
VDR rs7975232	CC	31 (41·3%)	25 (50·0%)	16 (41·0%)	n.s.*	22 (50·0%)	18 (42·9%)
	CA	32 (42·7%)	23 (46·0%)	19 (48·7%)		18 (40·9%)	22 (52·4%)
	AA	12 (16·0%)	2 (4·0%)	4 (10·3%)		4 (9·1%)	2 (4·7%)
	C allele	94 (62·7%)	73 (73·0%)	51 (65·4%)	n.s.*	62 (70·5%)	58 (69·0%)
	A allele	56 (37·3%)	27 (27·0%)	27 (34·6%)		26 (29·5%)	26 (31·0%)
VDR rs2228570	CC	25 (32·9%)	18 (36·7%)	9 (23·5%)	n.s.*	20 (45·5%)	23 (55·0%)
	CT	42 (55·3%)	27 (55·1%)	27 (67·5%)		19 (43·2%)	16 (40·0%)
	TT	9 (11·8%)	4 (8·2%)	4 (10·0%)		5 (11·3%)	2 (5·0%)
	C allele	92 (59·2%)	63 (64·3%)	45 (56·3%)	n.s.*	59 (67·0%)	60 (75·0%)
	T allele	60 (40·8%)	35 (35·7%)	35 (43·7%)		29 (33·0%)	20 (25·0%)
VDR rs1544410	AA	3 (4·7%)	0 (0%)	1 (2·8%)	n.s.*†	0 (0%)	2 (5·4%)
	AG	11 (17·2%)	4 (9·5%)	6 (16·7%)		7 (17·1%)	9 (24·3%)
	GG	50 (78·1%)	38 (90·5%)	29 (80·5%)		34 (82·9%)	26 (70·3%)
	A allele	17 (13·3%)	4 (4·8%)	8 (11·1%)		7 (8·5%)	13 (17·6%)
	G allele	111 (86·7%)	80 (95·5%)	64 (88·9%)		75 (91·5%)	61 (82·4%)
GC	Gc1Gc1	57 (61·7%)	21 (38·9%)	24 (66·7%)	0·0093*† 0·0109*	33 (82·5%)	25 (62·5%)
	Gc1Gc2	19 (31·7%)	32 (59·3%)	10 (27·8%)		18 (36·0%)	15 (32·5%)
	Gc2Gc2	4 (6·6%)	1 (1·8%)	2 (5·5%)		1 (2·0%)	0 (0%)
	Gc1 allele	93 (77·5%)	74 (68·5%)	58 (80·6%)	n.s.*	80 (80·0%)	65 (81·3%)
	Gc2 allele	27 (22·5%)	34 (31·5%)	14 (19·4%)		20 (20·0%)	15 (18·7%)
CYP2R1 rs10741657	GG	25 (40·3%)	26 (47·6%)	12 (30·0%)	n.s.* 0·0268*‡	20 (37·0%)	11 (30·5%)
	GA	26 (41·9%)	20 (53·8%)	22 (53·0%)		23 (42·6%)	19 (52·8%)
	AA	11 (17·8%)	11 (24·6%)	6 (15·0%)		11 (20·4%)	6 (16·7%)
	G allele	76 (61·3%)	72 (59·0%)	46 (57·5%)	n.s.*	63 (58·3%)	41 (56·9%)
	A allele	48 (38·7%)	50 (41·0%)	34 (42·5%)		45 (41·7%)	31 (43·1%)

Analysed by χ^2 tests or Fisher's exact test; *intractable GD versus GD in remission; †severe HD versus mild HD; ‡Gc1Gc1 versus Gc1Gc2 + Gc2Gc2; §AA versus GG + AA; n.s. = not significant.

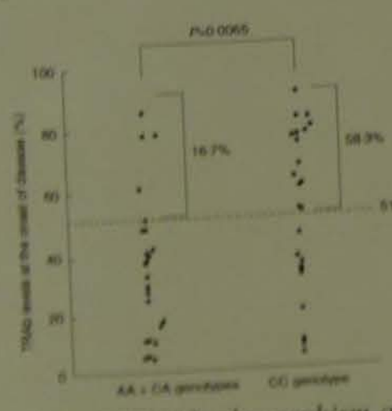

Fig 1 VDR rs7975232polymorphism and TRAb levels

Summary

1. ***VDR* rs731236 TT genotype: GD > HD (P=0.0147)**
2. ***VDR* rs7975232 C allele: GD > control (P=0.0349)**
   CC genotype > AA + CA genotypes (P=0.0065) (TRAb levels > 51%)
3. ***VDR* rs2228570 CC genotype: HD > control (P=0.0174)**
4. ***GC* Gc1Gc1 genotype, *CYP2R1* rs10741657 AG genotype:**
   intractable GD < GD in remission (P=0.0093, 0.0268)

Materials and Methods

Subjects

Severe HD: HD patients developed hypothyroidism before the age of 50 and were treated with thyroxine

Mild HD: HD patients over the age of 50 were left untreated and demonstrated euthyroid

Intractable GD: GD patients were euthyroid, had been treated with methimazole for at least five years and were still positive for TRAb

GD in remission: GD patients maintained a euthyroid state and were negative for TRAb for more than two years after discontinuing the anti-thyroid drug therapy

Control subjects: healthy volunteers who were euthyroid and negative for thyroid autoantibodies

***Methods*:** PCR-RFLP method

Conclusion

1. ***VDR* polymorphisms were associated with GD development and GD activity**
2. ***GC* and *CY2R1* polymorphisms were associated with GD intractability**

There were no conflict of interest

Molecular Diagnosis

PL-29

Telomeric regions of the spinal muscular atrophy locus are susceptible to structural variations.

Yoriko Noguchi, Yuji Nakamachi, Nobuhide Hayashi, Jun Saegusa, Seiji Kawano, Taku Nakagawa, Ai Shima, Hisahide Nishio

Kobe University Hospital

Background

- Spinal muscular atrophy(SMA) is a common neuromuscular disorder with an autosomal recessive inheritance trait. It is classified into three subtypes based on the age of onset and clinical severity: type1(severe), type2(intermediate), type3(mild).
- The SMA locus is mapped to chromosome 5q13, and can be divided into telomeric and centromeric parts because of the presence of a large inverted duplication in the chromosome. *SMN* exists in two nearly identical copies, *SMN1* (the telomeric copy) and *SMN2* (the centromeric copy).
- *SMN1* is now recognized as an SMA-causing gene.

Munsat TL, et al. Neuromuscul Disord. 1992; 2: 423-428.

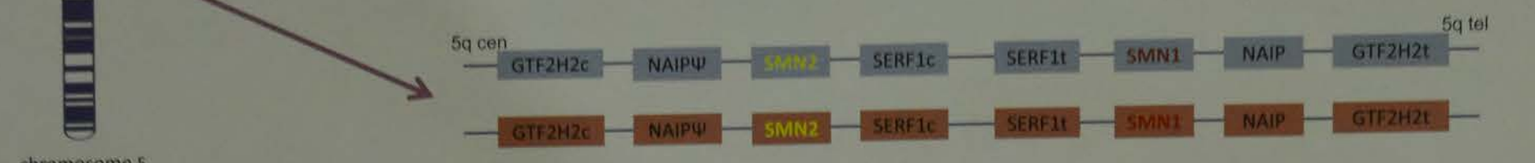

- Most SMA patients lack the *SMN1* . On the other hand, the copy number of *SMN2* is increased in many of these patients.
- The *SMN1* protein product SMN is essential in heterogeneous nuclear ribonucleoprotein biogenesis (a ubiquitous function) and in axonal transport (a motor neuron-specific function).
- *SMN2* also expresses SMN, albeit at considerably lower levels than *SMN1*. It was shown that a high copy number of *SMN2* can partially compensate for the lack of *SMN1*. Therefore, *SMN2* is also now considered to be an SMA-modifying gene.

Nurputra DK, et al. Ann Hum Genet. 2013; 77: 435-463.
Lefebvre S, et al. Cell. 1995; 80: 155-165.

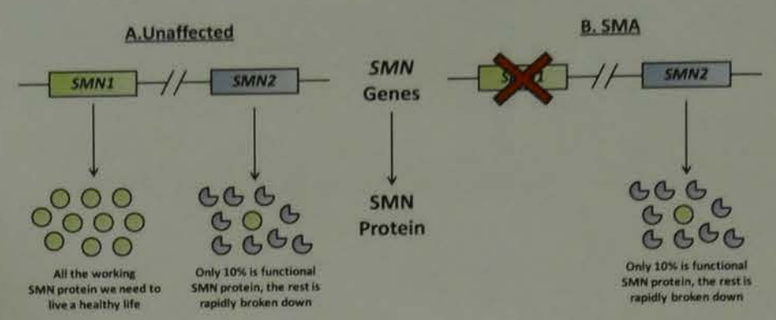

Spinal muscular atrophy support UK HP

Aim This study aimed to clarify the mechanism underlying these structural variations. We herein examined the copy number variation of SMA locus gene *NAIP*, *GTF2H2*, and *SERF1* using multiplex ligation-dependent probe amplification(MLPA).

Subjects and Methods

- We used the diagnosis criteria of SMA defined by the International SMA Consortium.
- A total of 74 SMA patients (28patients with type 1, 27 with type 2, 19 with type 3) and 22 controls participated in this study.
- Genomic DNA was extracted from whole blood using DNA extraction kit.
- MLPA was used to evaluate 5q13 region genes, and copy numbers of *SMN*, *NAIP*, *GTF2F2*, and *SERF1* in the DNA samples using the SALSA MLPA kit P021 (MRC-Holland, Amsterdam, the Netherlands) according to the manufacturer's recommendations.

Results

Fig.1 *SMN2* copy number

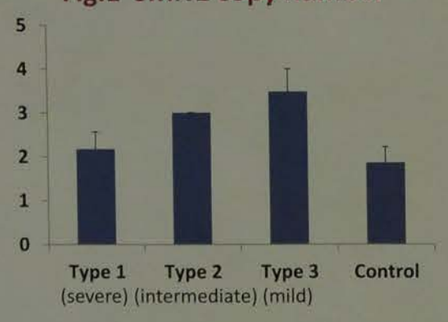

Fig.3 *NAIP* copy number

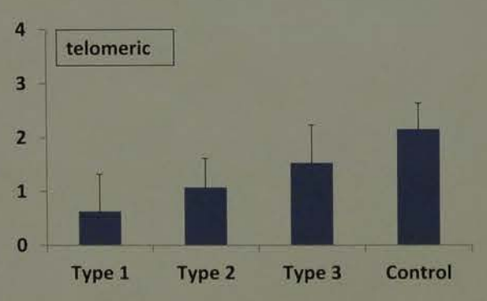

Fig.4 *GTF2H2* copy number

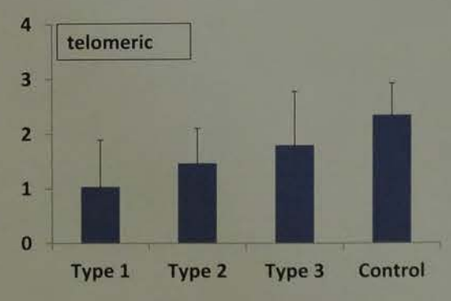

Fig.2 *SERF1*(teromeric+centromeric) copy number

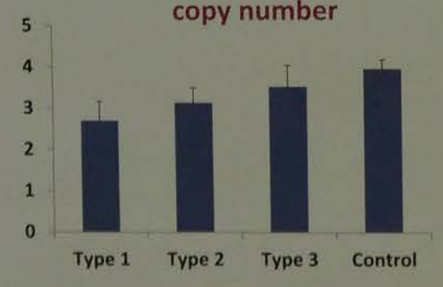

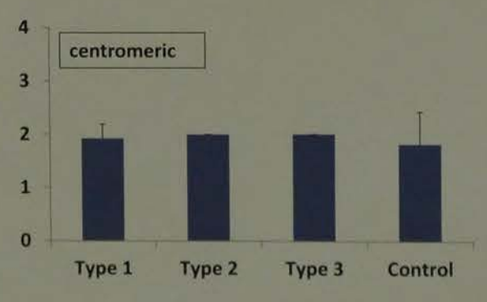

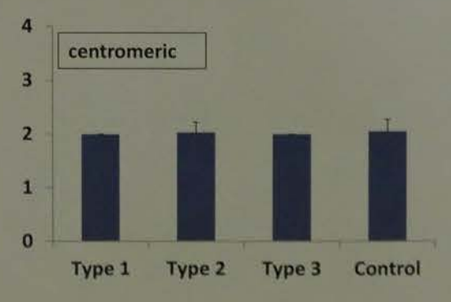

Table1 Spearman's correlation coefficient by rank test

	SERF1	*SMN2*	tel. *NAIP*	tel. *GTF2H2*
SERF1				
SMN2	0.786 ($p < 0.001$)			
tel. *NAIP*	0.555 ($p < 0.001$)	0.687 ($p < 0.001$)		
tel. *GTF2H2*	0.425 ($p < 0.001$)	0.543 ($p < 0.001$)	0.732 ($p < 0.001$)	

Summary

- The *SMN2* copy number was shown to vary widely, and to correlate with the disease severity of the patients.
- Telomeric *NAIP* and telomeric *GTF2H2* showed similar tendencies, and positive correlations showed among the copy number of *SMN2* and the telomeric genes of the SMA locus.
- However, the copy numbers of centromeric *NAIP* and centromeric *GTF2H2* were stable among the patients, with both approximating a value of 2.

Conclusion

- The telomeric region of the SMA locus appears to be susceptible to structural variation, while the centromeric region is stable.
- New *SMN2* copies may be generated in the telomeric region of the SMA locus, supporting the *SMN1*-to-*SMN2* gene conversion theory.

We have no COI with regard to our presentation.

D-2 D-2

Molecular Diagnosis

PL-30

Standardization of circulating miRNA analysis: Difference between plasma and serum miRNAs

Hiromichi Shiotsu[1,3], Kazuhiro Okada[1], Saki Shirahama[1], Chieri Kuroki[1], Saori Ueda[1], Katsuyoshi Ikeda[3], Hirotaka Matsui[3], Yuzo Kayamori[1], Tsukuru Umemura[1,2]

1. Department of Health Sciences, Graduate Scholl of Medical Sciences, Kyushu University, Fukuoka, Japan, 2. Department of Medical Technology and Sciences, International University of Health and Welfare, Fukuoka, Japan, 3. Department of central clinical laboratory of medicine, Kumamoto University Hospital, Kumamoto, Japan

Background:

MicroRNA(miRNA) is one of the short non-coding RNAs which negatively regulates gene expressions. It has been reported that values of miRNA are variable depending on measurement conditions, thus a standardization of miRNA is essential for the utilization in clinical laboratory.
Here we report several fundamental factors that cause variation of miRNA values.

Materials and methods

- Subject:
  22 males and 3 females (Subjects that meet condition of hunger and no smoking were collected.)
  Plasma and Serum (Centrifugation at 1900G, 10 minutes.)
- Extraction and RT-qPCR:
  Nucleospin (Takara), miRNA array assay (Thermo Fisher Scientific).
- Target of miRNA:
  hsa-miR-16-1, miR-451, miR-126, miR-223 and cel-miR-39 (as a spike-in control),

Results

1.Differences of miRNA level between plasma and serum.
When serum miRNA expression was defined as 1, relative expression of miR-126 and miR-223 in plasma were 93.9 and 32.2, respectively. miR-16 in plasma also showed higher value than serum relatively 14.9, while miR-451 in plasma was lower than serum, 0.42.

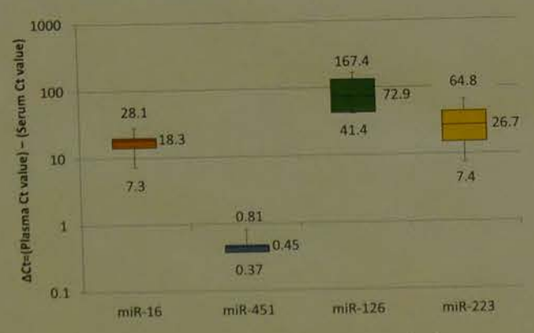

Fig.1 miRNA expression in serum and plasma

2. Influence of cell debris and platelets
Blood samples were centrifuged for 1 min at 10,000G. When serum miRNA expression was defined as 1, relative expression of miR-16 was 0.82 which is showed as average value of whole samples and miR-451 was 5.79. miR-126 and miR-223 were 0.79 and 3.07, respectively.

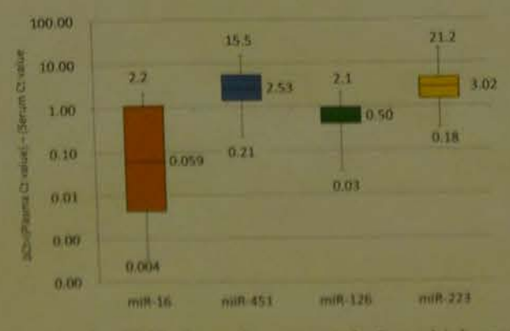

Fig.2 Levels of miRNA of samples extracted after a high speed centrifugation

3. Influence of normalizer selection between spike-in control and internal control
1 fmol cel-miR-39 was added as a spike-in control during the miRNA extraction. ΔΔCt method was adopted for analyze method. Values of miRNA is showed respectively and miRNA in serum was used as a standard. miR-16 in plasma was 1.07, miR-451 in plasma was 2.02. Expression of miR-126 was 0.69, miR-223 was 0.28.

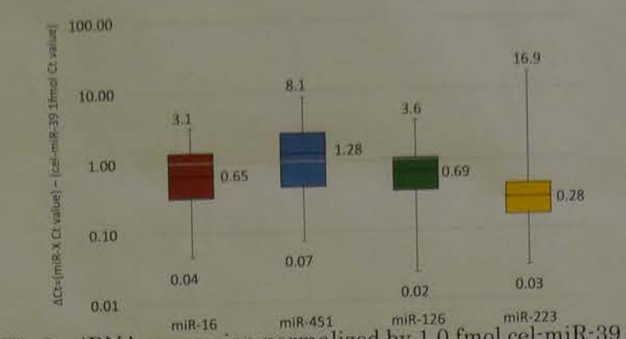

Fig.3 miRNA expression normalized by 1.0 fmol cel-miR-39

4. Influence of coagulation accelerator during sample preparation
Expression of miRNA between plasma and serum was changed depend on a normalizer selection that cel-miR-39 or serum.
An extra sample was prepared in the following manner ; plasma specimens removed from whole blood in EDTA tube was transferred to plain tube and was incubated for 30 minutes at room temperature before extraction.

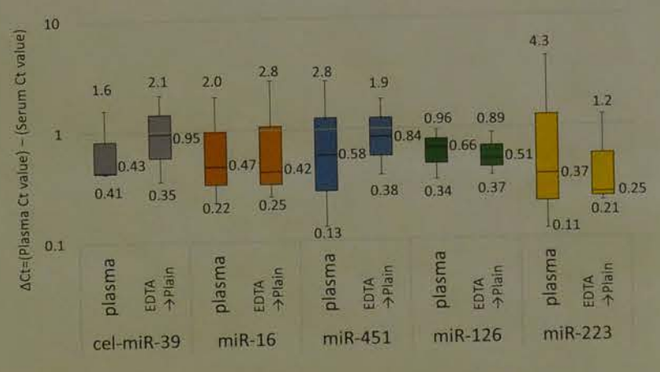

Fig.4 Influence of coagulation accelerator

There were no significant difference between miRNA values of plasma and EDTA → Plasma sample.

5. Usefulness of RNase Inhibitor to protect from miRNA degradation

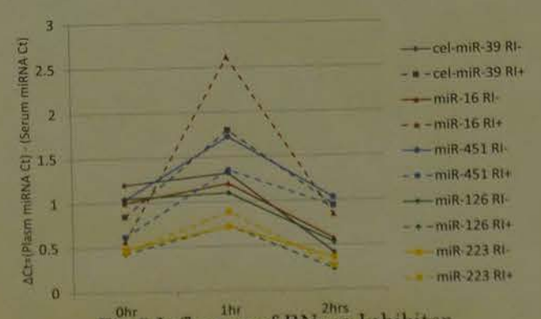

Fig.5 Influence of RNase Inhibitor

RNase Inhibitor(RI) was used at the concentration of 0.3M. When RI- and RI+ samples were compared, most of RI+ samples showed higher values than RI-.

Discussion

At first platelet-specific miRNA had been rich in plasma than serum, but this difference was presumed to be interfusion of platelets and platelet-derived debris. High speed centrifugation was effective to remove these components in sample. Most of miRNAs had no difference between plasma and serum when value of serum miRNA was defined as 1. Our data that the plasma level of miR-451 was significantly higher than in serum, but cause of this difference have not been clear.

Conclusion

Our data suggest that
- A large part of plasma miRNAs come from cellular miRNAs.
- Removal of cellular components from plasma is essential to analyze circulating miRNAs in various pathological state.

Molecular Diagnosis

PL-31

Development of a quenching probe PCR method distinguishing between *Chlamydophila pneumoniae* and *Chlamydophila psittaci*

Kyoko Hisada[a], Yukio Hida[a], Yousuke Kawashima[b], Yoshihiro Soya[b], Akihiro Shimada[a], Syouhei Sakaguchi[a], Hideki Kimura[a] and Masayuki Iwano[c]

Department of Clinical Laboratories of Fukui University Hospital[a], Tsuruga Institude of Biotechnology TOYOBO Co., LTD.[b], and Division of Nephrology, Department of Medicine, Faculty of Medical Sciences, University of Fukui[c]

Introduction

The family Chlamydiaceae infection is usually diagnosed by serological test. However, this test requires paired serum samples at an interval of 2 to 4 weeks and consequently provides only a retrospective diagnosis.

We newly developed a quenching probe PCR method using (GENECUBE®) to rapidly detect *Chlamydophila* with distinguishing between *C. pneumoniae* and *C. psittaci*.

Methods for detecting *Chlamydophila* in specimens

A total of 289 specimens from respiratory systems of candidates were preserved in a sucrose - phosphatase - glutamate(SPG).

1. A newly developed quenching probe PCR method using GENECUBE® (GENECUBE ® assay)

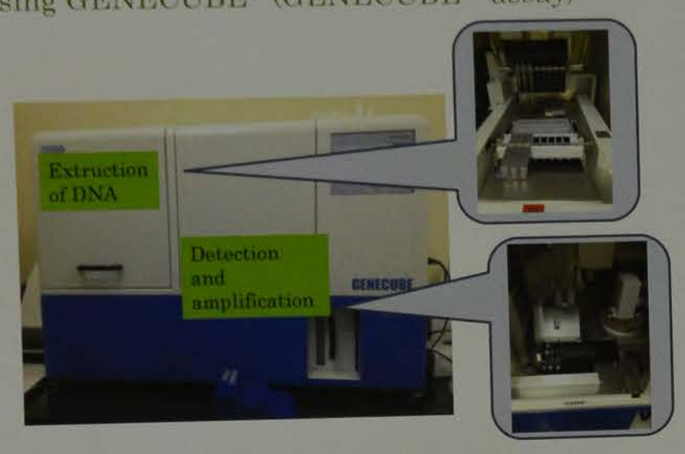

Oligonucleotide primers targeting *ompA* gene sequences were used for the GENECUBE® assay of *C. pneumoniae* and *C. psittasi*. We constructed quenching probes which can discriminate *C. pneumoniae* and *C. psittaci*, and analyzed specimens automatically using GENECUBE® with the primers and probe.

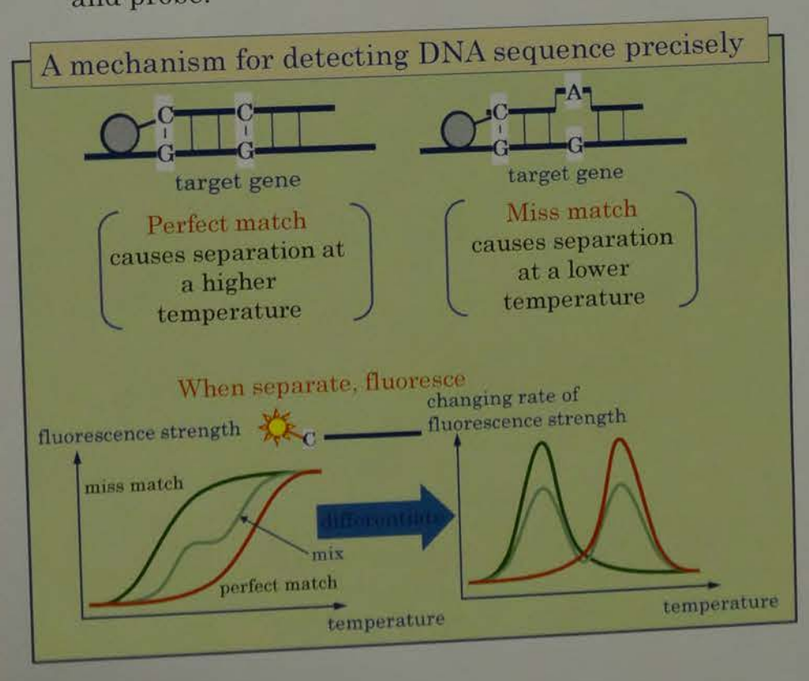

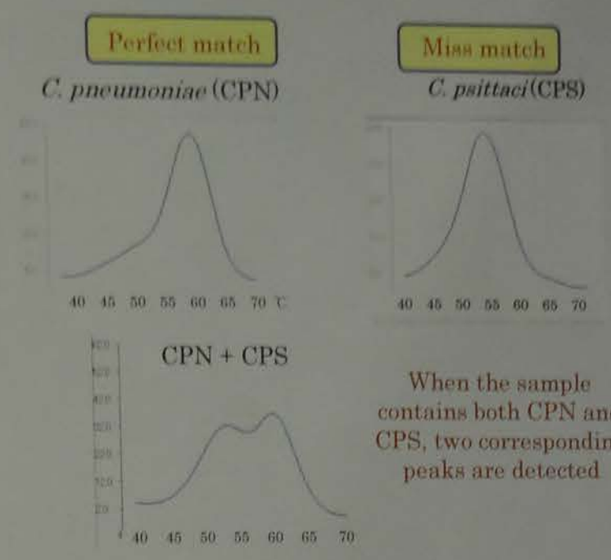

When the sample contains both CPN and CPS, two corresponding peaks are detected

2. A conventional method using cell culture

Small portions of specimens were added into Hela - 2 cell seeded at 2×10^5 cells in 24 - well plates. The cells thus treated were further incubated for 72h at 37℃ under 5% CO_2. After methanol fixation, *Chlamydia* inclusions were stained by a fluorescent antibody.

cell culture

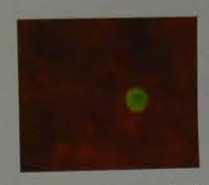

A fluorescent staining for *Chlamydia* inclusion

Result

Concordance rate was 96.5%(279/289), when results from the GENECUBE® assay were compared with those from the cell culture. Among the 10 mismatched cases, 7 samples were culture - positive and PCR - negative, and 3 samples were PCR - positive and culture - negative. No cross reaction was observed in test samples containing different and various bacterial strains.

		PCR +	PCR -
culture	+	3 ※1	7 ※2
	-	3 ※3	276

※1 *C. pneumoniae*(+), 2 ; *C. psittaci*(+), 1

※2 serological test : CPN IgM>1.25ng/mL, 2 ; positive by pared serum samples, 5

※3 *C. pneumoniae*(+)×3 , serological test : CPN IgM>2.01ng/mL, 3

Conclusion

GENECUBE® assay enabled us to specifically and rapidly identify *C. psittaci* from clinical specimen and to distinguish it from *C. pneumoniae* . Therefore, this assay may be a promising tool for rapid diagnosis of the Chlamydiaceae infection.

Molecular Diagnosis

PL-32

Basic Examination of Major BCR-ABL mRNA quantification with IS calibrator

INTRODUCTION

OBJECTIVE

SUBJECTS&METHODS

RESULTS

CONCLUSION

Molecular Diagnosis

PL-32

Basic examination of Major BCR-ABL mRNA quantification kit with IS calibrator

Hikaru Hattori[1], Yoko Kajiura[1], Yukako Yamamoto[1], Mayumi Takatsu[1], Hiroyuki Matsumoto[1], Mayuko Kishimoto[2], Nobuaki Suzuki[3], Tadashi Matsushita[4]

1 Dept. of Medical Technique, Nagoya Univ. Hosp., Nagoya, Aichi, Japan
2 Dept. of Clinical Laboratory, Nagoya Univ. Hosp., Nagoya, Aichi, Japan
3 Dept. of Transfusion Medicine, Nagoya Univ. Hosp., Nagoya, Aichi, Japan
4 Dept. of Clinical Laboratory&Transfusion Medicine, Nagoya Univ. Hosp., Nagoya, Aichi, Japan

2016 IFBLS Kobe Japan

INTRODUCTION

Major BCR-ABL mRNA quantification methods in Japan

Amp-CML (TMA method)
- ✓No normalizing mRNA levels
- ✓Cannot detect low-levels of BCR-ABL mRNA

Not used much now in Japan

BCR-ABL (RT-qPCR method)
- ✓The most **common method** in JAPAN
- ✓Variability among laboratory using **different protocols**

Data can not be compared between different facilities!

BCR-ABL^{IS} (RT-qPCR method)
- ✓Defined as the **International Scale(IS)** converted from measurements

Recommended in JALSG clinical guidelines

What is BCR-ABL^{IS}?

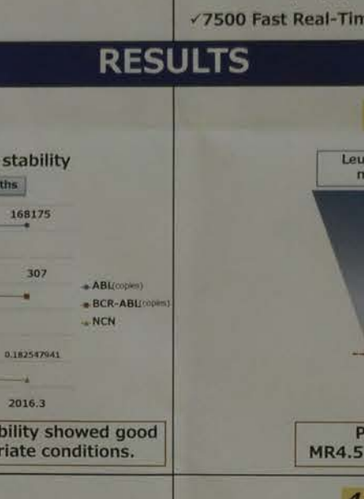

- ✓NCN is corrected that degradation of RNA
- ✓CF is corrected many factors of measurement

2-types of BCR-ABL^{IS} methods

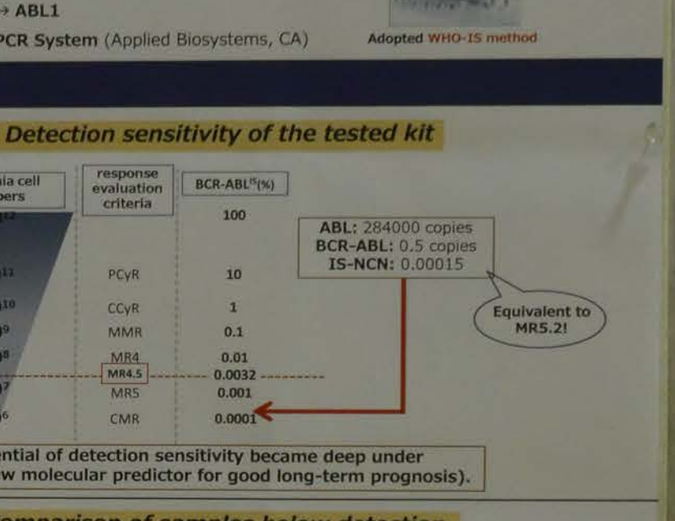

OBJECTIVE

The monitoring of chronic myeloid leukemia(CML) therapy is based on BCR-ABL mRNA levels by RT-qPCR. But, there is a problem relating to different measurement protocol among every institution. The ipsogen BCR-ABL1 Mbcr IS-MMR DX kit can report International Scale (IS) of BCR-ABL mRNA using a calibrator whose value is assigned to WHO 1st standard material. This time, we report performance of the kit and comparison with the measurements by the current RT-qPCR method.

SUBJECTS&METHODS

Subjects: **This test was approved by the ethics committee of Nagoya University graduate of medicine**

- ✓Residual samples of RNA from peripheral-blood mononuclear cells of the patients used for testing Major BCR-ABL mRNA in this hospital**(N=28)**
- ✓Pooling RNA of healthy volunteer peripheral-blood mononuclear cells**(N=6)**

Current method:
- ✓**RT-qPCR method** (K.Kawamura et al. 2002 *The Japanese journal of medical technology*)
- ✓**House-keeping gene → ABL1**
- ✓ **Light Cycler 2.0**(Roche, Swiss)

Tested BCR-ABL^{IS} measurement kit:
- ✓**ipsogen BCR-ABL1 Mbcr IS-MMR DX kit** (Sysmex, Japan)
- ✓**House-keeping gene → ABL1**
- ✓**7500 Fast Real-Time PCR System** (Applied Biosystems, CA)

Adopted WHO-IS method

RESULTS

1,Tests of IS calibrator within the kit

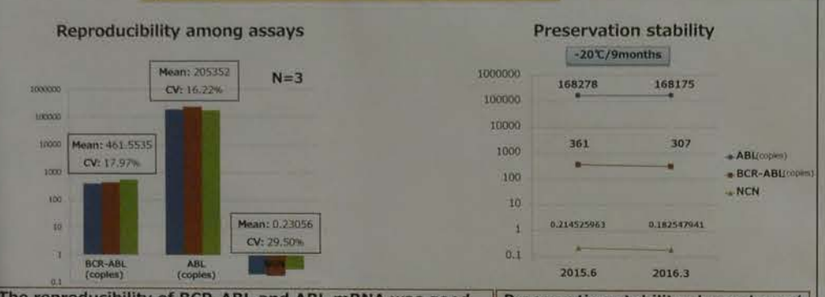

The reproducibility of BCR-ABL and ABL mRNA was good. Dispersion increased when results were expressed by NCN.

Preservation stability showed good under appropriate conditions.

3, Detection sensitivity of the tested kit

Potential of detection sensitivity became deep under MR4.5(new molecular predictor for good long-term prognosis).

2, Dilution linearity of the tested kit

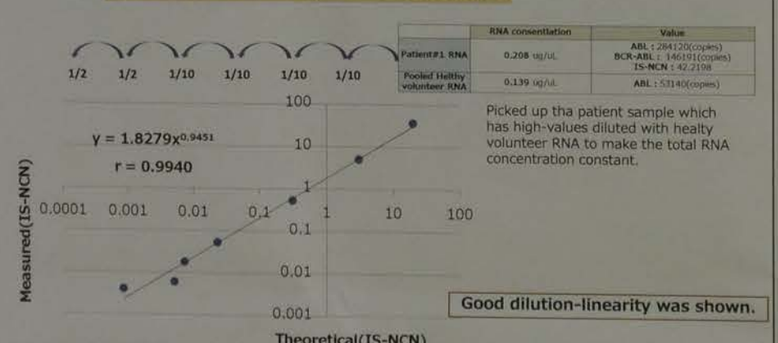

RNA consentiation	Value
Patient#1 RNA 0.208 ug/uL	ABL : 284120(copies) BCR-ABL : 146191(copies) IS-NCN : 42.2198
Pooled Helthy volunteer RNA 0.139 ug/uL	ABL : 53140(copies)

Picked up tha patient sample which has high-values diluted with healty volunteer RNA to make the total RNA concentration constant.

Good dilution-linearity was shown.

4, Comparison of samples below detection sensitivity by current method

N=10

Current \ Tested	Quantitative range	Less than detection sensitivity (>3copies)	Not detected
Less than detection sensitivity (>10^2copies)	5	2	0
Not detected	0	1	2

The quantitation limit of this kit was lower than the current method(10^2 vs. 3 copies), therefore more samples could be quantitated in this kit.

5, Correlation between current method and tested kit data

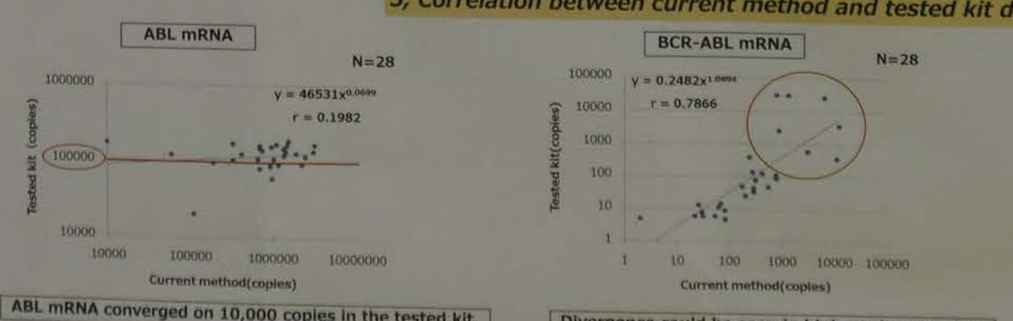

ABL mRNA converged on 10,000 copies in the tested kit.

Divergence could be seen in high-copies samples.

Almost samples located in the same point of order.

CONCLUSION

This examination confirmed that the ipsogen BCR-ABL1 Mbcr IS-MMR DX kit possessed **sufficient sensitivity** and **good dilution-linearity**. In addition, IS calibrator within the kit was **uniformity** and **stability**. But, correlation between current method and the kit data **showed divergence in some samples**. In preparation for switch from current method to new kits, it requires further consideration regarding the **clinical backgrounds** (ex. ABL mutation, breakpoint in fusion gene, Ph+ALL) of the patient's samples.

Hikaru Hattori :hhattori@med.nagoya-u.ac.jp

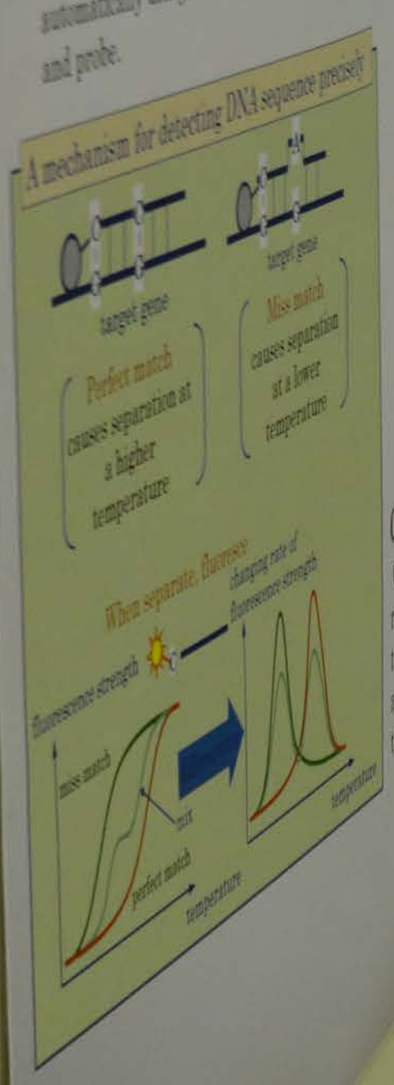

Molecular Diagnosis

PL-33

CALR and *MPL* mutation analysis in the patients suspected of myeloproliferative neoplasms without *JAK2* V617F

Manjiro Yamanaka, Tatsuya Negishi, Kazuyuki Matsuda, Shohei Shigeto, Satomi Furukawa, Mitsutoshi Sugano, Takayuki Honda.
Department of Laboratory Medicine, Shinshu University Hospital

Introduction

Polycythemia vera (PV), essential thrombocytosis (ET), and primary myelofibrosis (PMF), are pathologically classified as myeloproliferative neoplasms (MPN). A somatic mutation of the Janus kinase 2 gene (*JAK2*) V617F is most frequently identified in patients with MPN. Recent studies showed that calreticulin (*CALR*) mutation, which commonly involved deletion or insertion, and thrombopoietin receptor (*MPL*) W515L/K mutation were found in many of the patients without the *JAK2*V617F [Figure 1].

In this study, we examined the *CALR* and *MPL* mutations in the patients who were suspected of having MPN, but not the *JAK2*V617F.

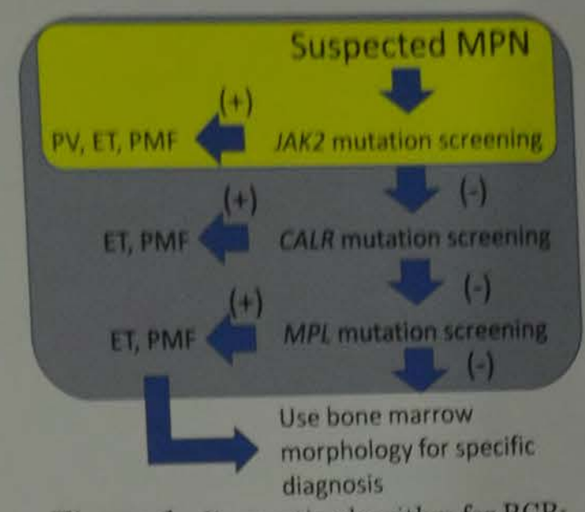

Figure 1. diagnostic algorithm for BCR-ABL negative MPN[1].

Material & Methods

Peripheral blood samples obtained from 45 patients who were suspected of having MPN, presenting splenomegaly or abnormalities in complete blood cell count (CBC) and/or pathological findings, were used in this study. The *JAK2*V617F was negative in all patients; the *BCR-ABL* fusion gene was negative in 8 and not evaluated in the remaining. The *CALR* mutation was examined by amplicon sizing with capillary electrophoresis and fragment length analysis after a PCR procedure[2]. The *MPL* W515L/K mutation was analyzed using the amplification refractory mutation system (ARMS)-PCR[3].

Results

Among the 45 patients, the *CALR* mutation was observed in 3 patients (A 19-bp deletion in patient 1,and a 52-bp deletion in patient2, 3). Patient 1 diagnosed as having myelofibrosis, and Patient 2, 3 were as having ET. [Figure 2, 3] No *MPL* W515L/K mutation was identified in all patients.[Figure 4, 5]

CALR mutation analysis

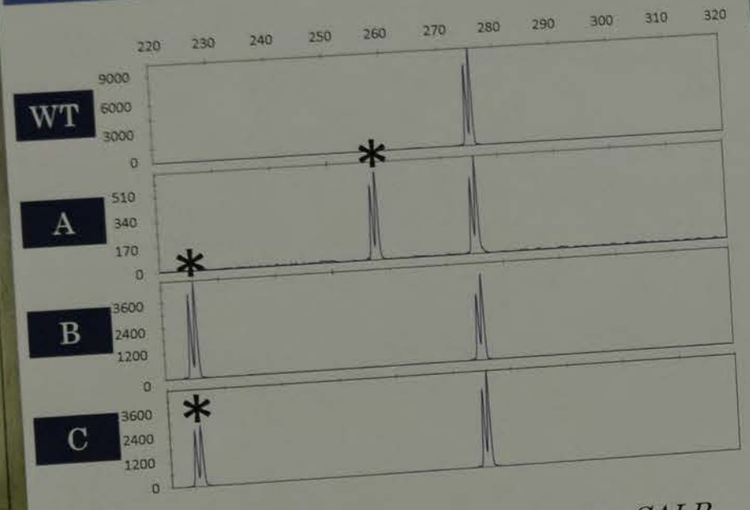

Figure 2. Fragment length analysis for *CALR* mutation. Astarisk, allele with a deletion. WT, wild type; A, patient 1; B, patient 2; C, patient 3.

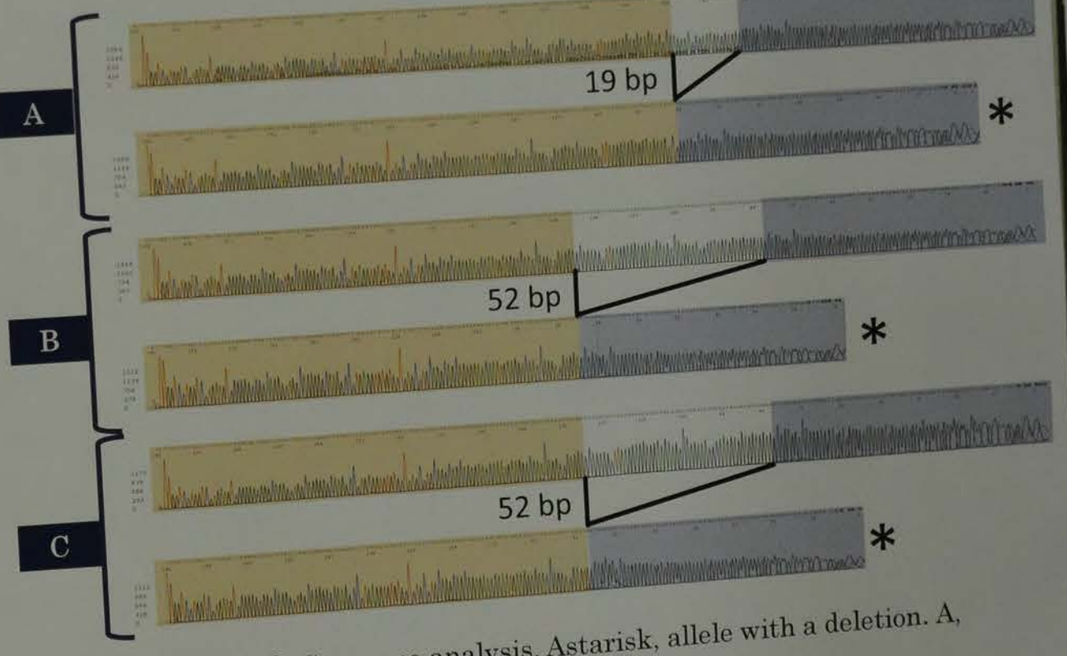

Figure 3. Sequence analysis. Astarisk, allele with a deletion. A, patient 1; B, patient 2; C, patient 3.

MPL mutation analysis

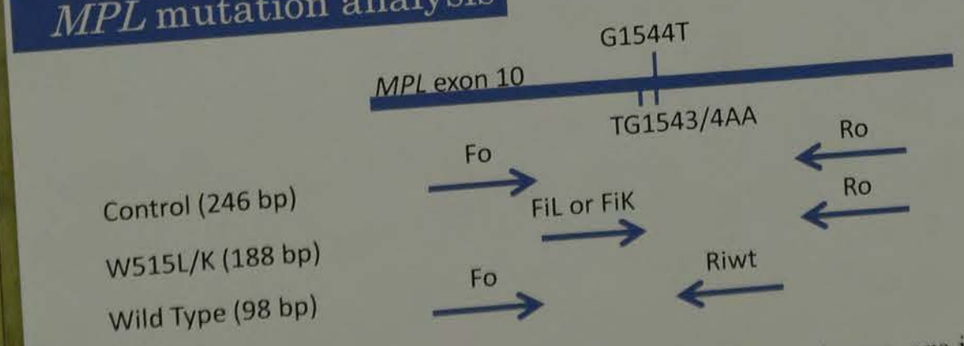

Figure 4. ARMS-PCR for *MPL* W515L/K. Four PCR primers are in one PCR. FiL-Ro primer pair designed for *MPL* W515L sized 188 bp. FiK primer was designed for *MPL* W515K instead of FiL primer. Fo-Riwt primer pair designed for wild type *MPL* fragment sized 246 bp.

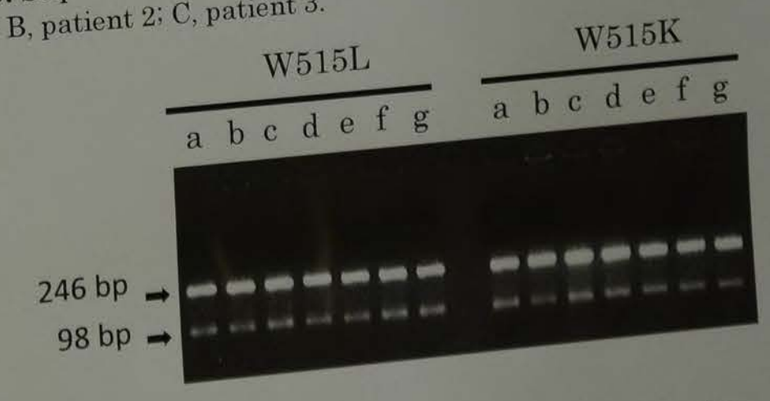

Figure 5. Result of *MPL* ARMS-PCR. Seven samples (a-g) out of 45 were shown in this figure.

Conclusion

Although an apparent increase of CBC parameters is one of the informative findings to suspect MPN, the patient with myelofibrosis, who showed no increase of CBC, had the *CALR* mutation. Therefore, the *CALR* mutation may be important to diagnose MPN even in the patients who show neither the *JAK2*V617F nor an increase of any CBC parameter levels. The diagnostic usefulness of the *MPL* mutation could not be proved in this study.

Reference

1. Tefferi A, Barbui T, et al. Polycythemia vera and essential thrombocythemia: 2015 update on diagnosis, risk-stratification, and management. Ame J Hem 2015;90:2
2. Cheryl LM, Kevin EF, et al. Development and Validation of *CALR* Mutation Testing for Clinical Diagnosis. AJCP 2015;144:738-745
3. Jian Z, Wenyong Z, et al. Sensitive detection of MPL W515L/K mutations by amplification refractory mutation system (ARMS)-PCR. Clinica Chimica Acta. 2010;411:122-123

Molecular Diagnosis

PL-34

Xeroderma pigmentosum (XP) genetic screening in Kobe University Hospital

Keiji Matsui[1)], Yoriko Noguchi[1)], Yoko Okazaki[1)], Yuji Nakamachi[1)], Taro Masaki[2)], Eiji Nakano[2)], Chikako Nishigori[2)]

1) Department of Clinical Laboratory, Kobe University Hospital, Japan
2) Department of Dermatology, Graduate School of Medicine, Kobe University

Background

In recent years , use of the practice of genetic testing is seen expanding. Our Department of clinical laboratory has performed the genetic testing of xeroderma pigmentosum (XP) in cooperation with our hospital dermatology since 2012. XP is autosomal recessive disease caused by dysregulated DNA repair. XP is classified into seven genetic complementation groups of nucleotide excision repair (NER)-deficient type, A-G (XPA-G), and a NER proficient xeroderma pigmentosum variant type (XP-V) (Figure 1). Because XP have a disability in DNA repair synthesis, there is a possibility that mutation of oncogene accumulate. In the result, Skin cancers characteristically develop in sun-exposed sites at much earlier ages. Here we report gene mutation of the 40 patients with XP (XPA: 6, XPD: 5, XPV: 30, total 41 tests) in our hospital since 2012 .

Method

DNA was extracted from peripheral blood using the QIAamp DNA Mini Kit(QIAGEN). Polymerase chain reaction (PCR) was performed on genomic DNA using primers XP-A (*XPA* gene), XP-D (*ERCC2* gene) and XP-V (*POLH* gene). Amplified products were directly sequenced using a BigDye terminator cycle-sequencing kit (Applied Biosystems). Unscheduled DNA synthesis (UDS) examined for NER activity was performed utilizing fibroblasts harvested from these patients.

Result

No.	age/sex	genome (NG_011642.1)	CDS (NM_000380.3)		UDS
1	0/M	15148	c.390-1G>C (IVS3-1G>C)	hetero	normal
2	0/M	15148	c.390-1G>C (IVS3-1G>C)	hetero	normal
3	1/F	15148	c.390-1G>C (IVS3-1G>C)	homo	9.67%

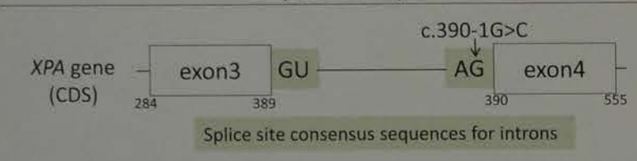

Table 1. Mutations of XPA gene found in this study.
Previously reported XPA mutation (c.390-1G>C) was detected in 3 patients, of which 2 were heterozygous mutant type. The patient with homozygote form showed decreased UDS level (9.67% of wild-type cell).

No.	age/sex	genome (NG_007067)	CDS (NM_000400.3)	protein		UDS
4	0/F	11829	c.1102C>T	p.Gln368X	hetero	normal
5	17/M	23236	c.2047C>T	p.Arg683Trp	homo	Not Date
6	33/F	23332	c.2143C>T	p.Gln715X	hetero	depression

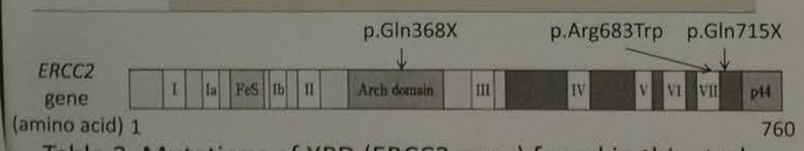

Table 2. Mutations of XPD (ERCC2 gene) found in this study.
Previously reported XPD mutation (p.Arg683Trp) was detected in 1 patient, and unreported mutations (p.Gln368X, p.Gln715X) were newly discovered in 2 patients. The UDS level was normal in the patient with p.Gln368X mutation and decreased in the patient with p.Gln715X mutation.

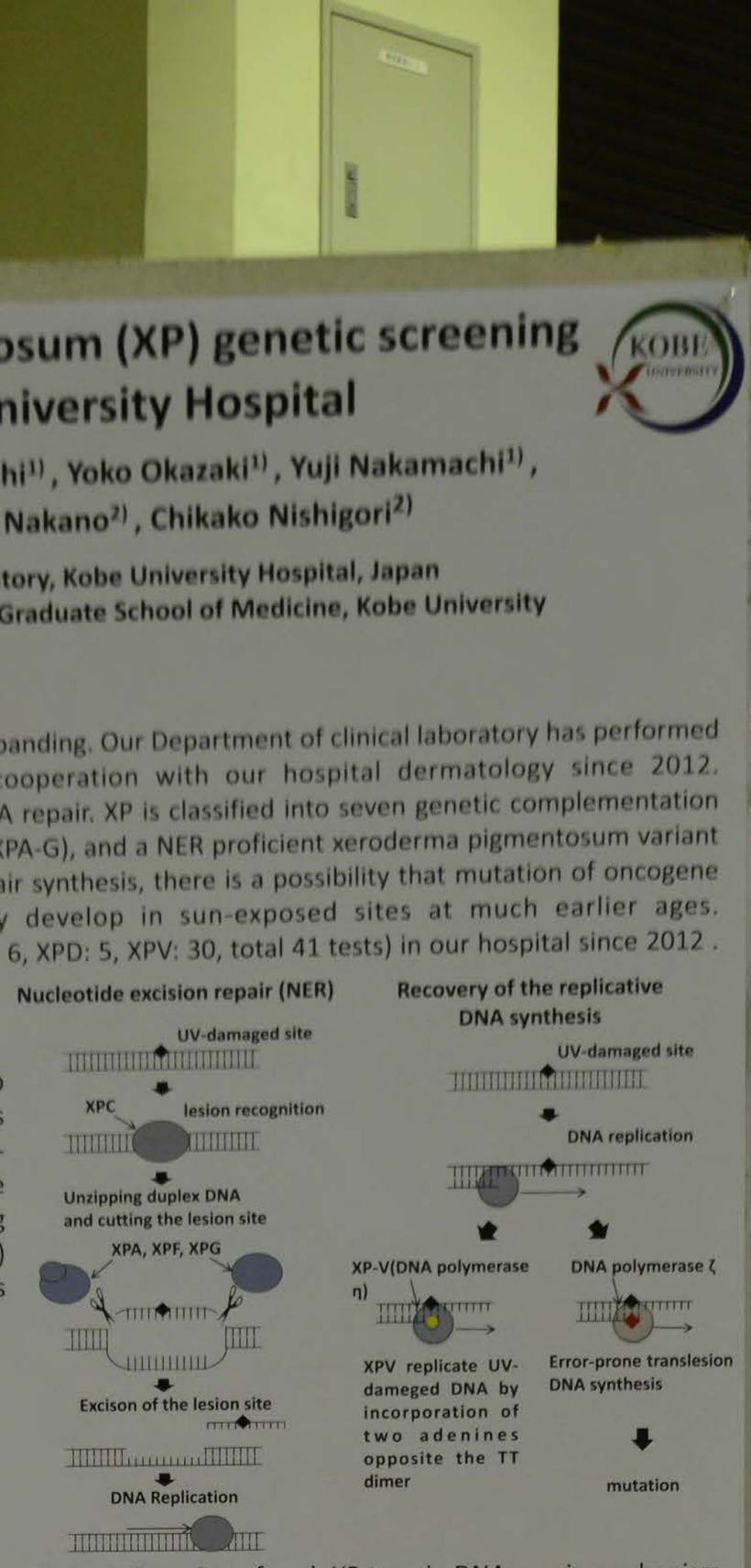

Figure 1. Function of each XP type in DNA repair mechanism

No.	age/sex	genome (NG_009252.1)	CDS (NM_006502.2)	protein	
7	61/M	16349	c.490G>T	Frameshift or large deletion	homo
8	29/F	16349	c.490G>T	Frameshift or large deletion	hetero
9	73/M	16208	c.349G>C	p.Ala117Pro	homo
10	57/M	16349	c.490G>T	Frameshift or large deletion	homo
11	56/M	16349	c.490G>T	Frameshift or large deletion	homo
		16349	c.490G>T	Frameshift or large deletion	hetero
12	6/F	26648-26653 or 26651-26656	c.583-588del or c.586-591del	p.Val195_Ile196del or p.Ile196_Val197del	hetero
		16208	c.349G>C	p.Ala117Pro	hetero
13	70/M	42936-42939	1661-1664のAの内一つがdelA	p.Asn554Thr fs 30X	hetero

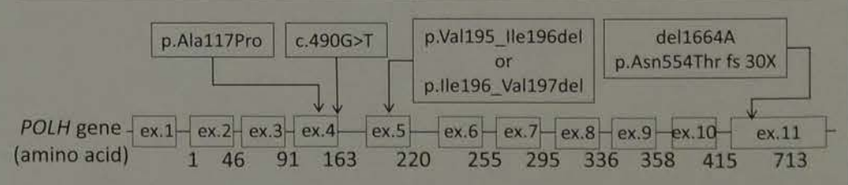

Table 3. Mutation of XPV (POLH gene) found in this study.
XPV mutation (c.490G>T) was detected in 5 patients, of which one was compound heterozygote type of six bases deletion (p.Val195_Ile196del or p.Ile196_Val197del) which is unknown. p.Ala117Pro mutation was detected in 2 patients, of which one was compound heterozygote type of c.1661delA. Among 40 patients, previously known mutation was detected in 10 patients, and unknown mutation was discovered in one patient.

Conclusion

Among 40 patients, previously known mutation was detected in 13 patients, and unknown mutation was discovered in 3 patients.